



THE UNIVERSITY *of* EDINBURGH

Edinburgh Research Explorer

Brain matters: Unveiling the Distinct Contributions of Region, Age, and Sex to Glia diversity and CNS Function

Citation for published version:

Seeker, L, Bestard-Cuche, N, Kazakou, N-L, Bøstrand, S, Wagstaff, L, Cholewa-Waclaw, J, Kilpatrick, A, van Bruggen, D, Kabbe, M, Baldivia Pohl, F, Moslehi, Z, Henderson, NC, Vallejos, CA, La Manno, G, Castelo-Branco, G & Williams, AC 2023, 'Brain matters: Unveiling the Distinct Contributions of Region, Age, and Sex to Glia diversity and CNS Function', *Acta Neuropathologica Communications*.
<https://doi.org/10.1186/s40478-023-01568-z>

Digital Object Identifier (DOI):

<https://doi.org/10.1186/s40478-023-01568-z>

Link:

[Link to publication record in Edinburgh Research Explorer](#)

Document Version:

Peer reviewed version

Published In:

Acta Neuropathologica Communications

Publisher Rights Statement:

For the Purpose of open access, the author has applied a CC-BY public copyright licence to any Author Accepted Manuscript version arising from this submission.

General rights

Copyright for the publications made accessible via the Edinburgh Research Explorer is retained by the author(s) and / or other copyright owners and it is a condition of accessing these publications that users recognise and abide by the legal requirements associated with these rights.

Take down policy

The University of Edinburgh has made every reasonable effort to ensure that Edinburgh Research Explorer content complies with UK legislation. If you believe that the public display of this file breaches copyright please contact openaccess@ed.ac.uk providing details, and we will remove access to the work immediately and investigate your claim.



Acta Neuropathologica Communications

Brain matters: Unveiling the Distinct Contributions of Region, Age, and Sex to Glia diversity and CNS Function --Manuscript Draft--

Manuscript Number:											
Full Title:	Brain matters: Unveiling the Distinct Contributions of Region, Age, and Sex to Glia diversity and CNS Function										
Article Type:	Research										
Funding Information:	<table border="1"> <tr> <td>Chan Zuckerberg Initiative (CZIF2019-002427)</td> <td>Dr Anna Williams</td> </tr> <tr> <td>Chan Zuckerberg Initiative (DAF2021-239069)</td> <td>Dr Anna Williams</td> </tr> <tr> <td>Medical Research Council (CZF2019-002427)</td> <td>Dr Anna Williams</td> </tr> <tr> <td>Multiple Sclerosis Society (MS Society UK Edinburgh Research Centre award reference 133)</td> <td>Dr Anna Williams</td> </tr> <tr> <td>British Heart Foundation (British Heart Foundation pilot grant RE/18/5/34216)</td> <td>Dr Anna Williams</td> </tr> </table>	Chan Zuckerberg Initiative (CZIF2019-002427)	Dr Anna Williams	Chan Zuckerberg Initiative (DAF2021-239069)	Dr Anna Williams	Medical Research Council (CZF2019-002427)	Dr Anna Williams	Multiple Sclerosis Society (MS Society UK Edinburgh Research Centre award reference 133)	Dr Anna Williams	British Heart Foundation (British Heart Foundation pilot grant RE/18/5/34216)	Dr Anna Williams
Chan Zuckerberg Initiative (CZIF2019-002427)	Dr Anna Williams										
Chan Zuckerberg Initiative (DAF2021-239069)	Dr Anna Williams										
Medical Research Council (CZF2019-002427)	Dr Anna Williams										
Multiple Sclerosis Society (MS Society UK Edinburgh Research Centre award reference 133)	Dr Anna Williams										
British Heart Foundation (British Heart Foundation pilot grant RE/18/5/34216)	Dr Anna Williams										
Abstract:	<p>The myelinated white matter tracts of the central nervous system (CNS) are essential for fast transmission of electrical impulses and are often differentially affected in human neurodegenerative diseases across CNS region, age and sex. We hypothesize that this selective vulnerability is underpinned by physiological variation in white matter glia. Using single nucleus RNA sequencing of human post-mortem white matter samples from the brain, cerebellum and spinal cord and subsequent tissue-based validation we found substantial glial heterogeneity with tissue region: we identified region-specific oligodendrocyte precursor cells (OPCs) that retain developmental origin markers into adulthood, distinguishing them from mouse OPCs. Region-specific OPCs give rise to similar oligodendrocyte populations, however spinal cord oligodendrocytes exhibit markers such as SKAP2 which are associated with increased myelin production and we found a spinal cord selective population particularly equipped for producing long and thick myelin sheaths based on the expression of genes/proteins such as HCN2. Spinal cord microglia exhibit a more activated phenotype compared to brain microglia, suggesting that the spinal cord is a more pro-inflammatory environment, a difference that intensifies with age. Astrocyte gene expression correlates strongly with CNS region, however, astrocytes do not show a more activated state with region or age. Across all glia, sex differences are subtle but the consistent increased expression of protein-folding genes in male donors hints at pathways that may contribute to sex differences in disease susceptibility. These findings are essential to consider for understanding selective CNS pathologies and developing tailored therapeutic strategies.</p>										
Corresponding Author:	Anna Williams University of Edinburgh UNITED KINGDOM										
Corresponding Author E-Mail:	anna.williams@ed.ac.uk										
Corresponding Author Secondary Information:											
Corresponding Author's Institution:	University of Edinburgh										
Corresponding Author's Secondary Institution:											
First Author:	Luise Seeker										
First Author Secondary Information:											
Order of Authors:	Luise Seeker										

	Nadine Bestard-Cuche
	Sarah Jaekel
	Nina-Lydia Kazakou
	Sunniva Bostrand
	Laura Wagstaff
	Justyna Cholewa-Waclaw
	Alastair M Kilpatrick
	David Van Bruggen
	Mukund Kabbe
	Fabio Baldivia Pohl
	Zahra Moslehi
	Neil Henderson
	Catalina Vallejos
	Gioele La Manno
	Goncalo Castelo-Branco
	Anna Williams
Order of Authors Secondary Information:	
Suggested Reviewers:	<p>marie Bechler SUNY Upstate Medical University Hospital BechlerM@upstate.edu expertise: Spinal cord vs. brain oligodendrocytes in mouse</p> <p>Tanja Kuhlmann Universitätsklinikum Münster: Universitätsklinikum Munster tanja.kuhlmann@ukmuenster.de expertise – human neuropathology, oligodendrocytes, including transcriptomics.</p>
Additional Information:	
Question	Response
Is this study a clinical trial?<hr><i>A clinical trial is defined by the World Health Organisation as 'any research study that prospectively assigns human participants or groups of humans to one or more health-related interventions to evaluate the effects on health outcomes'.</i>	No

[Click here to view linked References](#)

1
2
3
4
5
6
7
8
9
10
11
12
13
14
15
16
17
18
19
20
21
22
23
24
25
26
27
28
29
30
31
32
33
34
35
36
37
38
39
40
41
42
43
44
45
46
47
48
49
50
51
52
53
54
55
56
57
58
59
60
61
62
63
64
65

Brain matters: Unveiling the Distinct Contributions of Region, Age, and Sex to Glia diversity and CNS Function

Short title: Human glia diversity with CNS region, age and sex

Authors

Luise A. Seeker¹, Nadine Bestard-Cuche¹, Sarah Jaekel^{1,2,3}, Nina-Lydia Kazakou¹, Sunniva M. K. Bøstrand¹, Laura J. Wagstaff¹, Justyna Cholewa-Waclaw¹, Alastair M. Kilpatrick¹, David Van Bruggen⁴, Mukund Kabbe⁴, Fabio Baldivia Pohl⁴, Zahra Moslehi⁵, Neil C. Henderson^{6,7}, Catalina A. Vallejos^{7,8}, Gioele La Manno⁵, Goncalo Castelo-Branco^{4,9}, Anna Williams^{1*}

Affiliations

¹ Centre for Regenerative Medicine, Institute for Regeneration and Repair, Edinburgh Bioquarter, University of Edinburgh, 5 Little France Drive, Edinburgh EH16 4UU.

² Institute for Stroke and Dementia Research, Klinikum der Universität München, Ludwig-Maximilians-Universität, Munich, Germany.

³ Munich Cluster for Systems Neurology (SyNergy), Munich, Germany.

⁴ Laboratory of Molecular Neurobiology, Department of Medical Biochemistry and Biophysics, Karolinska Institutet, 171 77 Stockholm, Sweden.

⁵ Laboratory of Neurodevelopmental Systems Biology, Brain Mind Institute, School of Life Sciences, École Polytechnique Fédérale de Lausanne (EPFL), 1015 Lausanne, Switzerland.

⁶ Centre for Inflammation Research, The Queen's Medical Research Institute, Edinburgh BioQuarter, University of Edinburgh, Edinburgh, UK.

⁷ MRC Human Genetics Unit, Institute of Genetics and Cancer, University of Edinburgh, Western General Hospital, Edinburgh, EH4 2XU, UK.

⁸ The Alan Turing Institute, 96 Euston Road, London, NW1 2DB, UK.

⁹ Ming Wai Lau Centre for Reparative Medicine, Stockholm node, Karolinska Institutet, 171 77 Stockholm, Sweden.

* anna.williams@ed.ac.uk, +44 (0) 131 651 9500

1
35
36
37
38
39
40
41
42
43
44
45
46
47
48
49
50
51
52
53
54
55
56
57
58
59
60
61
62
63
64
65

Abstract

The myelinated white matter tracts of the central nervous system (CNS) are essential for fast transmission of electrical impulses and are often differentially affected in human neurodegenerative diseases across CNS region, age and sex. We hypothesize that this selective vulnerability is underpinned by physiological variation in white matter glia. Using single nucleus RNA sequencing of human post-mortem white matter samples from the brain, cerebellum and spinal cord and subsequent tissue-based validation we found substantial glial heterogeneity with tissue region: we identified region-specific oligodendrocyte precursor cells (OPCs) that retain developmental origin markers into adulthood, distinguishing them from mouse OPCs. Region-specific OPCs give rise to similar oligodendrocyte populations, however spinal cord oligodendrocytes exhibit markers such as *SKAP2* which are associated with increased myelin production and we found a spinal cord selective population particularly equipped for producing long and thick myelin sheaths based on the expression of genes/proteins such as *HCN2*. Spinal cord microglia exhibit a more activated phenotype compared to brain microglia, suggesting that the spinal cord is a more pro-inflammatory environment, a difference that intensifies with age. Astrocyte gene expression correlates strongly with CNS region, however, astrocytes do not show a more activated state with region or age. Across all glia, sex differences are subtle but the consistent increased expression of protein-folding genes in male donors hints at pathways that may contribute to sex differences in disease susceptibility. These findings are essential to consider for understanding selective CNS pathologies and developing tailored therapeutic strategies.

Key Words

Human glia, Developmental origin, spinal cord, ageing, myelin, OPCs

Introduction

The white matter of the human central nervous system (CNS) contains many non-neuronal cells called glia which include oligodendroglia (oligodendrocytes and their oligodendrocyte precursor cells - OPCs), astrocytes and microglia. Glia are of crucial importance for the physiology of the CNS and are also key players in the pathologies of demyelinating, neurodegenerative and neuropsychiatric disorders (reviewed in [5]). Some of these diseases have pathological biases to CNS region, are more common in one sex and increase in incidence with age. Animal model data suggest that functional differences in glia may

1
69 2
3
70 4
5
71 6
7
72 8
9
73 10
11
74 12
13
75 14
15
76 16
17
77 18
19
78 20
21
79 22
23
80 24
25
81 26
27
82 28
29
83 30
31
84 32
33
85 34
35
86 36
37
87 38
39
88 40
41
89 42
43
90 44
45
91 46
47
92 48
49
93 50
51
94 52
53
95 54
55
96 56
57
97 58
59
100 60
61
101 62
63
102 64
65

causally underpin this pathological variation, with particular importance attributed to oligodendroglial involvement in demyelinating diseases, which we focus on here. In mouse, there is morphological and functional diversity in oligodendroglia in different white matter regions [23, 44] linked to differences in tissue environment [79], axon caliber [3], extracellular matrix stiffness [66], and intrinsic factors related to their developmental origin [3, 14]. Regardless of CNS region, there is a functional shift in glia with age; aged rodent OPCs proliferate and differentiate slower [51, 72], aged rodent oligodendrocytes remyelinate white matter demyelinated lesions less efficiently [69], aged rhesus monkeys and humans show more pro-inflammatory activated phagocytic microglia [68, 71] and increasing age is the main risk factor for more severe disability in the demyelinating disease multiple sclerosis [64]. Sex dimorphism in neurodegenerative disease susceptibility suggests that gonosomal genes or hormones may affect CNS function [12, 34]: cultured female neonatal rat OPCs show more proliferation, migration and less differentiation than males [83], and there are more microglia with homeostatic markers in adult female mice [36].

However, despite these data from animal models and their presumed link to disease, white matter glial regional, age and sex diversity is not well understood in humans. Single-nucleus RNA sequencing (snRNAseq) data from post-mortem human samples have been very successfully used to study cellular changes in development [16, 19, 24, 31, 89] or disease [32, 46, 50, 65, 78]. ~~and We~~ we used this technology to address our hypothesis that in the normal human CNS, there is regional, age and sex-related glial diversity is an important mediator of region, age and sex differences in the normal human CNS and that if we better understand these differences, we will better understand region, age and sex susceptibilities to CNS diseases.

Here, we characterized human white matter nuclei of healthy post-mortem samples from three different CNS regions: Primary motor cortex (Brodmann area 4; BA4), cerebellum (CB) and cervical spinal cord (CSC), from donors of two different adult age groups (30 – 45y and 60 – 75y) and both sexes. We found significant regional heterogeneity with region-specific populations of OPCs and astrocytes, and spinal cord-enriched populations of oligodendrocytes and microglia. Transcriptional variation with age and sex was also identified, with most marked effects in OPCs, microglia and astrocytes. We discuss potential causes and the expected impact of these differences on health and targeting therapies in disease and provide an open-source atlas for researchers as a comparator for pathologies.

Materials and Methods

Experimental design

For the snRNAseq experiment ([Fig. 1A](#)), 20 donors were selected to equally represent two age groups ([10](#) "young adults": 30-45 years, [10](#) "old adults": 60-75 years) and two sex groups ([5](#) male, [5](#) female [within each age group](#)). Each donor donated fresh frozen white matter from the following three tissue regions: primary motor cortex (Brodmann area 4, BA4), arbor vitae cerebelli (CB) and fasciculi cuneatus and gracilis from and cervical spinal cord (CSC) [which resulted in a total of 60 samples](#) (Table S1). The samples were randomly allocated to 10X chromium chips and then again randomly pooled for cDNA sequencing to reduce batch effects. Validation of bioinformatics results was performed in formalin-fixed paraffin-embedded tissue of the same tissue regions donated by different donors of the same age and sex groups (Table S2).

Human donor tissue

Adult post-mortem unfixed fresh-frozen tissue and formalin-fixed paraffin-embedded tissue were obtained from the MRC Sudden Death Brain Bank in Edinburgh with full ethical approval (16/ES/0084). All samples are verified to have no detectable neuropathology by a consultant neuropathologist (Professor Colin Smith) [using published staging/ grading systems, including Braak, NIAA, Thal, Newcastle LBD criteria, LATE pTDP stages, and VCING. Each case has multiple samples assessed, from both hemispheres and multiple cortical, subcortical, cerebellar, brainstem regions plus the cervical spinal cord.](#) Formalin-fixed paraffin-embedded samples were sectioned at 4 μ m by the Shared University Research Facilities (SuRF, <https://surf.ed.ac.uk/about-us/>) (BA4) or by the MRC Sudden Death Brain Bank (CB and CSC).

~~Luxol-Fast-Blue (LFB)~~ staining [with Cresyl Violet counter stain \(LFB-CV\)](#)

Fresh frozen tissue was placed in Luxol Fast Blue (LFB) solution (0.1% LFB in 95% ethanol, 0.05% Acetic acid) and incubated at 60 °C overnight. Slides were rinsed with tap water and developed using a saturated Lithium Carbonate solution. Slides were washed and placed in Cresyl Fast Violet (0.1% in 0.07% acetic acid in water) and incubated for 10 minutes at 60 °C. After slides had cooled to room temperature, they were developed using 250 μ l Glacial acetic acid in 100% Ethanol. Slides were rinsed, dehydrated in increasing ethanol concentrations (70% - 100%) followed by incubation in xylene and then they were

1
2
3
4
5
6
7
8
9
10
11
12
13
14
15
16
17
18
19
20
21
22
23
24
25
26
27
28
29
30
31
32
33
34
35
36
37
38
39
40
41
42
43
44
45
46
47
48
49
50
51
52
53
54
55
56
57
58
59
60
61
62
63
64
65

mounted using Pertex mounting medium. LFB-CV stainings were used to identify white matter (WM) for snRNAseq.

Bulk RNA extraction and RNA integrity (RIN) - value measurement

RNA was extracted from each fresh-frozen sample by homogenizing multiple sections in 500 µl Trizol (Thermo Fisher Scientific, 15596-026). After 5 min incubation at room temperature 100 µl Chloroform (Vickers Labs LTDICKERS LABS LTD, che1570) were added, and samples were mixed by vigorous shaking. Samples were incubated at room temperature for 3 min and then centrifuged at 12,000 g for 15 min. The aqueous phase was mixed with the same volume of 70% ethanol and transferred to silica columns of the QIAGEN—Qiagen RNeasy Mini kit (QiagenIAGEN, 74104). The manufacturer's instructions were followed to isolate RNA. For RIN-value measurement 1 µl of RNA was mixed with 5 µl RNA screenTape buffer (Agilent, 5190-6506), incubated at 72 °C for 3 minutes and then loaded into a Tapestation 2200.

Nuclei isolation

For each sample, 20 tissue cryosections at 20 µm thickness were macro-dissected ~~while enriching for~~ selecting WM using ~~Luxol Fast Blue~~LFB-CV stainings of adjacent sections (Fig. 1A). For ~~one-one~~ out of ~~60-sixty~~ samples it was impossible to dissect white matter without capturing grey matter (cerebellum sample) and therefore it was removed from the experiment. The nuclei PURE isolation kit (Sigma, NUC201-1KT) was used to isolate nuclei: Samples were lysed in 200 µl lysis buffer (PURE lysis buffer containing 1 % 0.1 M DTT, 0.1 % Triton, 2 % SUPERase RNase inhibitor (Thermo Fischer Scientific AM2694)) on ice and homogenized using syringes and needles of descending needle size (first 27 Gauge then 29 Gauge). 360 µl sucrose cushion (PURE 5M sucrose solution containing 11% PURE Sucrose cushion buffer, 0.11% DTT and 0.02 % RNase inhibitors) was added to each sample and after mixing, samples were filtered through a 30 µm Sysmex/ Partec CellTrics cell strainer (Wolf Laboratories, 04-004-2326). The filtrate was carefully pipetted on top of 200 µl sucrose buffer. Samples were centrifuged for 45 min at 16,100 g and 4 °C. The supernatant was discarded, and the pellet was washed twice in ice-cold PURE storage buffer containing 0.2 U/ µl RNase inhibitors. After the second centrifugation at 1000 g for 5 min, the pellet was dissolved in 100 µl PURE storage buffer. Nuclei were stained with

1
168²
3 Trypan blue (Bio-Rad Laboratories, 1450013) and their concentration was measured using
169⁴
5 an automated cell counter (Biorad TC20) and standardized to 1,000,000 nuclei per ml.
170⁶

171⁷ 8 **10X loading and library preparation**

172⁹
173¹⁰ Samples were randomly allocated to 10X Genomics Chromium single cell 3' chips ([Fig. 1A](#)).
174¹¹
175¹² The 10X Genomics v3 beads, Gem kits and library kits were used according to the
176¹³
177¹⁴ manufacturer's instructions. Library quality was assessed using a Bioanalyzer (Labchip GX
178¹⁵
179¹⁶ Touch 24 nucleic acid analyzer, PerkinElmer ~~LAS (UK)Ltd., Chalfont Road, Seer Green,
180¹⁷
181¹⁸ Beaconsfield, Bucks HP9 2FX England, Chip and Kit used:~~ DNA 1K/12K/Hi Sensitivity
182¹⁹
183²⁰ Assay LabChip with kit DNA high sensitivity reagent kit CLS760672). If libraries failed to
184²¹
185²² have a pronounced peak at the expected fragment size of 450 nm – 500 nm, they were
186²³
187²⁴ removed from downstream analysis (1 out of 59).
188²⁵

189²⁶ 27 **Next Generation Sequencing**

190²⁸
191²⁹ Nine to ten cDNA libraries were randomly allocated to seven sequencing pools and added
192³⁰
193³¹ at an equimolar concentration of 5 nmol ([Fig. 1A](#)). Sequencing was performed by Edinburgh
194³²
195³³ Genomics using a Novaseq 6000 System and a S2 flow cell. Each pool was sequenced on
196³⁴
197³⁵ two different lanes to reduce batch effects. We aimed for a sequencing depth of 70,000 reads
198³⁶
199³⁷ per nucleus.
200³⁸

201³⁹ 40 **Genome alignment and raw matrix generation**

202⁴¹
203⁴² The transcriptome was demultiplexed and aligned with the human reference genome
204⁴³
205⁴⁴ GRCh38 using 10X Genomics Cellranger 3.0.2. Raw data included 33939 genes and 95992
206⁴⁵
207⁴⁶ nuclei.

208⁴⁷
209⁴⁸ To retrieve feature-count matrices for exonic and intronic reads separately Velocityto
210⁴⁹
211⁵⁰ (0.17.16) was used with a repeat mask for the human reference genome GRCh38 which was
212⁵¹
213⁵² downloaded from <https://genome.ucsc.edu/index.html>.

214⁵³ 215⁵⁴ **Data Quality control**

216⁵⁵
217⁵⁶ [After empty droplets were removed, doublets were detected within each sample using](#)
218⁵⁷
219⁵⁸ [scDblFinder v 1.6.0. After further quality control \(see below\), 2.2% of nuclei were potential](#)
220⁵⁹
221⁶⁰ [doublets \(Figure SX 1\) which were retained in the dataset as they marked populations that](#)
222⁶¹
223⁶² [could be transitional states. We provide doublet information in our metadata and shiny app](#)
224⁶³
225⁶⁴ [and discuss their potential effect on analysis results when relevant.](#) Genes with less than 200
226⁶⁵

1
202 2
3
203 4
5
204 6
7
205 8
9
206 10
11
207 12
13
208 14
15
209 16
17
210 18
19
211 20
21
212 22

copies across both the spliced and unspliced matrices were removed from the analysis. The nucleus quality control was conducted on the spliced and unspliced matrices separately using UMI counts, gene counts and percentage of mitochondrial RNA (only present on spliced matrix). Thresholds for excluding nuclei were first selected as 3 median absolute deviations using the R library Scater [47]. When Scater-set thresholds were too permissive and no nuclei were filtered, manually set thresholds were used. The combined (spliced + unspliced) filtered dataset included nuclei with a minimum of 231 detected genes (mean 1853) and a mean mitochondrial gene percentage of 2.59%. Library sizes did not correlate with post-mortem intervals or RNA integrity values (Fig. S1a-f), nor did PMI and RIN correlate (Fig. S1g).

213 22 23 **Normalization**

214 24
25
215 26
27
216 28
29
217 30
31
218 32

Scran [41] was used to normalize the combined matrix of spliced and unspliced reads for each tissue separately (because they may differ biologically in their amount of gene expression) and to transform data onto a logarithmic scale. Tissue-specific datasets were subsequently merged.

219 33 34 **Dimensional reduction and clustering**

220 35
36
221 37
38
222 39
40
223 41
42
224 43
44
225 45
46
226 47
48
227 49
50
228 51
52
229 53
54
230 55
56
231 57
58
232 59
60
233 61
62
234 63

Using Seurat [8], the 2000 most variable genes were selected, all genes were scaled and a principal component analysis was performed. The first 25 principal components were used for constructing a Shared Nearest Neighbor (SNN) graph ($k = 20$) and as input for a Uniform Manifold Approximation and Projection (UMAP). This process was repeated after sample and cluster quality control steps. Louvain clustering was performed at a resolution of 0.8 (0.5 and 1.3 were also tested). The clustering behavior was not influenced by the allocation of a sample to an individual chromium chip or sequencing batch (Fig. S1 h-i). A combination of the following statistics was used to filter for good quality samples: mean UMI count > 490, proportion of spliced vs. unspliced genes < 75%. This resulted in ten samples being removed from downstream analyses (4 BA4, 5 CB, 1 CSC; 6 young, 4 old; 5 male, 5 female). Human donors are known to be genetically diverse and therefore clustering may depend on the individual. Therefore, we considered following criteria to manually curate clusters: Clusters had to contain nuclei of at least 8 donors, while donors were only considered if they contributed at least 2% to the total cluster size.

235 64 65 **Cell type annotation and analysis of subsetted cell lineage datasets**

1
2
3
4
5
6
7
8
9
10
11
12
13
14
15
16
17
18
19
20
21
22
23
24
25
26
27
28
29
30
31
32
33
34
35
36
37
38
39
40
41
42
43
44
45
46
47
48
49
50
51
52
53
54
55
56
57
58
59
60
61
62
63
64
65

Canonical marker genes were used to annotate cell types as described in the main text and to select oligodendroglia, astrocytes, microglia and macrophages for separate downstream analysis. The 2000 most variable genes were selected, all genes were scaled and a PCA was performed. The first 10 principal components were used for constructing a shared nearest neighbor graph with 20 k- nearest neighbors and as input for a UMAP. Our clustering strategy involved repeated clustering at different resolutions from obvious under- to clear over-clustering and was considered in combination with differential gene expression analyses (see below) and measures of cluster stability at all those resolutions. If functional differences were recognized based on the expression of marker genes, they were considered in the annotation (e.g. excitatory vs. inhibitory neurons). Endothelial cells and pericytes can share the expression of genes that mark blood vessel types. We, therefore, used the scSorter [28] with weighted markers for blood vessel type annotation as we described in Quick et al. [56].

Differential gene expression analysis

Differential gene expression analyses for the identification of cluster marker genes and genes that are enriched in tissue, age and sex groups were performed using MAST [48] within Seurat (using test.use = "MAST") filtering genes for those that had a minimum positive log₂-fold change of 0.25 and were expressed by at least 25 % of cells within the cluster/group of interest. All genes that were expressed in less than 60% of nuclei outside the cluster/group of interest were considered for the visual screening of marker genes and as gene ontology input if they had a minimum log₂-Fold change of 0.7 and 0.4 respectively and a significant adjusted p-value (<0.05).

Compositional analysis

We used the R library miloR [15] for differential abundance testing. For buildGraph() 30 nearest neighbors and 30 dimensions were considered and for makeNhoods() the proportion of graph vertices sampled was set to 0.2. When testing for a tissue effect, a pairwise comparison (CSC vs. BA4, CB vs BA4 and CB vs. CSC) was employed with the exemplary additional argument model.contrasts = c("TissueCB - TissueBA4") in the testNhoods() function. Currently, no other fixed effects can be included in the same model when a contrast is investigated. Sex and age had a much smaller effect when tested alone and will not considerably affect tissue variance whereas it is possible that tissue origin may increase or mask age and sex effects. Therefore, we accounted for tissue and the other factor (sex in the

1
270 2 case of age and age in the case of sex) in the same model when testing those factors (Figure
3 SX 2).
271 4
5

272 6 7 **Label transfer and integration with other datasets**

273 8
9 Seurat's CCA label transfer and integration was applied to our oligodendroglia dataset and
274 10 a published human [32] and three mouse datasets [23, 43, 62]. Mouse gene symbols were
275 11 translated to human gene symbols using the R library biomaRt [17]. For the label transfer
276 12 and the integration, the first 30 and 20 dimensions respectively were used to specify the
277 13 neighbor search space. The integrated data was re-scaled and dimensionally reduced using
278 14 the first 20 principal components as input for a UMAP.
279 15
280 16
281 17
282 18
283 19
284 20
285 21
286 22
287 23
288 24
289 25
290 26
291 27
292 28
293 29
294 30
295 31
296 32
297 33
298 34
299 35
300 36
301 37
302 38
303 39
304 40
305 41
306 42
307 43
308 44
309 45
310 46
311 47
312 48
313 49
314 50
315 51
316 52
317 53
318 54
319 55
320 56
321 57
322 58
323 59
324 60
325 61
326 62
327 63
328 64
329 65

We created a correlation matrix between predicted and current labels by counting each occasion of a co-labelling and normalizing counts for cluster size and largest cluster to bring the results on a scale from zero to one. The R library corrplot [81] was used with the argument `is.corr = FALSE` to visualize cluster label correlations.

327 64 328 65 **Trajectory analysis**

Dynverse [59] was used for the selection of suitable trajectory inference methods for the complete oligodendroglia dataset and the oligodendroglia dataset divided by tissue. Slingshot [74], PAGA and PAGA tree, Angle and Scorpius were the top ranking methods for our dataset based on Dynverse and they were all tested within the Dynverse framework, setting PDGFRA expressing OPC nuclei as start point for the trajectories. Additionally, slingshot [74] and Monocle [77] were run outside of Dynverse [59] first separately for each tissue (BA4, CB, CSC), then for the tissues combined. In Monocle, the starting point was first not determined, but because we know that in vitro OPCs can generate oligodendrocytes, we set the start point to the OPC clusters. Lastly, we used scVelo [4] within R using velociraptor [58] on spliced and unspliced counts that were subsetted for nuclei that were retained in the final dataset. We superimposed UMAP projections onto the new dataset that included RNA velocity [42] calculations.

329 64 330 65 **Gene Ontology**

Cluster profiler [87] was used on all significantly differentially expressed genes (adjusted p-value < 0.05) with a log2-Fold change of at least 0.4 (which corresponds to at least ~30% difference) to identify significantly enriched biological processes in clusters, and tissue, sex and age groups. The function `compareCluster()` was used to compare clusters within each

1
2
304 3 cell lineage using the argument “enrichGO”, the human genome-wide annotation [10] and
4
5 a named list of cluster labels and their significantly differentially expressed genes as
6
7 ENTREZID. For more in-depth biological process results, enrichGO() was run for each
8
9 cluster separately and the 20 most enriched processes were plotted.
10

11 **Environment and code availability**

12
13 Earlier steps of the analysis (genome alignment) and computational intensive analyses (such
14
15 as Monocle [77] on oligodendroglia of all tissues) were performed on the University of
16
17 Edinburgh’s Linux compute cluster. For later steps R (version 4.1.1.) and RStudio (version
18
19 1.3.1056) were used on a MacBook Pro (64-bit) with macOS Big Sur 11.6.1. More
20
21 information on R library versions used for individual analyses can be found in the GitHub
22
23 repository (<https://gitfront.io/r/user-1167685/QNF6fMTSbeE6/Luise-Seeker-Human-WM-Glia/>).
24
25

26 **Immunofluorescence**

27
28
29 Human formalin-fixed paraffin-embedded tissue sections were de-waxed and re-hydrated
30
31 in 2 x 10 min in Xylene, 2 x 2 min in 100 % ethanol, then 2 min in each 95%, 80% and 70%
32
33 of ethanol. Antigen retrieval was performed by microwaving the samples for 15 minutes in
34
35 0.01 M citrate buffer (pH = 6, Vector Laboratories, H-3300) in Millipore water. Sudan Black
36
37 Autofluorescence Eliminator Reagent (Merck Millipore, 2160) was added to each slide for
38
39 30 s – 1 min which were then washed twice for 5 min in TBS with 0.001% Triton. Slides
40
41 were incubated in 3 % H₂O₂ for 10 min and washed. Serum block (TBS + 0.5% Triton +
42
43 10% horse serum) was added for 1 h at room temperature. Antibodies were diluted in serum
44
45 block and added to slides prior to an overnight incubation at 4°C. On the next day, slides
46
47 were washed in TBS + 0.001% Triton (2 x 5 min) and incubated with an appropriate
48
49 ImmPress HRP secondary antibody (see below) for 1 h. After washing the slides, OPAL
50
51 tyramide dye was added at a dilution of 1:500 for 10 minutes. After washing them, the slides
52
53 were boiled in 0.01 M citrate buffer (pH = 6) for either 2.5 minutes and then left in the hot
54
55 buffer for 20 minutes or boiled for 15 minutes if same-species primary antibodies were used
56
57 in a following step. Slides were washed (2 x 5 min) and incubated overnight at 4°C with the
58
59 second primary antibody diluted in serum block. The procedure of the second day was
60
61 repeated until the required number of antibody reactions was completed. On the last day,
62
63 samples were counterstained with Hoechst (10 min) after the tyramide reaction, washed (2
64
65 x 5 min) and mounted.

1
2
338 2 We used following antibodies at indicated dilutions SPARC (Abcam, ab225716,
3
339 4 RRID:AB_2924283, 1:100), OLIG2 (R&D Systems, AF2418, RRID:AB_2157554, 1:100),
4
5
340 6 RBFOX1 (Abcam, ab243727, RRID:AB_2924285, 1:100), FMN1 (Abcam, ab244482,
6
7
341 8 RRID:AB_2924284, 1:100), OPALIN (Abcam, ab121425, RRID:AB_11127935, 1:100),
8
9
342 10 HCN2 (Alomone Labs, APC-030, RRID:AB_2313726, 1:1000), GPNMB (Abcam,
10
11
343 11 ab227695, RRID:AB_2924286, 1:100), IBA1(ab178846, RRID:AB_2636859, 1:50).
11
12
344 13 Following secondary antibodies were used: ImmPress HRP secondary antibodies: horse
12
13
345 14 anti-rabbit (Vector Laboratories, MP-7401-15), horse anti-goat (Vector Laboratories, MP-
13
14
346 15 7405). Following OPAL Tyramide dyes were used: OPAL 570 (Akoya Biosciences, SKU
14
15
347 16 FP1488001KT), OPAL 650 (Akoya Biosciences, FP1496001KT) and OPAL 480 (SKU
15
16
348 17 FP1500001KT).
16
17
349 18
17
18
350 19
18
19
351 20
19
20
352 21
20
21
353 22
21
22
354 23
22
23
355 24
23
24
356 25
24
25
357 26
25
26
358 27
26
27
359 28
27
28
360 29
28
29
361 30
29
30
362 31
30
31
363 32
31
32
364 33
32
33
365 34
33
34
366 35
34
35
367 36
35
36
368 37
36
37
369 38
37
38
370 39
38
39
371 40
39
40
372 41
40
41
373 42
41
42
374 43
42
43
375 44
43
44
376 45
44
45
377 46
45
46
378 47
46
47
379 48
47
48
380 49
48
49
381 50
49
50
382 51
50
51
383 52
51
52
384 53
52
53
385 54
53
54
386 55
54
55
387 56
55
56
388 57
56
57
389 58
57
58
390 59
58
59
391 60
59
60
392 61
60
61
393 62
61
62
394 63
62
63
395 64
63
64
396 65
64
65

BaseScope duplex

We used a BaseScope duplex detection kit (ACD Bioscience, 323800) on formalin-fixed paraffin-embedded tissue according to the manufacturer's instruction with following optimized times: Target retrieval for 15 min. protease digestion for 20 min, AMP7 and AMP11 incubation for 1h each. We used following probes: PDGFRA (BA-Hs-PDGFRA-3EJ-C1, H1037431-C1), NELL1 (BA-HsNELL1-3zz-st-C2, 902681-C2) and PAX3 (BA-Hs-PAX3-3zz-st-C2, 902701-C2).

RNAScope

We used the RNAScope Multiplex Fluorescent Reagent kit v2 (323100) according to the manufacturer's instructions with 15 min target retrieval and 25 min protease treatment. We used following probes: Hs-EBF1-C2 (583141-C2) and PDGFRA (604481).

Imaging and analysis of imaging data

A Vetra Polaris slide scanner (Perkin Elmer) was used to image IF and colorimetric BaseScope Duplex stainings at 20x objective. RNAScope slides were imaged using an Opera Phenix Plus High-Content Screening System (Perkin Elmer) with an air objective at 20X. The exact number of samples quantified for each stain is shown in Table S2. For human IF and RNAScope stains, four fields of view within WM that measured 500 x 500 µm were used for each sample to quantify stainings in QuPath [2] by setting channel-specific thresholds for a positive detection for each field of view (IF) or constant across all fields of view (RNAScope) or by counting manually (FMN1 IF). RNAScope quantification

1
2
372 2 was performed automatically by using Qupath’s algorithm for cell detection and subcellular
3
373 4 detection. BaseScope duplex stainings were quantified by exporting each field of view as
4
5
374 6 separate image, randomize the file names for blinding and then manually counting single
6
7
375 8 and double positive cells where at least three PDGFRA mRNA molecules had to be detected
7
8
376 9 to mark an OPC. Most quantification results are visualised as box and whisker plots with
9
10
377 11 overlaid individual data points using the standard geom_boxplot() settings where the
11
12
378 13 horizontal line visualizes the median, the box the hinges the 25th and 75th percentile and the
13
14
379 15 whiskers the full data range within 1.5 inter-quartile ranges from the hinges. Data points
15
16
380 17 outside the whiskers may be interpreted as outliers. Data analysis methods were chosen to
17
18
381 19 best reflect the data structure of the individual datasets and included linear models and
19
20
382 21 Poisson models (**Table 1**).

22 23 383 24 **Data and materials availability**

25
385 26 All data necessary to reproduce the results of the present paper are available at
26
27
386 28 (link_inserted_upon_acceptance). R code (that also specifies R library versions) is available
28
29
387 30 at <https://gitfront.io/r/user-1167685/QNF6fMTSbeE6/Luise-Seeker-Human-WM-Glia/>.
30
31
388 32 We used ShinyCell [53] to generate interactive shiny apps that are accessible at
32
33
389 34 https://seeker-science.shinyapps.io/shiny_app_multi/.

36 37 **Results**

38 39 **Description and annotation of the complete dataset**

40
393 41 We used white matter from three anatomical CNS sites selected for their pronounced
41
42
394 43 structural differences: BA4, CB and CSC. We analyzed these samples over a cohort of 20
43
44
395 45 British Caucasian donors (60 samples in total) (Fig. 1 a, Table S1). Donors equally
45
46
396 47 represented both sexes and two different age groups “young adults” (30-45 y, 5 males and
47
48
397 48 5 females) and “old adults” (60-75 y, 5 males and 5 females). After strict sample, cluster
48
49
398 49 and nucleus quality control (see methods, Fig. S1), we retained 48 samples and 48,104
49
50
399 51 nuclei (mean number of genes per nucleus: 1853, mean number of UMIs per nucleus: 5450,
51
52
400 53 mean mitochondrial gene percentage 2.59%). We compared our data quality to three
53
54
401 55 previously published snRNAseq datasets of the human CNS [32, 46, 50] and found that our
55
56
402 57 filtering was more stringent which resulted in significantly better nucleus quality, based on
57
58
403 59 higher gene and unique molecular identifier (UMI) counts and a lower mitochondrial gene
59
60
404 61 percentage at the cost of slightly fewer nuclei per sample (Fig. S1 j-m). Post-mortem interval
61
62
405 62 and RNA integrity values do not predict nuclei quality in our data (Fig. S1 a-f). A first-level
62
63
406 63

1
2
3
406 4
5
6
7
8
9
10
11
12
13
14
15
16
17
18
19
20
21
22
23
24
25
26
27
28
29
30
31
32
33
34
35
36
37
38
39
40
41
42
43
44
45
46
47
48
49
50
51
52
53
54
55
56
57
58
59
60
61
62
63
64
65

cluster analysis and marker inspection revealed all expected major cell types: excitatory neurons (as marked by *SNAP25*, *SLC17A7*), inhibitory neurons (*SNAP25*, *GAD1*), REELIN-positive neurons (*SNAP25*, *RELN*), astrocytes (*GJA1*, *GFAP*), microglia and macrophages (*CD74*, *P2RY12*), endothelial cells and pericytes (*CLDN5*, *NOTCH3*), oligodendrocytes (*PLP1*, *CNP*), their precursor cells (*PDGFRA*, *PTPRZ1*) and immune cells (*HLA-A*, *PTPRC*) (Fig. 1 b-c). We subsetted the data for all main cell lineages and re-clustered each resulting dataset allowing finer distinction of cellular populations, identifying 11 oligodendroglia, 11 astrocyte, 6 microglia and macrophage, 11 vascular and 18 neuronal clusters that expressed distinct cluster marker genes (Fig. 1 b, Data S1).

Oligodendroglia are transcriptionally heterogeneous

In our analysis, we focused on oligodendroglia, the most abundant cell lineage in the human white matter. The cluster analysis revealed six oligodendrocyte clusters (positive for myelin genes such as *PLP1*, *MBP*, *MAG*), two OPC clusters (positive for *PDGFRA*, *CSPG4* and *BCAN*) and three committed oligodendrocyte precursor (COP) cell clusters (positive for *GPR17*, *GPC5* or *GAP43*), confirming that oligodendroglia are heterogeneous in the healthy adult human CNS (Fig. 2). We validated cluster markers (Fig. 2 a-b) using immunofluorescence stainings for oligodendrocytes (Fig. 2 c) and in situ hybridization (Fig. 2 d) for OPCs on formalin-fixed paraffin-embedded sections of different donors (Table S2) and our quantification shows that the proportion of single and double positive cells for each cluster marker pair is similar to the RNAseq data (Fig. 2 e-f).

We found three major populations of oligodendrocytes that are very different in their gene expression: Oligo_A, Oligo_B-E and Oligo_F. They almost mutually exclusively express the markers *OPALIN*, *RBFOX1* and *SPARC* respectively (Fig. 2 a-c, e-f), however, Oligo_B-E (*RBFOX1*+) are subclustered based on the expression of additional genes: Oligo_B: *AFF3*+ *LGALS1*- *FMN1*-; Oligo_C: *FMN1*; Oligo_D: *LGALS1*+ *FMN1*- *SPARC*-; Oligo_E: *HHIP*+ *OPALIN*- *AFF3*- (Fig. 2 a,b, Data S1). Oligo_A and F are *RBFOX1*-negative and strikingly different; Oligo_A expresses *OPALIN*, *PLXDC2*, *LAMA2* and *PALM2*, and Oligo_F expresses *SPARC*, *DHCR24*, *TUBA1A*, *TUBB2B*, *PMP2* and *HCN2* (Fig. 2 b). Gene ontology analysis shows functional differences among oligodendroglia clusters (Data S2). For example, for Oligo_A, 52 enriched pathways were identified (Data S2) including those important for interaction with neurons, such as axon development, regulation of neuronal projections and GTPase-mediated signal transmission (underpinned by genes such as *STARD13*, *AUTS2* and *ANK3*) and the expression of *ANK3* and *OPALIN*

1
2
3 suggests a link with paranodal development and/or maintenance [11, 86] (Fig. S2, Data S2).
4
5 Oligo_F expresses the novel oligodendrocyte marker *SPARC* and is mostly found in CSC
6 (see below). Gene ontology analysis for Oligo_F markers revealed 405 statistically enriched
7 terms (Data S2) including 19 terms based on genes such as *MIF* and *GSTP1* suggesting an
8 immune-related function (Fig. S3). However, these are different from the immune
9 oligodendroglia we previously described [20], as these oligodendrocytes do not express
10 MHC-2 genes, *CD74* nor *CTSS*, as expected in a healthy cohort. Instead, these immune-
11 related gene ontology terms may reflect the expression of genes related to membrane fusion
12 processes that have been shown to play a role in oligodendrocyte membrane extension, for
13 example by the expression of the vesicle-associated membrane protein 3 (VAMP3) [38]
14 which is indeed more highly expressed in Oligo_F (Fig. 2 b). Furthermore, Oligo_F also
15 shows enriched genes related to sterol, cholesterol and myelin production (Data S2), and
16 the highest levels of *HCN2*, a gene that is important for the formation of longer myelin
17 sheaths in mice [75] (Fig. 2 g). This suggests that Oligo_F is a spinal cord-enriched cluster
18 that contributes to the longer and thicker myelin sheaths of the human spinal cord compared
19 to the brain [3].
20
21
22
23
24
25
26
27
28
29
30
31

32 **Oligodendroglia clusters correlate with CNS region**

33
34 **Focussing on Oligo_F.** To statistically test whether **Oligo_F this cluster** is more abundant
35 in CSC, we used the R library Milo [15] which allows for differential abundance testing
36 based on subdividing clusters into neighborhoods and employs an algorithm borrowed from
37 differential gene expression analyses to test if those neighborhoods contain more nuclei of
38 one or the other CNS region. A pairwise comparison of each tissue region revealed that
39 indeed Oligo_F is enriched in CSC (Fig. 3 a-c, **also shown in Figure SX 3**). Validation using
40 two different immuno-fluorescence stainings on formalin-fixed paraffin-embedded samples
41 from different donors, based on the observation that Oligo_F is positive for *SPARC* and
42 *HCN2* but negative for *RBFOX1*, confirmed that Oligo_F is enriched in CSC: both
43 *SPARC*+*RBFOX1*- cells (Fig. 3 d) and *SPARC*+ *HCN2*+ cells (Fig. 3 e) are more abundant
44 in CSC compared to the other regions in the validation datasets.
45
46
47
48
49
50
51
52
53
54

55 The differential abundance testing also revealed that the two identified OPC clusters are
56 region-specific: OPC_A expresses the Paired Box 3 gene *PAX3* and the cation transporter
57 gene *SLC22A3* (Fig. 2 a-b,d) and is enriched in the posterior CNS-regions (CB and CSC),
58 while OPC_B is more abundant in the anterior BA4. OPC_B is marked by the expression
59 of *NELL1* (Fig. 2 a-b,d) which has epidermal growth factor like domains, is predicted to be
60
61
62
63
64
65

1
2
3
4
5
6
7
8
9
10
11
12
13
14
15
16
17
18
19
20
21
22
23
24
25
26
27
28
29
30
31
32
33
34
35
36
37
38
39
40
41
42
43
44
45
46
47
48
49
50
51

involved in cell differentiation and has not been previously described in OPCs. We confirmed this OPC segregation using BaseScope duplex by co-labelling *PDGFRA* with either *PAX3* or *NELL1* (Fig. 2 d; Fig. 3 f-g). In mouse spinal cord, *PAX3* is a marker for the third dorsal developmental wave of OPCs and oligodendrocytes derived from *PAX3*-positive OPCs have been shown to contribute more to remyelination of spinal cord lesions [91] which suggests that 1) human adult OPCs retain a subset of these developmental origin markers and 2) tissue-specific OPCs may vary in function. To explore this further, we performed a differential gene expression analysis between OPCs from the CSC versus BA4 (as the anatomically most distant regions) that revealed 871 differentially expressed genes (Log2FC > 0.25, adjusted p-value < 0.05, corresponding to at least 19 % upregulation) (Data S3, Data S4). Among those genes, we found that BA4 OPCs upregulate *FOXP1*, which plays a critical role in mouse forebrain development [82], and CSC OPCs express more *HOXB3*, which is important for mouse cervical spinal cord development (Fig. 3 h) [37]. This is surprising as human oligodendroglial development is known to be largely similar to rodents [33] and yet here we show that OPC patterning genes that are present at E13.5, but downregulated at P7 in mice [43] are retained in the human into adulthood (Fig. S4). To address the question if retaining these markers is associated with functional variation, we performed gene ontology analyses on differentially expressed genes between CSC and BA4 OPCs and found that BA4-enriched genes are mainly concerned with ion channel regulator activity (molecular function gene ontology), driven by genes such as *CACNG5*, *FGF12*, *FGF14*, *GRID2*, *KCNAB1*, *KCNIP4*, *KCNQ3*. For CSC OPCs, we found 80 significantly differentially regulated biological processes including glial differentiation, axon development and regulation of transcription, translation and protein secretion (Fig. 3i, Fig. S5). This indicates that human OPCs that are derived from different origins and/or have been exposed to different tissue environments vary in their function, with implications for the pathogenesis of diseases that affect the brain or spinal cord selectively.

All oligodendroglia clusters differentially regulate genes based on CNS region

52
53
54
55
56
57
58
59
60
61
62
63
64
65

We have shown above that Oligo_F, found more in the spinal cord, expresses key genes for the production of longer and thicker myelin sheaths including myelin genes such as *PLP1*, *CNP*, and *MAG* and also *HCN2* (known to control mouse myelin sheath length [75]) (Fig. 2 b,c,g). Next, we asked if other CSC oligodendrocytes also differ from the other two CNS regions. We performed differential gene expression analyses both pairwise between regions across all oligodendrocyte clusters (Fig. 3 j-l) and also cluster-wise and found that

1
2
3
4
5
6
7
8
9
10
11
12
13
14
15
16
17
18
19
20
21
22
23
24
25
26
27
28
29
30
31
32
33
34
35
36
37
38
39
40
41
42
43
44
45
46
47
48
49
50
51
52
53
54
55
56
57
58
59
60
61
62
63
64
65

oligodendrocytes differentially regulated 13, 170 and 191 genes in BA4, CB and CSC respectively (Log2FC > 0.25, adjusted p-value < 0.05). Among the upregulated genes in CSC oligodendrocytes were myelin genes and the Src Kinase-Associated Phosphoprotein 2 gene (*SKAP2*) (Fig. 3 j-k) which contributes to thicker myelin sheath formation in mouse spinal cord oligodendrocytes [27]. *SKAP2* is not only expressed by Oligo_F, but also by other spinal cord oligodendrocyte clusters (Fig. S6), indicating that these all contribute to differences with tissue region. Furthermore, gene ontology analysis performed on differentially expressed genes across all oligodendrocyte clusters confirms that, overall, human spinal cord oligodendrocytes upregulate genes important for cholesterol biosynthesis and myelination (Fig. 3 m, Fig. S7), consistent with mouse [35].

Age differences in oligodendroglia are largely restricted to OPCs

As myelin quality deteriorates with age [30] and increasing age is a risk factor for progressive disability in the demyelinating disease multiple sclerosis, we next investigated whether oligodendroglial transcriptional signatures also differ with age in our samples. We first tested for compositional differences using Milo [15] but found that oligodendroglia cluster composition largely did not correlate with donor age except for Oligo_E and COP_A, which show neighborhood enrichment in younger donors (Fig. 4 A, **Figure SX 2**). COPs represent the transition between OPCs and oligodendrocytes during differentiation, needed for myelin maintenance, but produced at a low rate in healthy adult brain. This reduction in COP_A abundance in older donors is consistent with the reduction of capacity of human OPCs to differentiate with age (as seen in rodents [39, 51, 72]) and subsequent reduced myelin integrity [30]. Differential gene expression analyses across the cell lineage-specific dataset, and for each of the oligodendrocyte and OPC cluster separately (Data S3, Data S4), showed that oligodendrocytes varied little with age, but OPCs showed more age-related transcriptional variation (Fig. 4 b-c). Old OPCs expressed less of the early myelin protein gene *PLP1* and less *PDGFRA* (Figure 4c), an OPC membrane receptor mediating proliferation, again consistent with a decline in human OPC function with age. In addition, the spinal cord and cerebellum-specific cluster OPC_A but not OPC_B showed a higher expression of the Early B-cell factor-1 (*EBF1*) in older donors which we validated using RNAScope (Fig. 4 c-f). *EBF1* is involved in Schwann cell myelination [49] and axonal pathfinding [55] (such proteins are often similarly used for OPC migration) and specific polymorphisms of this gene increase risk of multiple sclerosis [45], suggesting that it may be important to better understand its function in OPCs.

1
2
3
4
5
6
7
8
9
10
11
12
13
14
15
16
17
18
19
20
21
22
23
24
25
26
27
28
29
30
31
32
33
34
35
36
37
38
39
40
41
42
43
44
45
46
47
48
49
50
51
52
53
54
55
56
57
58
59
60
61
62
63
64
65

In summary, our results indicate that age-related oligodendrocyte and myelin changes may be influenced by transcriptional changes in the OPC.

Sex differences in oligodendroglia are subtle

Demyelinating diseases show a variation with biological sex: women are four times more likely to be affected by multiple sclerosis than men, while men show on average a faster progression [34]. Therefore, we next explored sex differences in oligodendroglial transcriptomic signatures. Differential abundance analysis showed few differences (Fig. 4 G, **Figure SX 2**) and differential gene expression analyses across and within clusters show that oligodendroglial gene expression variation with sex is considerably driven by gonosomal genes, such as XIST in female donors and Y-chromosomal genes in male donors: *NLGN4Y*, *TTY14*, *USP9Y*, *KDM5D*, *ZFY* and *UTY* (Fig. S8). Although this is not surprising, ~~these gonosomal genes may still have an important influence on neuropathology:~~ repression of Y-linked genes in a mouse model of Alzheimer's disease, led to more mitochondrial gene dysfunction and neuroinflammation [9]. Non-gonosomal genes that were differentially regulated between sexes included an upregulation of *NRXN1* in female oligodendrocytes (Fig. 4 h), which has previously been linked to Alzheimer's disease and multiple sclerosis, and of *HIF3A* in female OPCs which is related to oxidative stress (Fig. 4 i). Male donors consistently express more heat shock protein *HSPA1A* not only in OPCs and oligodendrocytes, but also in astrocytes and microglia, indicating that male glia may respond differently to stress and vary in their regulation of protein folding mechanisms, ~~which may contribute to sex differences in neuropathology~~ (Fig. 4 h-i, Fig. S8, Fig. S9).

Adult normal CNS oligodendroglia clusters do not represent transitional states of the differentiation pathway

We were next interested in whether our identified normal adult CNS oligodendrocyte clusters represent transitional states along a differentiation trajectory. This is more likely if 1) OPCs express cell-cycling markers indicating cell-turnover necessary for on-going replacement of differentiating cells, 2) if intermediate cells exist and 3) if similar trajectories can be identified using different methods.

There was no evidence for cycling OPCs (no expression of cell cycling markers e.g. *MKI67* and with Seurat's cell cycle annotation algorithm [8]) and few detectable intermediate COPs (though more in young donors as above). We used a variety of trajectory inference methods

1
2
3 both inside of Dynverse [59] (Angle, Scorpius, PAGA Tree) and standalone (Monocle [77],
4 Slingshot [74], scVelo [4]) but obtained conflicting results as to the overall trajectory and
5 the identity of the most immature oligodendrocyte cluster: Oligo_B (Slingshot, PAGA Tree)
6 or Oligo_A (Monocle, Angle, Scorpius) (Fig. S10). This is consistent with limited on-going
7 oligodendroglial differentiation in our non-diseased adult human CNS dataset, suggesting
8 either fixed cell end-states or dynamic switching between multiple states which current
9 trajectory inference methods struggle to identify.
10
11
12
13
14

15 16 17 **Integrated analysis of oligodendroglia datasets reveals a human-selective** 18 **oligodendrocyte subtype**

19
20 To determine how our 11 oligodendroglial clusters relate to published datasets, we
21 transferred the labels of our previous study by Jäkel & Agirre et al. (2019) [32] which
22 included human samples of subcortical white matter of donors affected by multiple sclerosis
23 and of disease-free controls onto our current dataset and then integrated both datasets (Fig.
24 5 A). The predicted labels fit well with our cluster labels, particularly for cluster Oligo_B
25 which mostly corresponds to cluster Oligo1 and Oligo_A which corresponds best to Oligo6
26 and Oligo4. Clusters Oligo2 and Oligo3 that are enriched in multiple sclerosis [32] are very
27 rare in our current dataset, confirming that those clusters are multiple sclerosis-selective
28 (Fig. 5 b). OPCs in Jäkel & Agirre et al. [32] are of mixed brain regions and correlate to
29 both of our OPC clusters (Fig. 5 b). Oligo_F does not map well to any cluster, underlining
30 its spinal cord selectivity (Fig. 5 b).
31
32

33
34 The mouse oligodendrocyte MOL2 expressing *Klk6* has been shown to be enriched in
35 specific regions of the spinal cord [23, 88]. To test whether there is an equivalent of Oligo_F
36 in mouse spinal cord, we also integrated our oligodendroglia dataset with three murine
37 datasets by Marques et al. [44] (different CNS regions of juvenile mice), Sathyarmurthy et
38 al. [62] (adult mouse lumbar spinal cord) and Floriddia et al. [23] (adult corpus callosum
39 and spinal cord) (Fig. 5 c-d). Human and mouse data integrated well, with OPC_A, Oligo_A
40 and Oligo_B correlating particularly well to mouse oligodendroglia. However, intermediate
41 cells between the state of OPCs and oligodendrocytes and newly formed oligodendrocytes
42 that are abundant in the mouse data, particularly in the juvenile data (Fig. 5 c-d) are rare the
43 human dataset, again suggesting that human adult CNS cells are not actively differentiating
44 in the absence of disease. The *SPARC*-positive, *RBFOX1*-negative human cluster Oligo_F
45 is missing in the mouse datasets, even in the adult mouse spinal cord samples, suggesting it
46 is human-selective (Fig. 5 d). There are known proteomic differences between human and
47
48
49
50
51
52
53
54
55
56
57
58
59
60
61
62
63
64
65

1
2
3
4
5
6
7
8
9
10
11
12
13
14
15
16
17
18
19
20
21
22
23
24
25
26
27
28
29
30
31
32
33
34
35
36
37
38
39
40
41
42
43
44
45
46
47
48
49
50
51
52
53
54
55
56
57
58
59
60
61
62
63
64
65

murine CNS myelin including the human-specific expression of Peripheral Myelin Protein 2 (*PMP2*) [25], which is highly expressed in our Oligo_F cluster (without expression of other Schwann cell markers; Fig. S11) and therefore this may contribute to the observed myelin proteomic species difference.

Region, age and sex variation in astrocytes

White matter oligodendroglia are in constant interaction with neighboring glia and so we also analyzed astrocytes and microglia in the same samples. Human grey matter astrocytes are known to be transcriptionally heterogeneous [70, 90], but data for human white matter astrocytes is much sparser [32, 65]. Our analyses identified twelve white matter astrocyte clusters (AS_1 – AS_12) with AS_9_ep representing transcriptionally closely related ependymal cells, all with distinct marker gene expression (Fig. 1 b, 6 a-b, Data S1). Gene ontology analysis suggests that astrocyte functional roles are distinct, with two types (AS_1 and 2) expressing genes concerned with neuronal interactions, axon guidance and synapse organization, three (AS_4, 6 and 12) related to synapses/synaptic vesicles, ~~two populations (AS_8 and 11) express myelin genes, as previously described in human astrocytes [67],~~ AS_5 relate to extracellular matrix organization, AS_7 to the blood brain barrier and AS_10 to cellular motility, signaling and histone modification. Ependymal cells (AS_9_ep) express motile cilia genes (*CFAP43*, *SPAG17*, *DNAH6*) in keeping with their function in promoting cerebrospinal fluid flow [73]. Two populations (AS 8 and 11) also express myelin genes. AS 8 contains some identified potential doublets (Figure SX 1), but these are not present in AS 11 and this has previously been described in human astrocytes [67],- (Fig. S12, Data S2).

Astrocytes also showed strong heterogeneity with white matter tissue region: Clusters AS_5 and 6 were specific for BA4, clusters AS_4 and 7 were specific for CB and clusters AS_1, 2, 3, 9_ep, 11 and 12 were more abundant in CSC (Fig. 6 c), and differential gene expression analyses between regions reflected differences in these cluster marker genes such as increased Adhesion G Protein-Coupled Receptor V1 (*ADGRV1*) in the BA4-specific cluster AS_5 (Fig. 6 d, Data S3). In addition, CSC astrocytes expressed more *SKAP2*, similarly to oligodendroglia and more Glial Fibrillary Acidic Protein (*GFAP*) as previously reported in mouse [85] (Fig. 6 d,f, Data S3). This astrocyte regional specificity may help us understand the regional variation in human astrocytopathies [7]. For example, *FAT3* gene mutations are associated with Spinocerebellar Ataxia (SCA), and is more highly expressed in CB astrocytes particularly of older donors (Fig. 6 e-g, Data S3). Furthermore, CSC astrocytes

1
2
3
4
5
6
7
8
9
10
11
12
13
14
15
16
17
18
19
20
21
22
23
24
25
26
27
28
29
30
31
32
33
34
35
36
37
38
39
40
41
42
43
44
45
46
47
48
49
50
51
52
53
54
55
56
57
58
59
60
61
62
63
64
65

express more genes associated with synapse formation and gliogenesis (Fig. S13 a) whereas BA4 astrocytes express more genes associated with the extracellular matrix (Fig. S13 b). Astrocytes change morphology and function upon injury or disease, previously categorized into a neurotoxic A1 type and a neuroprotective A2 type in mice [40], but now considered more of a spectrum [13], but we found no evidence of genes associated with astrocyte activation in our normal adult dataset, not even with increased age (Fig. S14). However, we did identify differentially expressed genes with older age in astrocytes which include *CACNB2* and *GREB1L*, important for calcium signaling and the potassium voltage-gated channel protein gene *KCND2* (Fig. 6 G, Data S1). Astrocytes of younger donors express more *BCAN*, which is important for experience-dependent neuroplasticity and normal cognitive function [21] (Fig. 6 g). Sex differences in the astrocyte population beyond the expression of gonosomal genes (discussed for oligodendroglia above) included more *LAMA2* in female astrocytes, related to the blood brain barrier, and more *CPAMD8* (associated with late-onset Alzheimer’s disease [22]) and heat shock protein gene (*HSPA1A*, *HSPA1B*) expression in male astrocytes (Fig. 6 h, Fig. S8).

Region, age and sex variation in microglia

We identified five microglia clusters (Microglia_1 – Microglia_5) and one cluster of border-associated macrophages (BAM – positive for *CD163*, *LYVE1*, *MRC1*) which express distinct marker genes (Fig. 1 b, 7 a-b.), but no cells with the phenotype of infiltrating monocyte-derived macrophages, expected to be absent in healthy tissue. Similarly to astrocytes, microglia can shift from a homeostatic to an activated phenotype, characterized by proliferation, chemoattractant-mediated migration, changes in cellular morphology and phagocytosis of damaged cells [29]. Microglia_1 (*RASGEF1C*, *AC008691.1*, *TLN2*) express markers for a homeostatic phenotype (*P2RY13* and *CX3CR1*) (Fig. 7 a, Fig. S15, Data S1, Data S2). Conversely, Microglia_2 (GPNMB) and Microglia_4 (*ACSL1*, *CXCR4*) appear more activated, expressing the phagocytotic markers *CD68* and *TREM2* (Fig. 7 a) and with significant leukocyte activation and degranulation gene ontology terms, in spite of being derived from healthy tissue (Data S2). However, even in normal adult tissue, activated microglia are needed for regulation of neuronal survival in development, and pruning of synapses, important for circuit refinement [57]. Microglia_3 and 5 express genes classical for neurons or glia such as *NTM*, *MAGI2*, *SCD*, *PLP1*, *NRG3*. Some of these are identified as potential doublets (Figure SX 1) but they may also, suggesting microglial engulfment of oligodendrocytes and/or synapses (Fig. 7 a, Data S1, Data S2).

1
2
3 The homeostatic Microglia_1 cluster was found similarly in all three tissues but activated
4
5 Microglia_2 and Microglia_4 were mostly found in CSC (Fig. 7 c-e). Microglia_2 expresses
6
7 *GPNMB* which labels lipid-associated microglia in mice [1], is expressed in microglia in
8
9 Alzheimer's disease [63] and which we detected in a subset of microglia using immuno-
10
11 fluorescence (Fig. 7 f). CSC microglia express more major histocompatibility genes and
12
13 more *CD74* than in other regions, particularly BA4 (Fig. 7 g-i), and these findings may be
14
15 as the blood spinal cord barrier is more permeable than the blood brain barrier, resulting in
16
17 increased microglial responses to blood-borne stressors. CSC and CB microglia also express
18
19 more *GRID2* (Fig. 7 g-i), previously detected in brain microglia of Alzheimer's disease
20
21 donors [26], and more *HIF1A* and *NEAT1*, which may indicate a hypoxic stress response
22
23 (Data S3 Data S4, Data S5). Border associated macrophages (BAM) were mostly captured
24
25 for CSC (Fig. 7 c-e), probably as meninges, including the perivascular space in which
26
27 BAMs reside, were captured for this region. (Gene ontology terms for regional differences
28
29 and activation/homeostatic markers are shown in Fig. S16 & Fig. S17.)

30
31 Previous literature suggests that microglia express more activation genes with increased age
32
33 [60, 68], and our data confirm this; *CD74*, *NEAT1* and *HLA-C* are more highly expressed in
34
35 old microglia (Fig. 7 J) and markers of homeostasis such *CX3CR1* and *P2RY12* decline with
36
37 age (Fig. 7 j, Data S3). However, the relatively subtle difference seen here may be bigger
38
39 in vivo as snRNAseq is thought to underestimate the expression levels of microglia
40
41 activation genes in comparison to scRNAseq [76].

42
43 Sex differences in the microglia population include more pro-inflammatory genes such as
44
45 *HLA-DRB5* and *IFI44L* in female microglia (Fig. 7 k, Data S3), and higher expression of
46
47 *DUSP1* which modulates microglia towards a homeostatic phenotype [80] in male microglia
48
49 (Fig. 7 k, Data S3). Like the other glia, male microglia also express more heat shock protein
50
51 genes such as *HSPA1A*. These changes suggest sex differences in the link between
52
53 inflammation and ageing, and may explain some sex dimorphism in neurodegenerative
54
55 disease susceptibility.

56
57 In summary, we show here that in normal adult human WM glia, there is striking variation
58
59 in transcriptional signatures of all broad cell groups with region, finding both region-
60
61 specific and region-selective cell populations, with much less variation with age and sex.

62 Discussion

1
2
3 We predicted that there would be diversity in normal human glial transcriptional signatures
4 as a read-out of functional variation across CNS regions, age groups and between sexes, to
5 explain the influence of these factors on susceptibility to neurological diseases. We found
6 that transcriptional diversity with CNS region was greater than with age and sex across all
7 glial types, and the striking regional differences between the spinal cord and the brain
8 indicate that we can no longer assume their parity in physiological, pathological or
9 therapeutic response.
10

11
12
13 Within the oligodendroglia, we found a brain (BA4)-specific and a spinal cord and
14 cerebellum-specific OPC cluster, which retain expression of different developmental
15 markers – unlike in the mouse, where, for example *Hox* genes that label spinal cord OPCs
16 and *Foxg1* that labels brain OPCs are repressed with age [43]. The continued expression of
17 developmental transcriptional factors in our human data indicates that they are needed for
18 adulthood function, differently from mouse. Spinal cord OPCs give rise to similar
19 oligodendrocytes to brain OPCs but have the added capability to differentiate into Oligo_F
20 oligodendrocytes which are selective for the CSC and appear absent in mice. These
21 oligodendrocytes express markers such as *HCN2* that leads to the production of longer and
22 thicker myelin sheaths [75] and high levels of *PMP2* but no other Schwann cell markers.
23 Del Rio Hortega described a Schwannoid and spinal cord-specific oligodendrocyte type
24 (Oligo IV) in the cat CNS (reviewed in [54]), which matches this Oligo_F transcriptional
25 signature. In multiple sclerosis, remyelination of spinal cord lesions is less successful than
26 brain lesions [6] but it is unclear why. We speculate that the functional differences of spinal
27 cord OPCs may alter their ability to differentiate into remyelinating oligodendrocytes and/or
28 that Oligo_F oligodendrocytes, and spinal cord oligodendrocytes generally may be more
29 difficult to replace because of their longer and thicker myelin sheaths. Analysis of
30 snRNAseq data from spinal cord white matter in donors with multiple sclerosis [78] and
31 improving functional in vitro assays for adult human oligodendroglia may shed further light
32 onto their different functions in health and disease.
33

34
35
36 Other CSC glial differences may relate to the more ‘open’ blood spinal cord barrier
37 compared to the blood brain barrier, therefore likely exposing CSC cells to more blood-
38 derived inflammatory cells/factors explaining activation markers in CSC microglia and
39 alterations in CSC astrocytes, of relevance to pathologies which predominantly affect the
40 spinal cord and for better targeting therapeutics.
41

42
43
44 In our dataset, age differences were more subtle and we hypothesize that a bigger age
45 disparity, by including a child/adolescent group, would show larger effects. However, *EBF1*

1
2
3 746
4 747
5
6 748
7
8 749
9
10 750
11 751
12
13 752
14
15 753
16
17 754
18
19 755
20
21 756
22
23 757
24
25 758
26
27 759
28 760
29
30 761
31
32 762
33
34 763
35
36 764
37
38 765
39
40 766
41
42 767
43 768
44
45 769
46
47 770
48
49 771
50
51 772
52
53 773
54
55 774
56
57 775
58
59 776
60
61 777
62
63 778
64
65 779

has emerged as a marker of aged adult human OPCs, which would be predicted from rodent work [52] to be poorer at initiating remyelination than young OPCs, and this may help us dissect these differences in humans. Changes with age or sex that affect lowly expressed genes will be hard to detect by snRNA-seq [76], and so cell sorting strategies on larger cohorts based on markers identified in the present study with subsequent bulk RNAseq may help highlight such differences. Other physiologically relevant age and sex-related differences may also be post-transcriptional, metabolic or only detectable in response to certain stressors/diseases. Finally, determining whether the subtypes we discovered are associated with local microenvironment or specific cell-cell interactions will require more multiplexed spatially-resolved techniques.

Our results show that human post-mortem tissue is an invaluable source of information highlighting human-specificity of some cellular phenotypes which are difficult to otherwise identify due to the current lack of faithful adult human in vitro models. However, by definition, human post-mortem tissue is limited as it only presents a single snapshot of transcriptional activity without a time course. We attempted to infer a ‘pseudotime’ trajectory between oligodendroglial clusters, but the lack of OPC proliferation and sparsity of intermediate COP stages suggest little oligodendroglia turnover in adulthood in the absence of disease, in agreement with previous radioisotope studies [84], and different from our previous multiple sclerosis dataset [32] with more intermediate cells and disease-specific signatures. Understanding these transitions and how they change in disease will only be solved by use of reporter genes for identified clusters in improved human cell models.

Our findings of marked regional cellular and gene expression differences in normal human post-mortem white matter are critical to consider in strategies for more effective therapeutics for region-specific/selective diseases. For example, our results predict that we will require different pro-remyelinating therapies for successful treatment of spinal cord multiple sclerosis demyelinated lesions compared to brain. For success in translating therapies, we need to embed the consideration of cellular regional, sex and age effects in health and disease throughout our pipeline from preclinical screens to clinical trials - a ‘precision medicine’ approach. We provide these data as an open resource for others for appropriate comparisons with future diseased human CNS cohorts in line with the Human Cell Atlas Project, and in a Shiny app for easy browsing https://seeker-science.shinyapps.io/shiny_app_multi/.

1
2
3
4
5
6
7
8
9
10
11
12
13
14
15
16
17
18
19
20
21
22
23
24
25
26
27
28
29
30
31
32
33
34
35
36
37
38
39
40
41
42
43
44
45
46
47
48
49
50
51
52
53
54
55
56
57
58
59
60
61
62
63
64
65

Declarations

Ethics approval and consent to participate

Adult post-mortem unfixed fresh-frozen tissue and formalin-fixed paraffin-embedded tissue were obtained from the MRC Sudden Death Brain Bank in Edinburgh with full ethical approval (16/ES/0084).

Consent for publication

Not applicable

Availability of data and material

All data necessary to reproduce the results of the present paper are available at (link_inserted_upon_acceptance). R code (that also specifies R library versions) is available at <https://gitfront.io/r/user-1167685/QNF6fMTSbeE6/Luise-Seeker-Human-WM-Glia/>. We used ShinyCell [53] to generate interactive shiny apps that are accessible at https://seeker-science.shinyapps.io/shiny_app_multi/.

Competing interests

All authors declare that they have no competing interests.

Funding

Our work was funded by the following grants: Medical research Council grant CZF2019-002427, Chan Zuckerberg Foundation CZIF2019-002427, DAF2021-239069, MS Society UK Edinburgh Research Centre award reference 133 and the British Heart Foundation pilot grant RE/18/5/34216

Authors' contributions

Conceptualization: AW, GCB, GL, CAV, LAS, NLK, SB, AMK, DVB, MK, FBP, ZM

Investigation: LAS, SJ

Validation: LAS

Formal analysis: LAS, NBC

Resources: NH

Data Curation: LAS, NBC

Visualization: LAS, JCW, AW

Supervision: AW, GCB, GL, CAV

Writing—original draft: LAS, AW

Writing—review & editing: AW, GCB, GL, CAV, LAS, NLK, SB, AMK, DVB, MK, FBP, ZM

Acknowledgements

1
2
3 We thank the following people and facilities at the University of Edinburgh for their help:
4
5 The MRC brain bank for providing tissue, Prof. Colin Smith for the neuropathological
6
7 examination of donors, Pamela Brown from the Biomolecular Core facility for Bioanalyzer
8
9 measurements, SuRF Histology for cutting paraffin samples, and Matthieu Vermeren from
10
11 the CRM imaging facility for his continued imaging support. We also thank Alex Lederer
12
13 and Alan O’Callaghan for discussions about the bioinformatics analysis and their advice.
14
15 Next Generation Sequencing of cDNA was carried out by Edinburgh Genomics at the
16
17 University of Edinburgh. Some figures were created with BioRender.com. This work has
18
19 made use of the resources provided by the Edinburgh Compute and Data Facility (ECDF)
20
21 (<http://www.ecdf.ed.ac.uk/>).

22 **References**

- 23 1. Androvic P, Schifferer M, Anderson KP, Cantuti-Castelvetri L, Ji H, Lui L, et al. (2022)
24 Spatial Transcriptomics-correlated Electron Microscopy. *bioRxiv* 1–19
- 25 2. Bankhead P, Loughrey MB, Fernández JA, Dombrowski Y, McArt DG, Dunne PD, et al.
26 (2017) QuPath: Open source software for digital pathology image analysis. *Sci Rep* 7:1–7.
27 doi: 10.1038/s41598-017-17204-5
- 28 3. Bechler ME, Byrne L, Bechler ME, Byrne L (2015) CNS Myelin Sheath Lengths Are an
29 Intrinsic Property of Oligodendrocytes. *Curr Biol* 25:2411–2416. doi:
30 10.1016/j.cub.2015.07.056
- 31 4. Bergen V, Lange M, Peidli S, Wolf FA, Theis FJ (2020) Generalizing RNA velocity to
32 transient cell states through dynamical modeling. *Nat Biotechnol* 38:1408–1414. doi:
33 10.1038/s41587-020-0591-3
- 34 5. Bøstrand SMK, Williams A (2021) Oligodendroglial Heterogeneity in Neuropsychiatric
35 Disease. *Life* 11:125. doi: 10.3390/life11020125
- 36 6. Bramow S, Frischer JM, Lassmann H, Koch-Henriksen N, Lucchinetti CF, Sørensen PS, et
37 al. (2010) Demyelination versus remyelination in progressive multiple sclerosis. *Brain*
38 133:2983–2998. doi: 10.1093/brain/awq250
- 39 7. Bugiani M, Plug BC, Man JHK, Breur M, van der Knaap MS (2022) Heterogeneity of
40 white matter astrocytes in the human brain. *Acta Neuropathol* 143:159–177
- 41 8. Butler A, Hoffman P, Smibert P, Papalexi E, Satija R (2018) Integrating single-cell
42 transcriptomic data across different conditions, technologies, and species. *Nat Biotechnol*
43 36:411–420. doi: 10.1038/nbt.4096
- 44 9. Caceres A, Jene A, Esko T, Perez-Jurado LA, Gonzalez JR (2020) Extreme
45 downregulation of chromosome Y and Alzheimer’s disease in men. *Neurobiol Aging*
46 90:150.e1-150.e4
- 47 10. Carlson M (2019) org.Hs.eg.db: Genome wide annotation for Human. R package version
48 3.8.2
- 49 11. Chang KJ, Zollinger DR, Susuki K, Sherman DL, Makara MA, Brophy PJ, et al. (2014)
50 Glial ankyrins facilitate paranodal axoglial junction assembly. *Nat Neurosci* 17:1673–1681.
51 doi: 10.1038/nn.3858
- 52 12. Chowen JA, Garcia-Segura LM (2021) Role of glial cells in the generation of sex
53 differences in neurodegenerative diseases and brain aging. *Mech Ageing Dev* 196:111473.
54 doi: 10.1016/j.mad.2021.111473
- 55 13. Clarke LE, Liddel SA, Chakraborty C, Münch AE, Heiman M, Barres BA (2018)

- 1
2
3
4
5
6
7
8
9
10
11
12
13
14
15
16
17
18
19
20
21
22
23
24
25
26
27
28
29
30
31
32
33
34
35
36
37
38
39
40
41
42
43
44
45
46
47
48
49
50
51
52
53
54
55
56
57
58
59
60
61
62
63
64
65
- Normal aging induces A1-like astrocyte reactivity. *Proc Natl Acad Sci U S A* 115:E1896–E1905. doi: 10.1073/pnas.1800165115
14. Crawford AH, Tripathi RB, Richardson WD, Franklin RJM (2016) Developmental Origin of Oligodendrocyte Lineage Cells Determines Response to Demyelination and Susceptibility to Age-Associated Functional Decline. *Cell Rep* 15:761–773. doi: 10.1016/j.celrep.2016.03.069
15. Dann E, Henderson NC, Teichmann SA, Morgan MD, Marioni JC (2022) Differential abundance testing on single-cell data using k-nearest neighbor graphs. *Nat Biotechnol* 40:245–253. doi: 10.1038/s41587-021-01033-z
16. Darmanis S, Sloan SA, Zhang Y, Enge M, Caneda C, Shuer LM, et al. (2015) A survey of human brain transcriptome diversity at the single cell level. *Proc Natl Acad Sci U S A* 112:7285–7290. doi: 10.1073/pnas.1507125112
17. Durinck S, Spellman PT, Birney E, Huber W (2009) Mapping identifiers for the integration of genomic datasets with the R/Bioconductor package biomaRt. *Nat Protoc* 4:1184–1191. doi: 10.1038/nprot.2009.97
18. Escartin C, Galea E, Lakatos A, O’Callaghan JP, Petzold GC, Serrano-Pozo A, et al. (2021) Reactive astrocyte nomenclature, definitions, and future directions. *Nat Neurosci* 24:312–325. doi: 10.1038/s41593-020-00783-4
19. Eze UC, Bhaduri A, Haeussler M, Nowakowski TJ, Kriegstein AR (2021) Single-cell atlas of early human brain development highlights heterogeneity of human neuroepithelial cells and early radial glia. *Nat Neurosci* 24:584–594. doi: 10.1038/s41593-020-00794-1
20. Falcão AM, van Bruggen D, Marques S, Meijer M, Jäkel S, Agirre E, et al. (2018) Disease-specific oligodendrocyte lineage cells arise in multiple sclerosis. *Nat Med* 24:1837–1844. doi: 10.1038/s41591-018-0236-y
21. Favuzzi E, Marques-Smith A, Deogracias R, Winterflood CM, Sánchez-Aguilera A, Mantoan L, et al. (2017) Activity-Dependent Gating of Parvalbumin Interneuron Function by the Perineuronal Net Protein Brevican. *Neuron* 95:639-655.e10. doi: 10.1016/j.neuron.2017.06.028
22. Fernández M V., Budde J, Del-Aguila JL, Ibañez L, Deming Y, Harari O, et al. (2018) Evaluation of gene-based family-based methods to detect novel genes associated with familial late onset Alzheimer disease. *Front Neurosci* 12. doi: 10.3389/fnins.2018.00209
23. Floriddia EM, Lourenço T, Zhang S, van Bruggen D, Hilscher MM, Kukanja P, et al. (2020) Distinct oligodendrocyte populations have spatial preference and different responses to spinal cord injury. *Nat Commun* 11:1–15. doi: 10.1038/s41467-020-19453-x
24. Fu Y, Yang M, Yu H, Wang Y, Wu X, Yong J, et al. (2021) Heterogeneity of glial progenitor cells during the neurogenesis-to-gliogenesis switch in the developing human cerebral cortex. *Cell Rep* 34:108788. doi: 10.1016/j.celrep.2021.108788
25. Gargareta V-I, Reuschenbach J, Siems SB, Sun T, Piepkorn L, Mangana C, et al. (2022) Conservation and divergence of myelin proteome and oligodendrocyte transcriptome profiles between humans and mice. *Elife* 11
26. Gerrits E, Brouwer N, Kooistra SM, Woodbury ME, Vermeiren Y, Lambourne M, et al. (2021) Distinct amyloid- β and tau-associated microglia profiles in Alzheimer’s disease. *Acta Neuropathol* 141:681–696. doi: 10.1007/s00401-021-02263-w
27. Ghelman J, Grewing L, Windener F, Albrecht S, Zarbock A, Kuhlmann T (2021) SKAP2 as a new regulator of oligodendroglial migration and myelin sheath formation. *Glia* 69:2699–2716. doi: 10.1002/glia.24066
28. Guo H, Li J (2021) scSorter: assigning cells to known cell types according to marker genes. *Genome Biol* 22:69. doi: 10.1186/s13059-021-02281-7
29. Hanisch UK, Kettenmann H (2007) Microglia: Active sensor and versatile effector cells in the normal and pathologic brain. *Nat Neurosci* 10:1387–1394. doi: 10.1038/nn1997

- 1
2
306 2 30. Hill RA, Li AM, Grutzendler J (2018) Lifelong cortical myelin plasticity and age-related
3 degeneration in the live mammalian brain. *Nat Neurosci* 21:683–695. doi: 10.1038/s41593-
4 018-0120-6
5
6 31. Huang W, Bhaduri A, Velmeshev D, Wang S, Wang L, Rottkamp CA, et al. (2020) Origins
7 and Proliferative States of Human Oligodendrocyte Precursor Cells. *Cell* 182:594-608.e11.
8 doi: 10.1016/j.cell.2020.06.027
9
10 32. Jäkel S, Agirre E, Falcão AM, Bruggen D, Lee KW, Knuesel I, et al. (2019) Altered human
11 oligodendrocyte heterogeneity in multiple sclerosis. *Nature* 566:543–547. doi:
12 10.1038/s41586-019-0903-2
13
14 33. Jakovcevski I, Filipovic R, Mo Z, Rakic S, Zecevic N (2009) Oligodendrocyte
15 development and the onset of myelination in the human fetal brain. *Front Neuroanat* 3:5.
16 doi: 10.3389/neuro.05.005.2009
17
18 34. Kalincik T, Vivek V, Jokubaitis V, Lechner-Scott J, Trojano M, Izquierdo G, et al. (2013)
19 Sex as a determinant of relapse incidence and progressive course of multiple sclerosis.
20 *Brain* 136:3609–3617. doi: 10.1093/brain/awt281
21
22 35. Khandker L, Jeffries MA, Chang YJ, Mather ML, Evangelou A V., Bourne JN, et al.
23 (2022) Cholesterol biosynthesis defines oligodendrocyte precursor heterogeneity between
24 brain and spinal cord. *Cell Rep* 38:110423. doi: 10.1016/j.celrep.2022.110423
25
26 36. Kodama L, Gan L (2019) Do Microglial Sex Differences Contribute to Sex Differences in
27 Neurodegenerative Diseases? *Trends Mol Med* 25:741–749. doi:
28 10.1016/j.molmed.2019.05.001
29
30 37. Kwan CT, Tsang SL, Krumlauf R, Sham MH (2001) Regulatory analysis of the mouse
31 *Hoxb3* gene: Multiple elements work in concert to direct temporal and spatial patterns of
32 expression. *Dev Biol* 232:176–190. doi: 10.1006/dbio.2001.0157
33
34 38. Lam M, Takeo K, Almeida RG, Cooper MH, Wu K, Iyer M, et al. (2022) CNS myelination
35 requires VAMP2/3-mediated membrane expansion in oligodendrocytes. *Nat Commun* 13
36
37 39. Leong SY, Rao VTS, Bin JM, Gris P, Sangaralingam M, Kennedy TE, et al. (2014)
38 Heterogeneity of oligodendrocyte progenitor cells in adult human brain. *Ann Clin Transl*
39 *Neurol* 1:272–283. doi: 10.1002/acn3.55
40
41 40. Liddelow SA, Guttenplan KA, Clarke LE, Bennett FC, Bohlen CJ, Schirmer L, et al.
42 (2017) Neurotoxic reactive astrocytes are induced by activated microglia. *Nature* 541:481–
43 487. doi: 10.1038/nature21029
44
45 41. Lun ATL, Mccarthy DJ, Marioni JC (2016) A step-by-step workflow for low-level analysis
46 of single-cell RNA-seq data with Bioconductor. *F1000Research* 5:1–69
47
48 42. La Manno G, Soldatov R, Zeisel A, Braun E, Hochgerner H, Petukhov V, et al. (2018)
49 RNA velocity of single cells. *Nature* 560:494–498. doi: 10.1038/s41586-018-0414-6
50
51 43. Marques S, van Bruggen D, Vanichkina DP, Floriddia EM, Munguba H, Våremo L, et al.
52 (2018) Transcriptional Convergence of Oligodendrocyte Lineage Progenitors during
53 Development. *Dev Cell* 46:504-517.e7. doi: 10.1016/j.devcel.2018.07.005
54
55 44. Marques S, Zeisel A, Codeluppi S, van Bruggen D, Mendanha Falcão A, Xiao L, et al.
56 (2016) Oligodendrocyte heterogeneity in the mouse juvenile and adult central nervous
57 system. *Science* (80-) 352:1326–1329. doi: 10.1126/science.aaf6463
58
59 45. Martínez A, Mas A, de las Heras V, Arroyo R, Fernández-Arquero M, de la Concha EG, et
60 al. (2005) Early B-cell Factor gene association with multiple sclerosis in the Spanish
61 population. *BMC Neurol* 5:19. doi: 10.1186/1471-2377-5-19
62
63 46. Mathys H, Davila-Velderrain J, Peng Z, Gao F, Mohammadi S, Young JZ, et al. (2019)
64 Single-cell transcriptomic analysis of Alzheimer’s disease. *Nature* 570:332–337. doi:
65 10.1038/s41586-019-1195-2
66
67 47. McCarthy DJ, Campbell KR, Lun ATL, Wills QF (2017) Scater: Pre-processing, quality
68 control, normalization and visualization of single-cell RNA-seq data in R. *Bioinformatics*

- 1
2
33:1179–1186. doi: 10.1093/bioinformatics/btw777
- 956 2
3
48. McDavid A, Finak G, Yajima M (2020) MAST: Model-based Analysis of Single Cell
957 4
5 Transcriptomics.
- 958 5
49. Moruzzo D, Nobbio L, Sterlini B, Consalez GG, Benfenati F, Schenone A, et al. (2017)
959 6
7 The Transcription Factors EBF1 and EBF2 Are Positive Regulators of Myelination in
960 7
8 Schwann Cells. *Mol Neurobiol* 54:8117–8127. doi: 10.1007/s12035-016-0296-2
- 961 8
9
962 9
50. Nagy C, Maitra M, Tanti A, Suderman M, Thérroux JF, Davoli MA, et al. (2020) Single-
963 10
11 nucleus transcriptomics of the prefrontal cortex in major depressive disorder implicates
964 11
12 oligodendrocyte precursor cells and excitatory neurons. *Nat Neurosci* 23:771–781. doi:
965 12
13 10.1038/s41593-020-0621-y
- 966 13
14
967 14
51. Neumann B, Baror R, Zhao C, Segel M, Dietmann S, Rawji KS, et al. (2019) Metformin
968 15
16 Restores CNS Remyelination Capacity by Rejuvenating Aged Stem Cells. *Cell Stem Cell*
969 16
17 25:473–485.e8. doi: 10.1016/j.stem.2019.08.015
- 970 17
18
971 18
52. Neumann B, Segel M, Chalut KJ, Franklin RJM (2019) Remyelination and ageing:
972 19
20 Reversing the ravages of time. *Mult Scler J* 25:1835–1841. doi:
973 20
21 10.1177/1352458519884006
- 974 21
22
975 22
53. Ouyang JF, Kamaraj US, Cao EY, Rackham OJL (2021) ShinyCell: simple and sharable
976 23
24 visualization of single-cell gene expression data. *Bioinformatics* 1–3. doi:
977 24
25 10.1093/bioinformatics/btab209
- 978 25
26
979 26
54. Pérez-Cerdá F, Sánchez-Gómez MV, Matute C (2015) Pío del Río hortega and the
980 27
28 discovery of the oligodendrocytes. *Front Neuroanat* 9:7–12. doi:
981 28
29 10.3389/fnana.2015.00092
- 982 29
30
983 30
55. Prasad BC, Ye B, Zackhary R, Schrader K, Seydoux G, Reed RR (1998) unc-3, a gene
984 31
32 required for axonal guidance in *Caenorhabditis elegans*, encodes a member of the O/E
985 32
33 family of transcription factors. *Development* 125:1561–1568. doi: 10.1242/dev.125.8.1561
- 986 33
34
987 34
56. Quick S, Procter T V, Moss J, Seeker L, Walton M, Lawson A, et al. (2022) Loss of the
988 35
36 heterogeneous expression of flippase ATP11B leads to cerebral small vessel disease in a
989 36
37 normotensive rat model. *Acta Neuropathol*. doi: 10.1007/s00401-022-02441-4
- 990 37
38
991 38
57. Reemst K, Noctor SC, Lucassen PJ, Hol EM (2016) The Indispensable Roles of Microglia
992 39
40 and Astrocytes during Brain Development. *Front Hum Neurosci* 10:1–28. doi:
993 40
41 10.3389/fnhum.2016.00566
- 994 41
42
995 42
58. Rue-Albrecht K, Lun A, Sonesson C, Stadler M (2021) velociraptor: Toolkit for Single-Cell
996 43
44 Velocity
- 997 43
45
998 44
59. Saelens W, Cannoodt R, Todorov H, Saeys Y (2019) A comparison of single-cell trajectory
999 45
46 inference methods. *Nat Biotechnol* 37:547–554. doi: 10.1038/s41587-019-0071-9
- 1000 46
47
1001 47
60. Safaiyan S, Besson-Girard S, Kaya T, Cantuti-Castelvetri L, Liu L, Ji H, et al. (2021)
1002 48
49 White matter aging drives microglial diversity. *Neuron* 109:1100–1117.e10. doi:
1003 49
50 10.1016/j.neuron.2021.01.027
- 1004 50
51
1005 51
61. Sanmarco LM, Wheeler MA, Gutiérrez-Vázquez C, Polonio CM, Linnerbauer M, Pinho-
1006 52
53 Ribeiro FA, et al. (2021) Gut-licensed IFN γ + NK cells drive LAMP1+TRAIL+ anti-
1007 53
54 inflammatory astrocytes. *Nature* 590:473–479. doi: 10.1038/s41586-020-03116-4
- 1008 54
55
1009 55
62. Sathyamurthy A, Johnson KR, Matson KJE, Dobrott CI, Li L, Ryba AR, et al. (2018)
1010 56
57 Massively Parallel Single Nucleus Transcriptional Profiling Defines Spinal Cord Neurons
1011 57
58 and Their Activity during Behavior. *Cell Rep* 22:2216–2225. doi:
1012 58
59 10.1016/j.celrep.2018.02.003
- 1013 59
60
1014 60
63. Satoh J, Kino Y, Yanaizu M, Ishida T, Saito Y (2019) Microglia express GPNMB in the
1015 61
62 brains of Alzheimer’s disease and Nasu-Hakola disease. *Intractable Rare Dis Res* 8:120–
1016 62
63 128
- 1017 63
64
1018 64
64. Scalfari A, Neuhaus A, Daumer M, Ebers GC, Muraro PA (2011) Age and disability
1019 65
66 accumulation in multiple sclerosis. *Neurology* 77:1246–1252. doi:

- 1
2
3
4
5
6
7
8
9
10
11
12
13
14
15
16
17
18
19
20
21
22
23
24
25
26
27
28
29
30
31
32
33
34
35
36
37
38
39
40
41
42
43
44
45
46
47
48
49
50
51
52
53
54
55
56
57
58
59
60
61
62
63
64
65
- 10.1212/WNL.0b013e318230a17d
65. Schirmer L, Velmeshev D, Holmqvist S, Kaufmann M, Werneburg S, Jung D, et al. (2019) Neuronal vulnerability and multilineage diversity in multiple sclerosis. *Nature* 573:75–82. doi: 10.1038/s41586-019-1404-z
66. Segel M, Neumann B, Hill MFE, Weber IP, Viscomi C, Zhao C, et al. (2019) Niche stiffness underlies the ageing of central nervous system progenitor cells. *Nature* 573:130–134. doi: 10.1038/s41586-019-1484-9
67. Sharma A, Song W-M, Farrell K, Whitney K, Zhang B, Crary JF, et al. (2021) Single-cell atlas of progressive supranuclear palsy reveals a distinct hybrid glial cell population. *bioRxiv*. doi: <https://doi.org/10.1101/2021.04.11.439393>
68. Shobin E, Bowley MP, Estrada LI, Heyworth NC, Orczykowski ME, Eldridge SA, et al. (2017) Microglia activation and phagocytosis: relationship with aging and cognitive impairment in the rhesus monkey. *GeroScience* 39:199–220. doi: 10.1007/s11357-017-9965-y
69. Sim FJ, Zhao C, Penderis J, Franklin RJM (2002) The Age-Related Decrease in CNS Remyelination Efficiency Is Attributable to an Impairment of Both Oligodendrocyte Progenitor Recruitment and Differentiation. *J Neurosci* 22:2451–2459. doi: 10.1523/JNEUROSCI.22-07-02451.2002
70. Smith AM, Davey K, Tsartsalis S, Khozoe C, Fancy N, Tang SS, et al. (2022) Diverse human astrocyte and microglial transcriptional responses to Alzheimer’s pathology. *Acta Neuropathol* 143:75–91
71. Soreq L, Rose J, Soreq E, Hardy J, Trabzuni D, Cookson MR, et al. (2017) Major Shifts in Glial Regional Identity Are a Transcriptional Hallmark of Human Brain Aging. *Cell Rep* 18:557–570. doi: 10.1016/j.celrep.2016.12.011
72. Spitzer SO, Sitnikov S, Kamen Y, Evans KA, Kronenberg-Versteeg D, Dietmann S, et al. (2019) Oligodendrocyte Progenitor Cells Become Regionally Diverse and Heterogeneous with Age. *Neuron* 101:459–471.e5. doi: 10.1016/j.neuron.2018.12.020
73. Sterpka A, Chen X (2018) Neuronal and astrocytic primary cilia in the mature brain. *Pharmacol Res* 137:114–121. doi: 10.1016/j.phrs.2018.10.002
74. Street K, Risso D, Fletcher RB, Das D, Ngai J, Yosef N, et al. (2018) Slingshot: cell lineage and pseudotime inference for single-cell transcriptomics. *BMC Genomics* 19:477. doi: 10.1186/s12864-018-4772-0
75. Swire M, Assinck P, McNaughton PA, Lyons DA, Ffrench-Constant C, Livesey MR (2021) Oligodendrocyte hcn2 channels regulate myelin sheath length. *J Neurosci* 41:7954–7964. doi: 10.1523/JNEUROSCI.2463-20.2021
76. Thrupp N, Sala Frigerio C, Wolfs L, Skene NG, Fattorelli N, Poovathingal S, et al. (2020) Single-Nucleus RNA-Seq Is Not Suitable for Detection of Microglial Activation Genes in Humans. *Cell Rep* 32:108189. doi: 10.1016/j.celrep.2020.108189
77. Trapnell C, Cacchiarelli D, Grimsby J, Pokharel P, Li S, Morse M, et al. (2014) The dynamics and regulators of cell fate decisions are revealed by pseudotemporal ordering of single cells. *Nat Biotechnol* 32:381–386. doi: 10.1038/nbt.2859
78. Trobisch T, Zulji A, Stevens NA, Schwarz S, Wischniewski S, Öztürk M, et al. (2022) Cross-regional homeostatic and reactive glial signatures in multiple sclerosis. *Acta Neuropathol* 144:987–1003. doi: 10.1007/s00401-022-02497-2
79. Viganò F, Möbius W, Götz M, Dimou L (2013) Transplantation reveals regional differences in oligodendrocyte differentiation in the adult brain. *Nat Neurosci* 16:1370–1372. doi: 10.1038/nn.3503
80. Wang X, Jiang Y, Li J, Wang Y, Tian Y, Guo Q, et al. (2021) DUSP1 Promotes Microglial Polarization toward M2 Phenotype in the Medial Prefrontal Cortex of Neuropathic Pain Rats via Inhibition of MAPK Pathway. *ACS Chem Neurosci* 12:966–978. doi: 10.1021/acschemneuro.1c00000

- 1
1056² 10.1021/acscemneuro.0c00567
1057³ 81. Wei T, Simko V (2021) R package “corrplot”: Visualization of a Correlation Matrix.
1058⁴ 82. Xuan S, Baptista CA, Balas G, Tao W, Soares VC, Lai E (1995) Winged helix
1059⁵ transcription factor BF-1 is essential for the development of the cerebral hemispheres.
1060⁶ Neuron 14:1141–1152. doi: 10.1016/0896-6273(95)90262-7
1061⁷ 83. Yasuda K, Maki T, Kinoshita H, Kaji S, Toyokawa M, Nishigori R, et al. (2020) Sex-
1062⁸ specific differences in transcriptomic profiles and cellular characteristics of
1063⁹ oligodendrocyte precursor cells. Stem Cell Res 46:101866. doi: 10.1016/j.scr.2020.101866
1064¹⁰ 84. Yeung MSY, Djelloul M, Steiner E, Bernard S, Salehpour M, Possnert G, et al. (2019)
1065¹¹ Dynamics of oligodendrocyte generation in multiple sclerosis. Nature 566:538–542. doi:
1066¹² 10.1038/s41586-018-0842-3
1067¹³ 85. Yoon H, Walters G, Paulsen AR, Scarisbrick IA (2017) Astrocyte heterogeneity across the
1068¹⁴ brain and spinal cord occurs developmentally, in adulthood and in response to
1069¹⁵ demyelination. PLoS One 12:e0180697. doi: 10.1371/journal.pone.0180697
1070¹⁶ 86. Yoshikawa F, Sato Y, Tohyama K, Akagi T, Hashikawa T, Nagakura-Takagi Y, et al.
1071¹⁷ (2008) Opalin, a Transmembrane Sialylglycoprotein Located in the Central Nervous
1072¹⁸ System Myelin Paranodal Loop Membrane. J Biol Chem 283:20830–20840. doi:
1073¹⁹ 10.1074/jbc.M801314200
1074²⁰ 87. Yu G, Wang LG, Han Y, He QY (2012) ClusterProfiler: An R package for comparing
1075²¹ biological themes among gene clusters. Omi A J Integr Biol 16:284–287. doi:
1076²² 10.1089/omi.2011.0118
1077²³ 88. Zeisel A, Hochgerner H, Lönnerberg P, Johnsson A, Memic F, van der Zwan J, et al.
1078²⁴ (2018) Molecular Architecture of the Mouse Nervous System. Cell 174:999-1014.e22. doi:
1079²⁵ 10.1016/j.cell.2018.06.021
1080²⁶ 89. Zhong S, Zhang S, Fan X, Wu Q, Yan L, Dong J, et al. (2018) A single-cell RNA-seq
1081²⁷ survey of the developmental landscape of the human prefrontal cortex. Nature 555:524–
1082²⁸ 528. doi: 10.1038/nature25980
1083²⁹ 90. Zhou Y, Song WM, Andhey PS, Swain A, Levy T, Miller KR, et al. (2020) Human and
1084³⁰ mouse single-nucleus transcriptomics reveal TREM2-dependent and TREM2-independent
1085³¹ cellular responses in Alzheimer’s disease. Nat Med 26:131–142. doi: 10.1038/s41591-019-
1086³² 0695-9
1087³³ 91. Zhu Q, Whittlemore SR, Devries WH, Zhao X, Kuypers NJ, Qiu M (2011) Dorsally-
1088³⁴ derived oligodendrocytes in the spinal cord contribute to axonal myelination during
1089³⁵ development and remyelination following focal demyelination. Glia 59:1612–1621. doi:
1090³⁶ 10.1002/glia.21203
1091³⁷
1092³⁸
1093³⁹
1094⁴⁰
1095⁴¹
1096⁴²
1097⁴³
1098⁴⁴
1099⁴⁵
1100⁴⁶
1101⁴⁷
1102⁴⁸
1103⁴⁹
1104⁵⁰
1105⁵¹
1106⁵²
1107⁵³
1108⁵⁴
1109⁵⁵
1110⁵⁶
1111⁵⁷
1112⁵⁸
1113⁵⁹
1114⁶⁰
1115⁶¹
1116⁶²
1117⁶³
1118⁶⁴
1119⁶⁵

1
2
3
4
5
6
7
8
9
10
11
12
13
14
15
16
17
18
19
20
21
22
23
24
25
26
27
28
29
30
31
32
33
34
35
36
37
38
39
40
41
42
43
44
45
46
47
48
49
50
51
52
53
54
55
56
57
58
59
60
61
62
63
64
65

1094 **Figures and Tables**

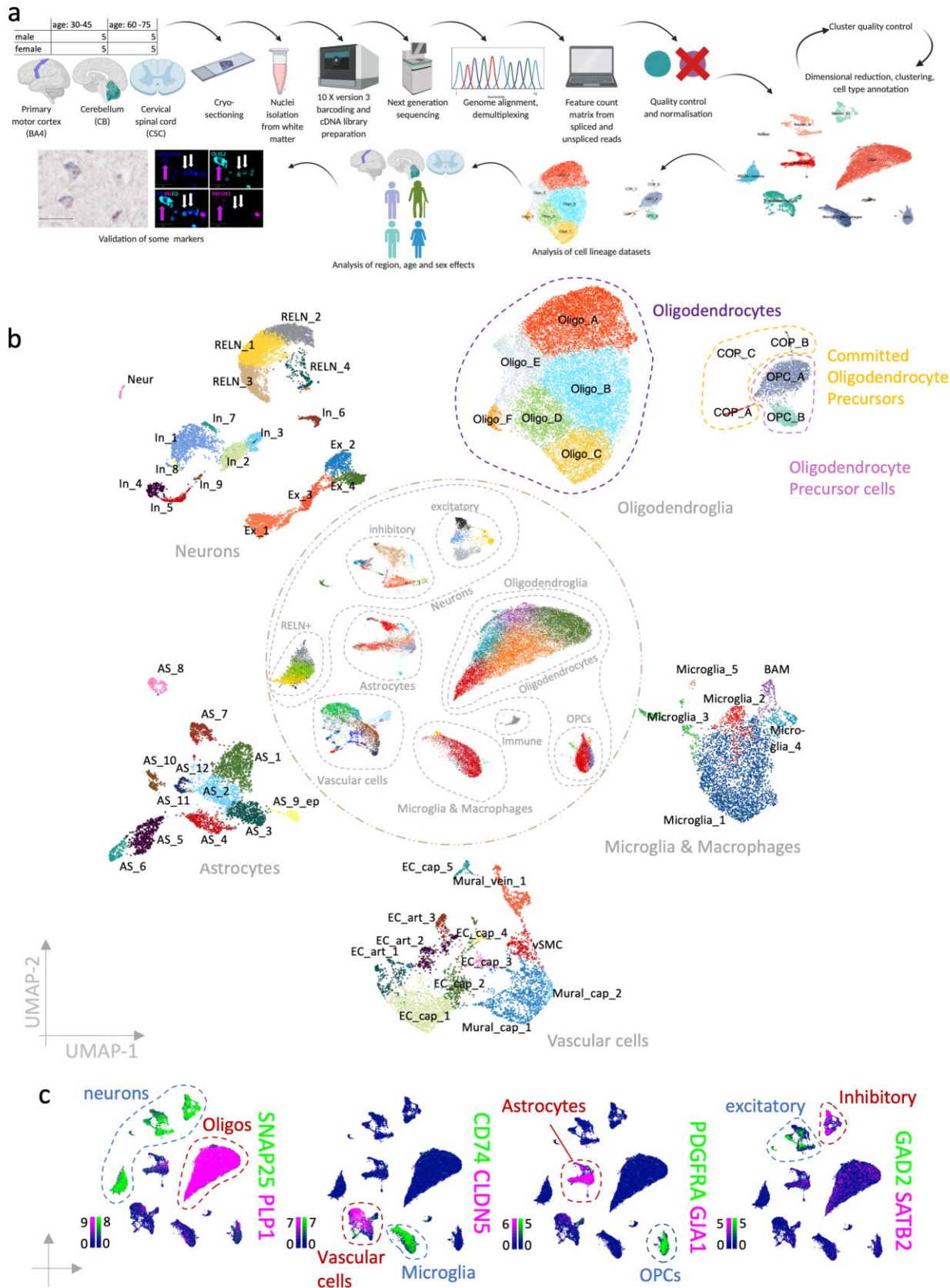


Fig. 1 Complete dataset. (a) Schematic of the workflow. (b) UMAP representation of the complete dataset in the centre and clustered cell lineage datasets at the circumference. (c) Feature plots of a

1
2
3
4
5
6
7
8
9
10
11
12
13
14
15
16
17
18
19
20
21
22
23
24
25
26
27
28
29
30
31
32
33
34
35
36
37
38
39
40
41
42
43
44
45
46
47
48
49
50
51
52
53
54
55
56
57
58
59
60
61
62
63
64
65

[Selection of canonical cell lineage marker genes expression in the complete dataset \(scale bars show LogNormalized counts\)](#). Oligos = Oligodendrocytes, excitatory= excitatory neurons, inhibitory=inhibitory neurons.

1
2
3
4
5
6
7
8
9
10
11
12
13
14
15
16
17
18
19
20
21
22
23
24
25
26
27
28
29
30
31
32
33
34
35
36
37
38
39
40
41
42
43
44
45
46
47
48
49
50
51
52
53
54
55
56
57
58
59
60
61
62
63
64
65

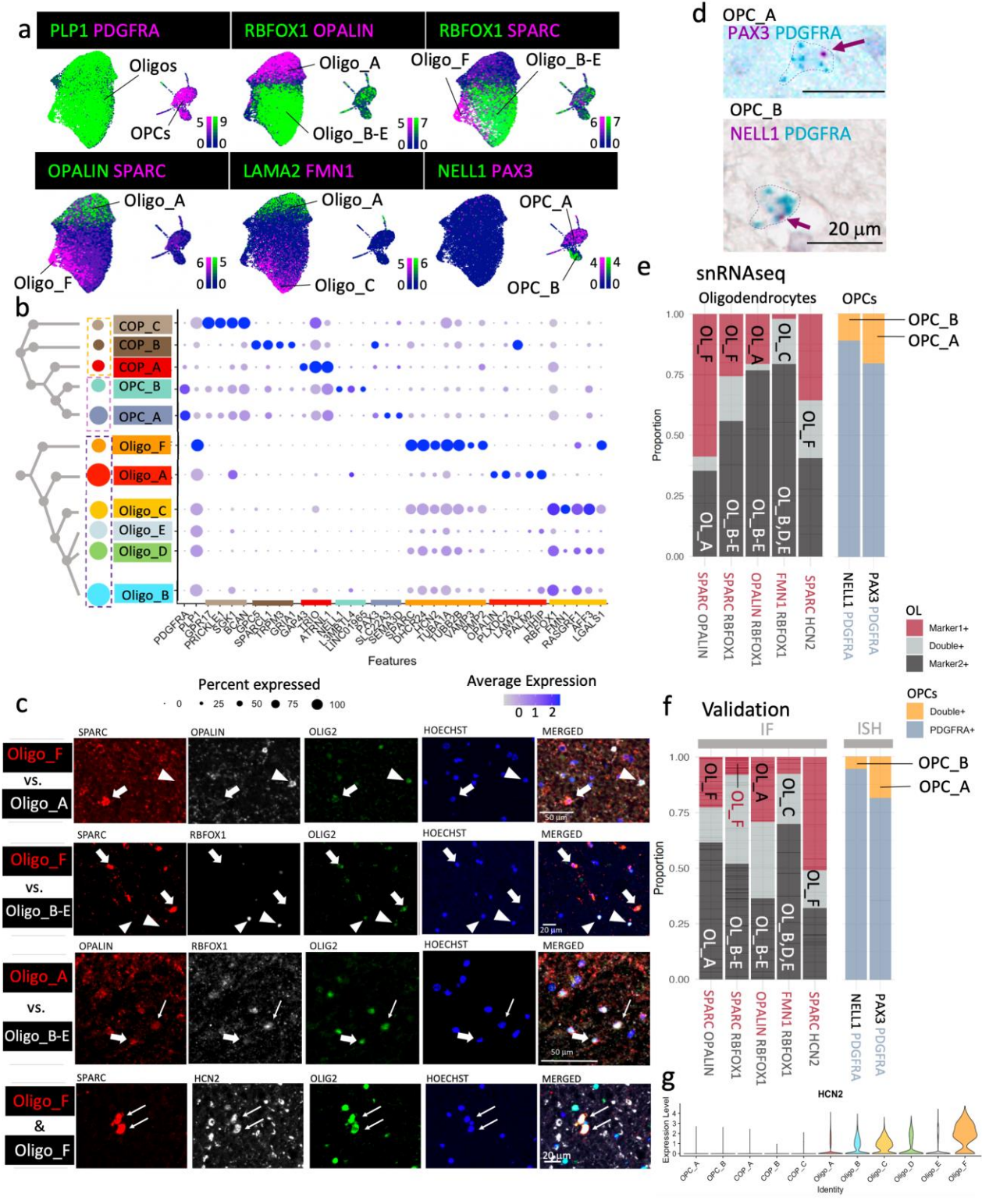


Fig. 2 Oligodendroglia cluster segregation and validation. (a) Feature plots of subsetted oligodendroglia that qualitatively show the expression of lineage marker and cluster marker genes (scale bars show LogNormalized counts). *PLP1* marks oligodendrocytes (Oligo) and *PDGFRA* oligodendrocyte precursor cells (OPCs). (b) Dot plot of a selection of marker genes for committed oligodendrocyte precursor cells (COP_A-C), oligodendrocyte precursors (OPC_A & B) and oligodendrocytes (Oligo_A-F) showing cluster segregation. The dendrogram visualizes the relationship of clusters based on 2000 most variable genes. (c) Validation of oligodendrocyte

1
1111 2 cluster markers by immuno-fluorescence stainings at the protein level. OLIG2-positive
1112 3 oligodendrocytes show either one cluster marker (fat arrow) or a second cluster marker
1113 4 (arrowhead), only with the occasional double-positive cell (thin arrow). Oligo_F-positive SPARC-
1114 5 positive Oligo F cells also express HCN2. **(d)** BaseScope duplex stainings for OPC cluster
1115 7 validation. Dotted line delineates the cell boundary with arrow pointing at cluster marker signal.
1116 8 PDGFRA marks all OPCs with PAX3 labelling OPC_A and NELL1, OPC_B. **(e,f)** Proportion of
1117 9 oligodendroglia expressing cluster markers by pairs in our snRNAseq dataset **(e)** colour-coded by
1118 10 single markers or overlap and **(f)** in the validation datasets by immunofluorescence
1119 12 (oligodendrocytes (OL), OLIG2+) or BaseScope Duplex (OPCs – PDGFRA+), showing good
1120 13 concordance. For example, OL_F (cluster Oligo_F) is SPARC- positive but RBFOX1-negative
1121 14 (second bar in (f)) and as positive for HCN2 and SPARC (5th bar in (f)). IF = immuno-fluorescence,
1122 15 ISH = In situ hybridization. **(g)** Violin plot showing that most HCN2 expression is in the Oligo_F
1123 16 cluster.

1124 18
1125 19
1126 20
1127 21
22
23
24
25
26
27
28
29
30
31
32
33
34
35
36
37
38
39
40
41
42
43
44
45
46
47
48
49
50
51
52
53
54
55
56
57
58
59
60
61
62
63
64
65

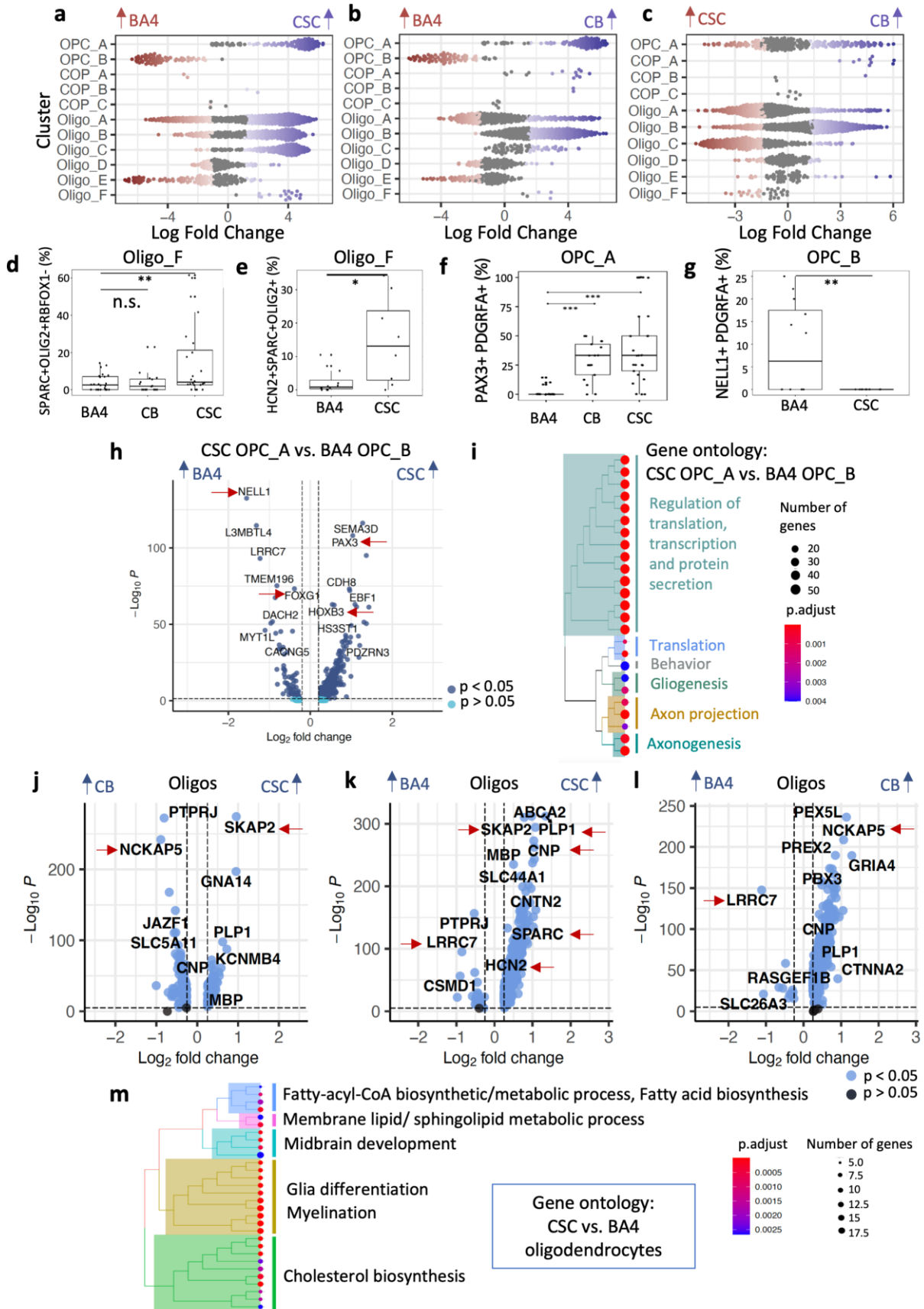


Fig. 3 Regional variation in the oligodendroglial population. Differential abundance analysis using Milo shows regional differences between (a) CSC and BA4, (b) CB and BA4 and (c) CB and CSC. Significant increases are coloured in red/blue according to region (FDR<0.1). Each dot represents a neighbourhood consisting of an average of 50 - 100 cells. OPC_A is more abundant in CB and CSC, and OPC_B in BA4. Oligo_C and Oligo_F are enriched in the spinal cord compared to the other regions. Oligo_F is a smaller cluster but strikingly different from the other oligodendrocytes in its transcriptome including genes associated with astrocytes (such as SPARC) and Schwann cells (MPZ) while clearly not being an astrocyte or Schwann cell based on the absence of relevant lineage markers. (d,e) Quantification by immunofluorescence (shown in Fig. 2c) showing the increased abundance of Oligo_F in the human spinal cord using the markers (d) SPARC+OLIG2+RBFOX1- and (e) HCN2+ SPARC+OLIG2+. (f,g) Quantification by BaseScope duplex of regional selectivity of OPC_A and B (example in Fig. 2d) showing that (f) PAX3-positive OPC_A are more abundant in CB and CSC and (g) NELL1-positive OPC_B are BA4 specific. Plots visualize percentage of total OLIG2 (d,e) or PDGFRA (f,g) -positive cells. Boxes in plots visualize median and 25th and 75th percentiles and whiskers mark range up to 1.5 * inter-quartile ranges to show potential outliers. See Table 1 for number of samples, statistical tests used and results and Table S2 for sample information. (h) Volcano plot showing differential gene expression between BA4 OPC_B and CSC OPC_A. (i) Gene ontology analysis based on differentially expressed genes of CSC OPC_A in comparison to BA4 OPC_B as shown in h) (complete version in Fig. S5). Differentially expressed genes in oligodendrocytes (oligos) with tissue region (j) – (l) with red arrows indicating genes that are discussed in the main text. (m) Gene ontology terms of genes enriched in spinal cord oligodendrocytes in comparison to brain oligodendrocytes. (Complete version in Fig. S7).

1
2
3
4
5
6
7
8
9
10
11
12
13
14
15
16
17
18
19
20
21
22
23
24
25
26
27
28
29
30
31
32
33
34
35
36
37
38
39
40
41
42
43
44
45
46
47
48
49
50
51
52
53
54
55
56
57
58
59
60
61
62
63
64
65

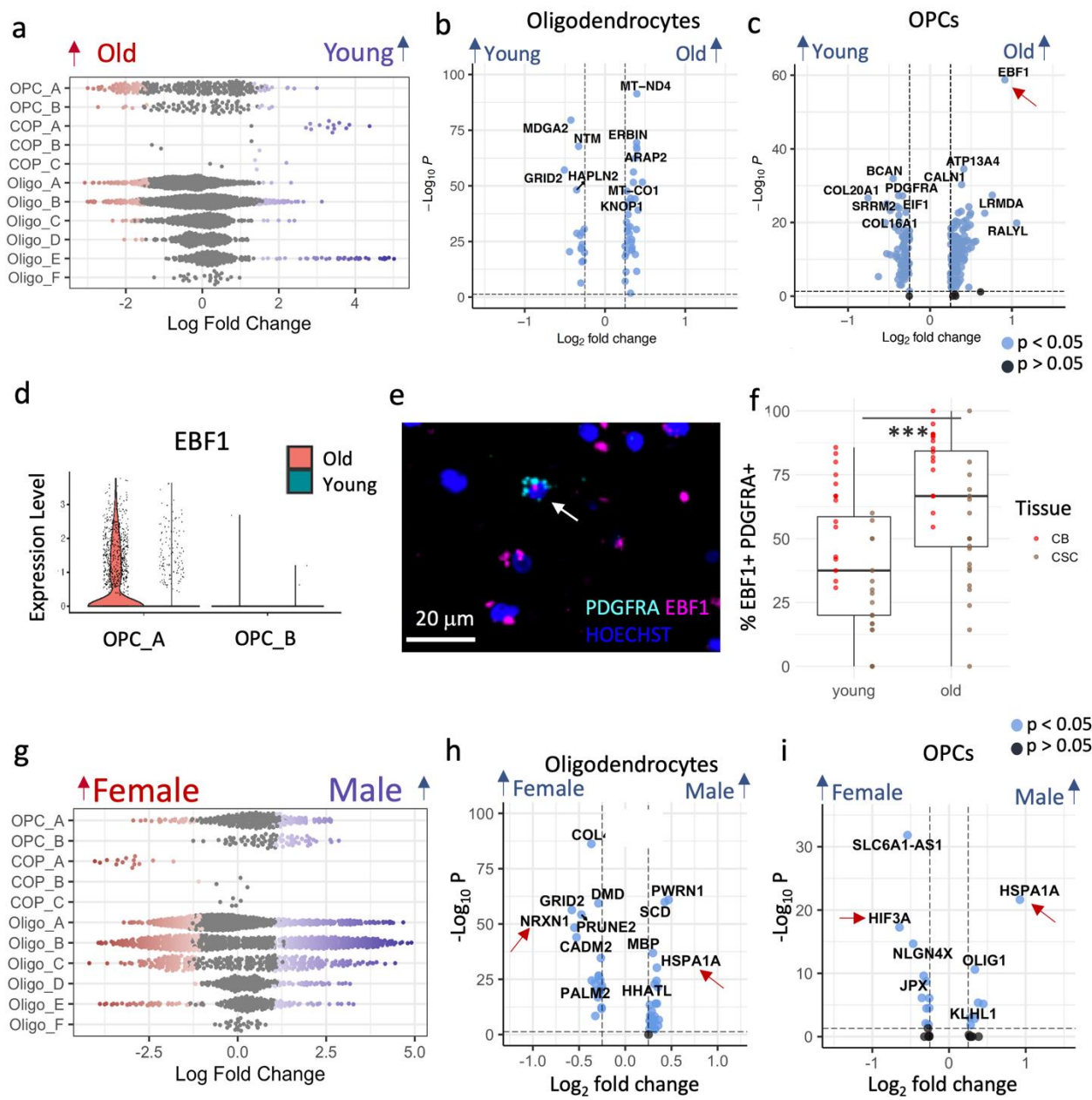


Fig. 4 Variation with age and sex in oligodendroglia. (a) Beeswarm plots showing compositional differences with age in oligodendroglia, with red showing significantly more in “old” and blue, significantly more in “young”. Volcano plots showing differentially expressed genes between young and old in oligodendrocytes (b) and OPCs (c). (d-f) There is increased *EBF1* expression in OPC_A in older donors, shown by violin plot (d), with RNAscope example of *EBF1* (pink) in *PDGFRA*+ OPCs (cyan) with Hoechst (blue) in old donor CSC (e), and quantification of double-positive *EBF1* & *PDGFRA* cells in validation dataset (f). (Linear model estimate of old age = 0.18, SE = 0.05, p <0,001, N =18 (see Table S2), 4 fields of view each, full model shown in Table 1; boxes visualize median and 25th and 75th percentiles and whiskers mark range up to 1.5 * interquartile ranges to mark potential outliers). (g) Compositional sex differences explored using Milo.

1
1163 2
1164 3
4
5
1165 6
1166 7
8
9
10
11
12
13
14
15
16
17
18
19
20
21
22
23
24
25
26
27
28
29
30
31
32
33
34
35
36
37
38
39
40
41
42
43
44
45
46
47
48
49
50
51
52
53
54
55
56
57
58
59
60
61
62
63
64
65

Differentially expressed genes with sex in oligodendrocytes (**h**) and OPCs (**i**). (Gonosomal genes excluded, but shown in Fig. S8).

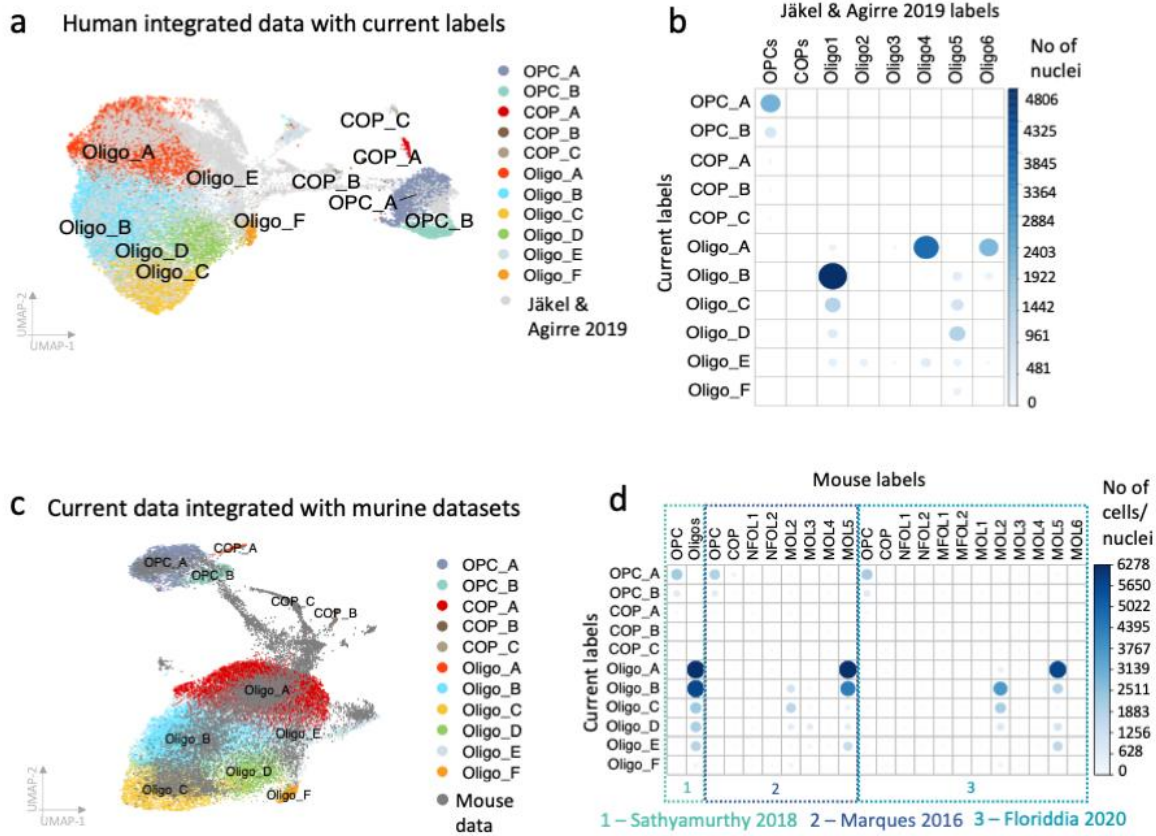
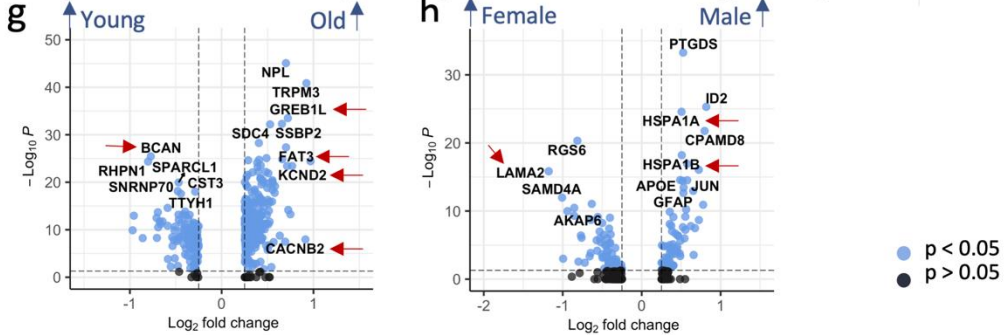
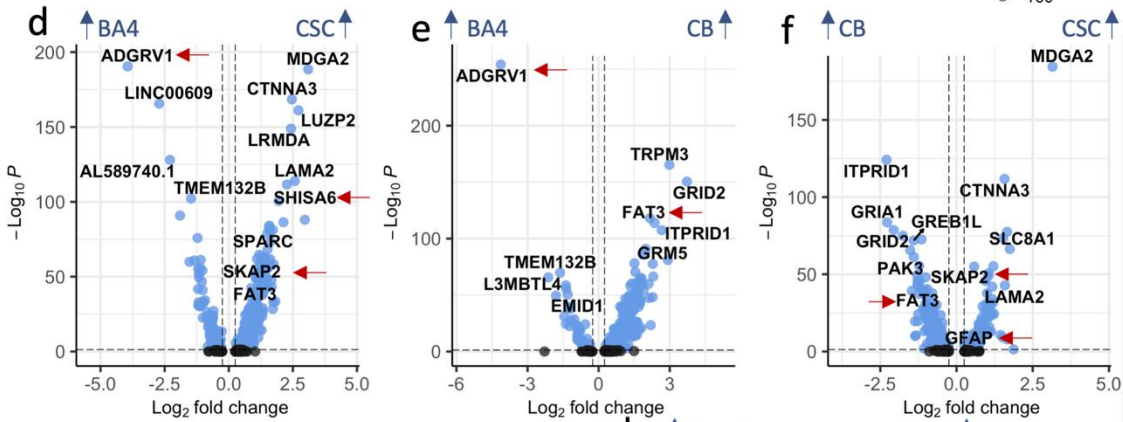
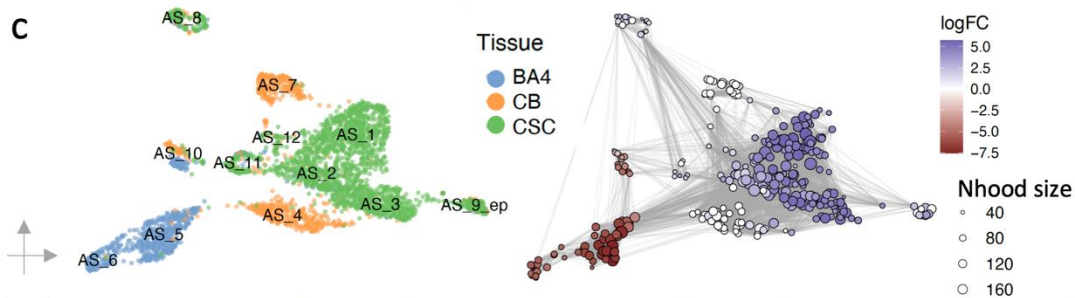
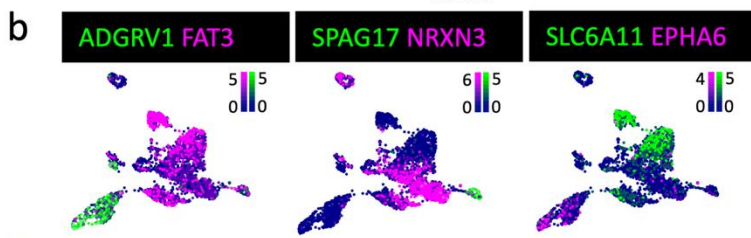
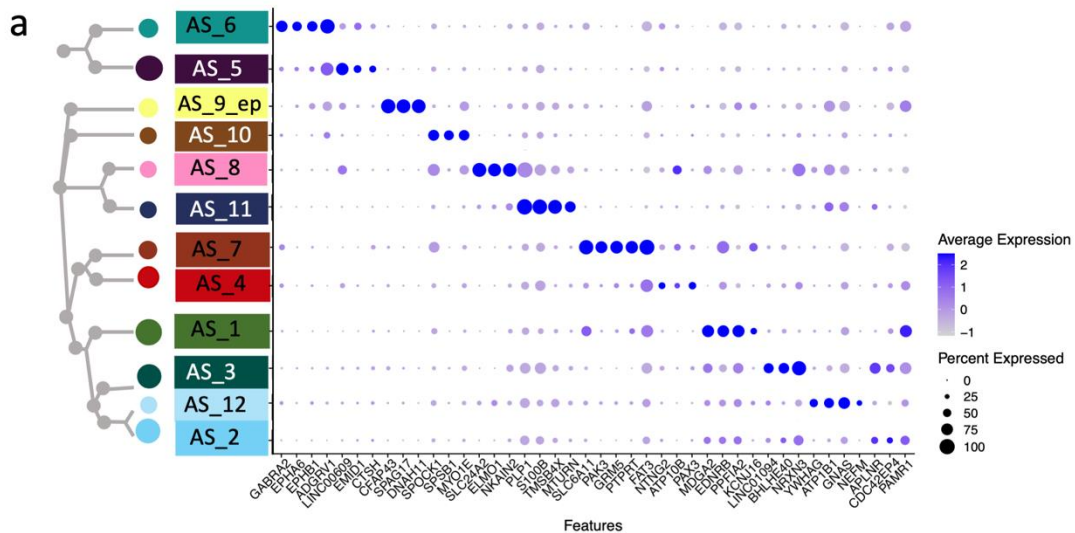


Fig. 5 Integration with previously published human and mouse datasets. Current cluster labels include letters to clearly distinguish them from previous cluster labels. **(a)** Integration with human dataset that includes multiple sclerosis and control brain samples [32]. **(b)** Correlation of transferred and new labels shows that human datasets overlap well and confirms that oligodendrocyte clusters Oligo2 and 3 are selective for multiple sclerosis whereas Oligo_F is missing in the Jäkel et al. dataset, supporting that Oligo_F is spinal cord-selective. **(c) – (d)** Integration with mouse datasets [23, 44, 62] is consistent with the lack of Oligo_F in mouse, even in datasets from spinal cord.



1
1181 2
1182 3
1183 4
1184 5
1185 6
1186 7
1187 8
1188 9
1189 10
1190 11
1191 12
13
14
15
16
17
18
19
20
21
22
23
24
25
26
27
28
29
30
31
32
33
34
35
36
37
38
39
40
41
42
43
44
45
46
47
48
49
50
51
52
53
54
55
56
57
58
59
60
61
62
63
64
65

Fig. 6 Astrocyte heterogeneity. (a) – (b) Dot plot (a) and feature plots (b) showing astrocyte cluster separation by different markers. (Scale bars show LogNormalized counts) (c) Astrocytes vary considerably with CNS region with enrichment of Milo neighborhoods in CSC in blue, depletion in CSC (and enrichment in BA4) in red, and white are CB selective. Pairwise DGE analysis across all astrocyte clusters shows variation in gene expression between (d) CSC vs. BA4, (e) CB vs. BA4 and (f) CSC vs. CB, (g) old and young and (h) male and female donors. (Gonosomal genes excluded, but shown in Fig. S8). Red arrows indicate genes discussed further in the main text.

1
1192 2
1193 3
1194 4
1195 5
1196 6
1197 7
1198 8
1199 9
1200 10
1201 11
1202 12
13
14
15
16
17
18
19
20
21
22
23
24
25
26
27
28
29
30
31
32
33
34
35
36
37
38
39
40
41
42
43
44
45
46
47
48
49
50
51
52
53
54
55
56
57
58
59
60
61
62
63
64
65

Fig. 7 Microglia heterogeneity. (a, b) Dot plot (a) and feature plots (b) showing microglial cluster separation by different markers. (Scale bars show LogNormalized counts). (c–e) Microglia vary with CNS region using Milo [15]. (f) Immuno-fluorescence validates that a subset of IBA1-positive microglia expresses the Microglia_2 cluster marker GPNMB (full arrow marks positive cell, arrow head marks negative cell). Pairwise differential gene expression analysis across all microglia clusters shows considerable variation in gene expression between (g) CSC vs. BA4, (h) CB vs. BA4 and (i) CSC vs. CB, (j) old and young and (k) male and female donors. (Gonosomal genes excluded, but shown in Fig. S8). Red arrows indicate genes discussed further in the main text.

Table 1. Statistical analysis methods and results for validation data. IF: Immuno-
fluorescence; CB: cerebellum; CSC: cervical spinal cord; Est: Estimate; SE: Standard Error.

Validation	Method	Model	Model output					Other statistical output		Number of samples (4 fields of view each quantified)
			Predictor	Est	SE	t-value	p-value			
SPARC+RBFOX1-OLIG2+ (IF)	Linear Model	cube root (percentage of SPARC+RBFOX1-OLIG2+) ~ tissue region + age*sex	(Intercept)	1.2	0.3	4.06	<0.001	NA	BA4: 6 CB: 4 CSC: 6	
			Tissue: CB	-0.17	0.36	-0.47	0.64			
			Tissue: CSC	0.74	0.32	2.34	0.023			
			Age Group: Young	-0.43	0.46	-0.931	0.356			
			Sex: Male	-0.02	0.39	-0.07	0.94			
			Young : Male	0.35	0.61	0.578	0.565			
HCN2+ SPARC+ OLIG2+ (IF)	Wilcoxon Rank Sum test	proportion of HCN2+ SPARC+ oligodendrocytes ~ tissue	NA					W = 18.5	p-value = 0.025	BA4: 3 CSC: 2
PAX3+ PDGFRA+ (BaseScope duplex)	Poisson Model	Count of double positive cells ~ total count of PDGFRA positive + tissue	(Intercept)	-1.31	0.34	-3.82	<0.001	NA	5 BA4 5 CB 7 CSC	
			total count PDGFRA	0.05	0.02	1.97	0.048			
			Tissue: CB	1.50	0.31	4.87	<0.001			
			Tissue: CSC	1.65	0.30	5.56	<0.001			
NELL1+ PDGFRA+ (BaseScope duplex)	Linear Model	NELL1+ PDGFRA+ ~ tissue region	(Intercept)	0.67	0.16	4.3	<0.001	NA	3 BA4 3 CSC	
			Tissue: CSC	-0.67	0.22	-2.97	0.007			
EBF1+ PDGFRA+ (RNAscope)	linear model	Proportion EBF1+ PDGFRA+ ~ age group + tissue + mean cellular autofluorescence	(Intercept)	0.43	0.2	4.09	<0.001	NA	CB old: 4 CB young: 4 CSC old: 5 CSC young: 5	
			Age Group	0.18	0.05	3.64	<0.001			
			Tissue (CSC)	-0.32	0.05	-7.05	<0.0001			
			cellular auto-fluorescence	44.00	26.27	1.68	0.099			



THE UNIVERSITY of EDINBURGH
Institute for Regeneration and Repair

Centre for Regenerative Medicine

Centre for Regenerative Medicine

Institute for Regeneration and Repair
The University of Edinburgh
Edinburgh BioQuarter
5 Little France Drive
Edinburgh
EH16 4UU

Tel: +44 (0) 131 651 9500

Fax: +44 (0) 131 651 9501

regenerative-medicine@ed.ac.uk

www.ed.ac.uk/regenerative-medicine

www.ed.ac.uk/regeneration-repair

10-04-2023

Dear Editor,

We submit our manuscript entitled '**Brain matters: Unveiling the Distinct Contributions of Region, Age, and Sex to Glia Diversity and CNS Function**' by Seeker et al., for consideration for publication in *Acta Neuropathologica Communications*. This is an agreed transfer and revision from the sister journal *Acta Neuropathologica*. We provide a supplementary file fully addressing the comments from the reviewers from this submission.

This is a descriptive paper using human post-mortem central nervous system emphasising the real need to consider regional CNS variation, age and sex in assessment of disease – both in pathology and therapeutics.

Summary:

The myelinated white matter tracts of the human central nervous system are commonly affected in neurodegenerative diseases, which often show regional variation, an increased risk with age and different susceptibilities between males and females. We hypothesised that this is secondary to physiological functional variation in white matter glia (oligodendroglia, astrocytes and microglia) with region, age and sex. To test this, we focussed on glia using single nucleus RNA sequencing and subsequent RNA/protein validation on human post-mortem white matter of the primary motor cortex (BA4), cerebellum and cervical spinal cord from 48 samples donated by 20 individuals without neurological disease of both sexes and two age groups (30-45 and 60-75 years).

Our advances:

1) **Regional differences in glia are striking, especially between brain and spinal cord**

All glia show regional transcriptome differences most conspicuous between the brain and the spinal cord. For example, spinal cord oligodendrocyte transcriptomic signatures explain why spinal cord myelin has longer and thicker myelin sheaths than brain, the different developmental origin of oligodendrocyte precursor cells from brain and spinal cord is reflected in their markers which are retained even in adulthood (different from mice), spinal cord-enriched microglia have a more activated phenotype than in brain and there is distinct astrocyte regional variation indicating functional segregation. We highlight differences between human and mouse glia, which may contribute to the fact that many of these diseases are uniquely human and emphasises the need to study human biology/pathology.

2) **Age and sex glial differences are less pronounced**

Age is the biggest risk factor for neurodegenerative diseases, and there are sex differences in susceptibility. We detected transcriptional variation with age, such as markers of reduced oligodendrocyte differentiation, correlating with known myelin changes, and increased microglial activation markers indicating an increased inflammatory environment. We also detect an ageing signature of human oligodendrocyte precursor cells in the cerebellum and spinal cord that is not present in the brain, suggesting that cells from diverse anatomical sites may 'age' differently. Sex variation was mostly specific for each glia type but male donor glia had a global increase in the expression of chaperone protein genes indicating altered protein folding mechanisms.

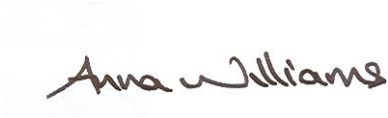
This is important as these distinct variations in regional gene/protein expression predict different responses to pathology and force us to change how we develop therapeutic strategies for region-specific diseases (e.g. astrocyte genetic neurodegenerative diseases) and global diseases (e.g. multiple sclerosis) where brain and spinal cord pathology are likely to require different therapeutics. It also reminds us that for success in translating therapies, we need to embed the consideration of cellular regional, sex and age effects in health and disease throughout our pipeline from preclinical screens to clinical trials - a 'precision medicine' approach.

We provide an open-source resource of normal adult brain and spinal cord tissue data for use by the scientific community, as part of the Human Cell Atlas Project with a user-friendly Shiny app.

None of this material has been published or is under consideration for publication elsewhere. There are no conflicts of interest. All tissue is from the Medical Research Council Brain Bank in the UK, with next-of-kin consent for tissue donation with full ethical approval. We will deposit snRNAseq data in GEO, bioinformatic code will be available on GitHub (and to the reviewers using a gitfront link currently indicated in the manuscript file) and there are no restrictions on data availability.

With best wishes,


Luisse Seeker and Anna Williams on behalf of the authors

A handwritten signature in black ink that reads "Anna Williams". The signature is written in a cursive, flowing style.


Anna Williams

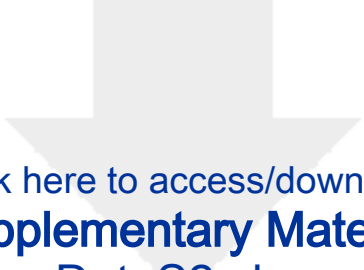
BSc (Med Sci), MB ChB (Hons), PhD, FRCP (UK)

Professor of Regenerative Neurology and Honorary Consultant Neurologist

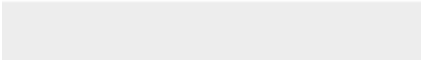




Click here to access/download
Supplementary Material
DataS1.xlsx







Click here to access/download
Supplementary Material
DataS2.xlsx







Click here to access/download
Supplementary Material
DataS3.xlsx






Click here to access/download
Supplementary Material
DataS4.xlsx





Click here to access/download
Supplementary Material
DataS5.xlsx





[Click here to access/download](#)

Supplementary Material

Revised additional supplementary figures.docx

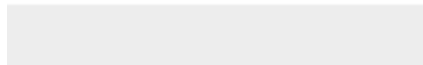
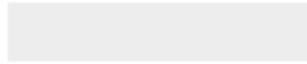




Click here to access/download

Supplementary Material

[anpc_supplementary_materials_Seeker.docx](#)



10th April 2023
Edinburgh

Brain matters: Unveiling the Distinct Contributions of Region, Age, and Sex to Glia diversity and CNS Function by Seeker et al.

This article is an agreed transfer and revision from the sister journal *Acta Neuropathologica*. We feel that the reviewers' comments are very addressable, and summarise the salient points here, before addressing each comment in detail below.

In summary, we make no apology for striving to understand differences in the normal human brain and spinal cord. We have uncovered marked differences in glial cellular signatures between the brain and the spinal cord which have not been known before. These differences help to explain the regional variation of diseases of the central nervous system - and we give examples of 1) regional differences in oligodendroglia, of relevance to known regional differences in remyelination in multiple sclerosis, 2) astrocyte regional differences that may be implicated in Spinocerebellar Ataxia and 3) microglial regional differences, which may reflect blood-brain and blood-spinal cord barrier disparity. We believe that these findings are of great interest to neuropathologists, neurologists and neuroscientists, leading to a strategy change for future therapeutics tailored for region rather than assuming all of the CNS is equal. We have emphasised this more in the text, and simplified/clarified our figures as requested by reviewer 1. We have very much taken on board the comment from Reviewer 1 that our figures (and legends) should be understandable to the 'intelligent lay reader' rather than the expert.

Our second reviewer has concerns about the technical aspects of the study which we are happy to put to rest, as we carefully designed this experiment to match our samples at the sample, chip and sequencing stage, avoiding batch effects, with strict QC, and careful, appropriate analysis. We can reassure the reviewer that we ran a doublet detection algorithm on these data, and flagged potential doublets (2.2%). We detected nuclei with expression of markers of more than one broad cell type, but these are now well-recognised to co-exist not simply for technical reasons and this is of increasing interest in the field. Therefore, we chose to retain these in our dataset, although these do not drive our findings. We report them simply to allow others to analyse them further if they wish, in the spirit of open science.

We carefully considered our clustering strategy, which was iterative as we explain below. We made much effort to ensure that our strategy and analysis was robust, but clearly bioinformatic analysis only provides hypotheses which should be validated. We chose to validate what we consider to be the most biologically interesting features, on a different set of human tissues (for biological rather than technical validation), and as successful, provides support for our bioinformatic strategy. In spite of known differences between RNA and protein levels of the same molecule, our on-tissue validation is consistent with our bioinformatics findings. More validation is clearly possible in a revision, although we are aware that this paper is already data-heavy (to quote Reviewer 1) and we tried to focus on validating what we felt were the key results.

We have tracked/highlighted changes in the attached files, and added supplementary figures as Figures SX1-3 in a separate file.

Thank you for your time in considering our revised paper.

Anna Williams and Luise Seeker, on behalf of all authors.

Detailed comments:

Reviewer #1: Introduction

I was getting very interested in this study, until I discovered that the researchers are using 'normal' brain tissue - this inevitably means that they are extrapolating when it comes to demyelinating diseases like MS

I think they need to compare their findings with the same regions in MS brains, or else this paper becomes an interesting physiological study of little relevance to MS, and maybe they need to either reframe the discussion or reframe the results

We make no apology for using normal tissue here, as our aim was to investigate differences between regions of the human CNS, as well as changes with age and sex. These studies are needed to provide understanding of normal before we can compare with disease, and this is the remit of the international 'Human Cell Atlas' project for this very reason. It is correct that we then want to compare normal with diseased, and our findings are of high relevance in explaining the different susceptibilities of different regions to disease, including with oligodendroglial changes in multiple sclerosis, astrocyte changes in spinocerebellar ataxia etc. We hope that the reviewer/reader will find the marked differences as exciting as we do in their relevance to a variety of different neurodegenerative diseases involving glia. We have reframed the introduction to make this even clearer.

Methods

Experimental design: '20 donors were selected to equally represent two age groups' Does this mean that you had 20 brains in each of the groups (young male, young female, old male, old female)? Needs clarification

We clarified the text (L 105-110) to state how many samples we included and their distribution over tissue region, age and sex groups. We also referenced Figure 1A, which the reviewer found helpful for understanding the experimental design, at the beginning of the methods section and throughout when appropriate to further help understanding.

Human donor tissue: How did Prof Smith confirm that the samples you used had 'no neuropathology'? Did he review slides for every region and every case?

Prof. Smith (as a clinical neuropathologist) assessed each donor brain using published staging/ grading systems, including Braak, NIAA, Thal, Newcastle LBD criteria, LATE pTDP stages, VCING etc. Each case has multiple samples assessed, from both hemispheres and multiple cortical, subcortical, cerebellar, brainstem regions plus the cervical spinal cord. We have added this information to the methods (L 120-123).

LFB staining: You are actually describing LFB-CV staining, with CV as the counterstain

This is correct and we have corrected this in the manuscript text in L 128.

Caps: The use of capital letters for the companies supplying reagents is irritating! Is there a good reason this is being done?

We have changed this.

Nuclei isolation: 'enriching for WM' : you are using LFB-CV to determine localization in white matter, so this isn't a matter of enriching but of localizing in white matter - it is either white matter or it isn't!

We indeed used LFB-CV to locate and select white matter for our experiments. We chose this language simply in case low volumes of border areas were included, but are happy to change this (L 153).

'For one out of 60': please state numbers numerically or with text but not both in one sentence ie '1 out of 60' or 'one out of sixty'

We have changed this (e.g. L 156).

Again, it is not clear why there are 60 samples here - if you were using 20 brains from each group, you would have 80 samples, please clarify!

We have ensured this is now clear at the beginning of our methods section. It is 20 donors across both age and sex groups that donated 3 tissue regions each, totalling 60 samples.

10X loading library preparation: No need to list the full address and postcode of the maker here!

Removed as requested L 175.

Results

Finally, we have the numbers! 5 donors in each of the 4 groups, 3 samples from each donor. I assume the age ranges were selected on purpose, not because they actually tell you anything about young versus old? This was presumably determined by the tissue available?

We indeed selected our age groups on purpose from the Edinburgh Brain bank, which has a choice of suitable donors in the age ranges we were interested in. We excluded very young donors (younger than 25 years) to avoid changes associated with brain development and also very old donors (avoiding the 'super' old).

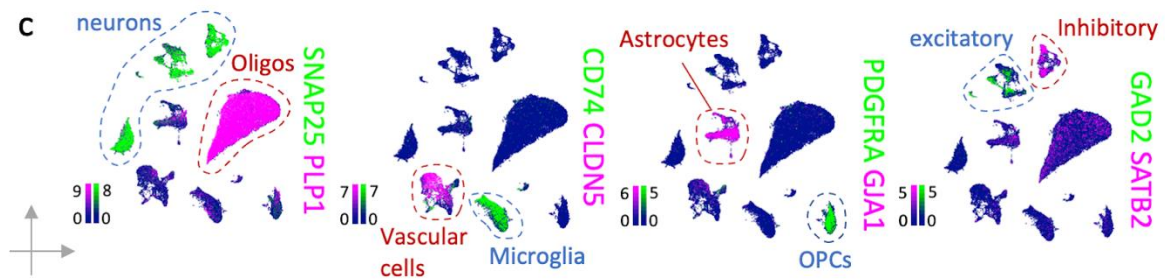
Fig 1a is much to be welcomed, since the methods tend to sound like gobbledegook - I suggest you put this figure at the start of the methods and refer to it constantly as you go through the tedious process of stating each stage of the methods

We are glad this figure panel is helpful and reference it now at the beginning of the methods and throughout the methods when appropriate. The methods are purposely detailed so that they can be reproduced by other scientists/bioinformaticians performing similar experiments (which is not the case in many similar articles). However, if this remains problematic, we could provide a summary of methods in the main paper, with supplementary more detailed methods for the experts.

1b is clear

1c would be clearer if you explained on the figure (using a key for instance) what each marker delineates ie SNAP25=neurons - you can look from 1c to 1b and vice versa to do the same thing, but it would be much easier if this was spelt out

We have added cell type annotation and scales to those plots as follows:



I note that your 60 samples got whittled down to 48 - I assume the effect on the data will be revealed in the subsequent text!

This is correct. The experiment was performed with 60 samples and after strict sample quality control we retained 48 good quality samples for downstream analysis. This is inevitable when working with post mortem human tissue which varies in quality, and is difficult to predict this in advance.

Fig 2 - This is a very confusing figure and the authors must unpack this to make it crystal clear to the intelligent lay reader, who doesn't have the gene names at their fingertips. Please start off by telling me what the different groups mean: Oligo A-F, OPC A and OPC B and COP A-C

We have added details to both the figure and the legend to make this clearer to lay readers. Oligodendrocytes (OligoA-F) all express myelin genes such as PLP1, OPCs are precursor cells that are PDGFRA positive and COPs are committed oligodendrocyte precursor cells that represent a differentiation stage between OPCs and oligodendrocytes.

It is no good showing panel a before panel b, because I have no idea what these markers mean unless you spell it out clearly. Start off with panel b - then do something to emphasize which genes characterize which oligo/OPC subtype, and then show me panel a with additional labels to tell me what I am meant to be looking at

We have added descriptions of the markers to the feature plots showing the separation of cluster gene expression qualitatively, followed by panel b, which includes more genes quantitatively. We also improved the figure legends and added scales to a).

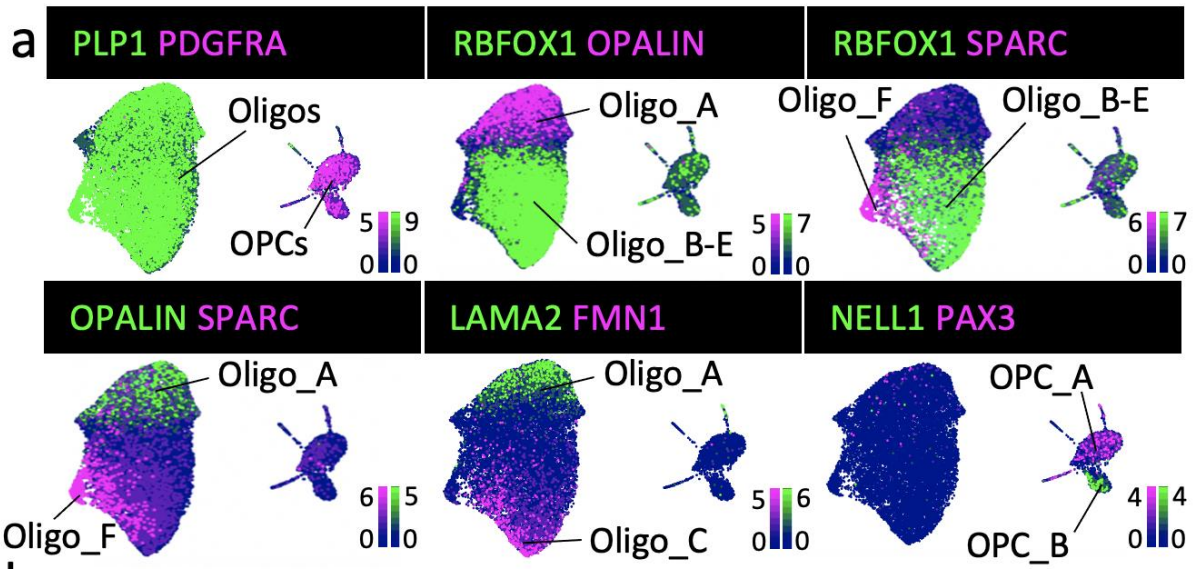


Fig 2c is equally meaningless - does each row show me a different type of cell? If so, what cell - put in a label to clarify the matter

Here, we simply show that different oligodendrocytes express markers of the different clusters using immuno-fluorescence (IF). We have changed the order of the IF panels and also added a description of which oligodendrocyte clusters we compare in each row, to help understanding.

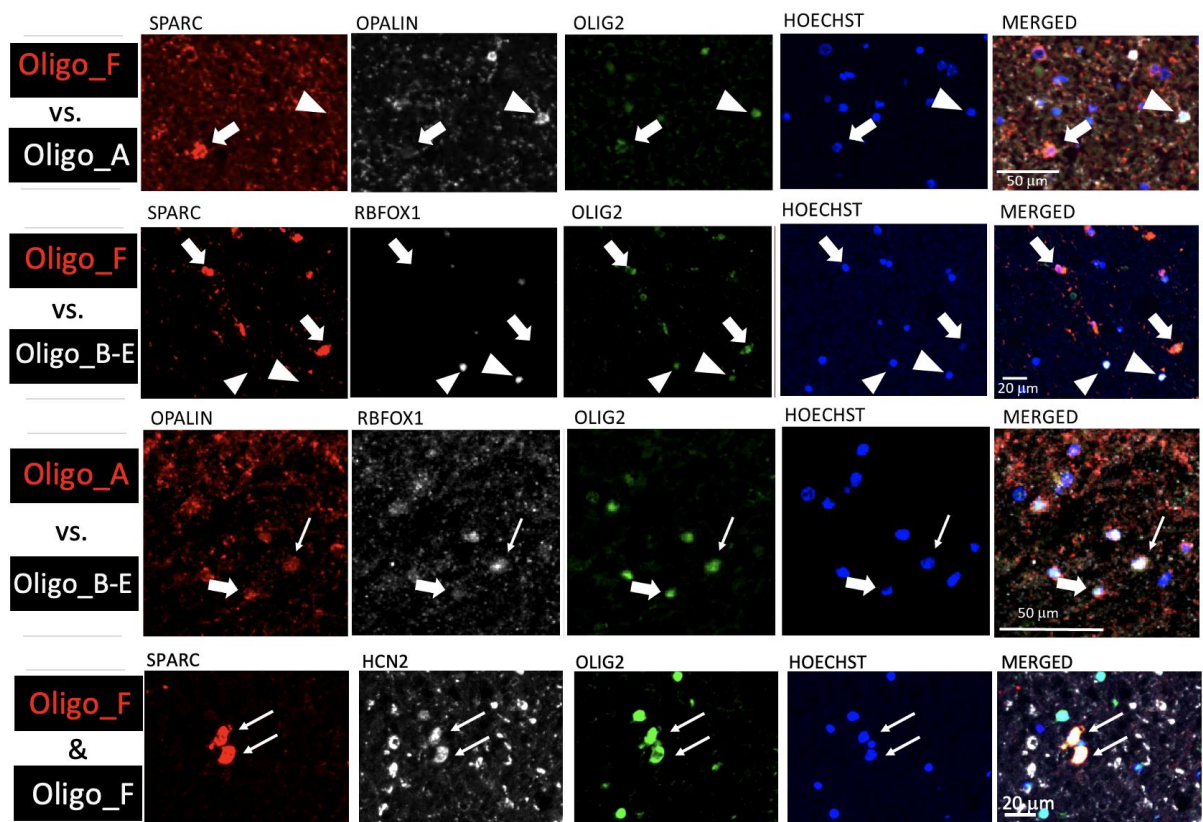


Fig 2d likewise - you are showing me something about OPCs but what?

This is in situ hybridisation using a PDGFRA probe as a marker for OPCs and PAX3 and NELL1 probes as markers for our two OPC clusters OPC_A and OPC_B respectively as example pictures to support the quantitative data in Figure 1f. We have added to the legend to make this clearer.

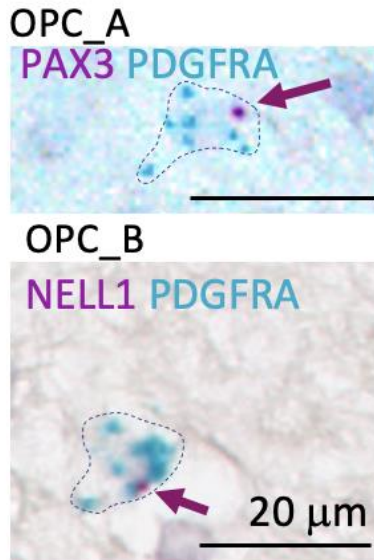


Fig 2e and f are baffling - what is this meant to be showing me?

Here, we represent the proportion of oligodendroglia in different clusters by RNAseq (e) and then by immunofluorescence/in situ hybridisation (f) using markers for these clusters (quantification of the examples shown in c and d). This is on-tissue validation of our cluster analysis by using other methods. We have put labels on as requested and expanded the legend explanation to make it clearer.

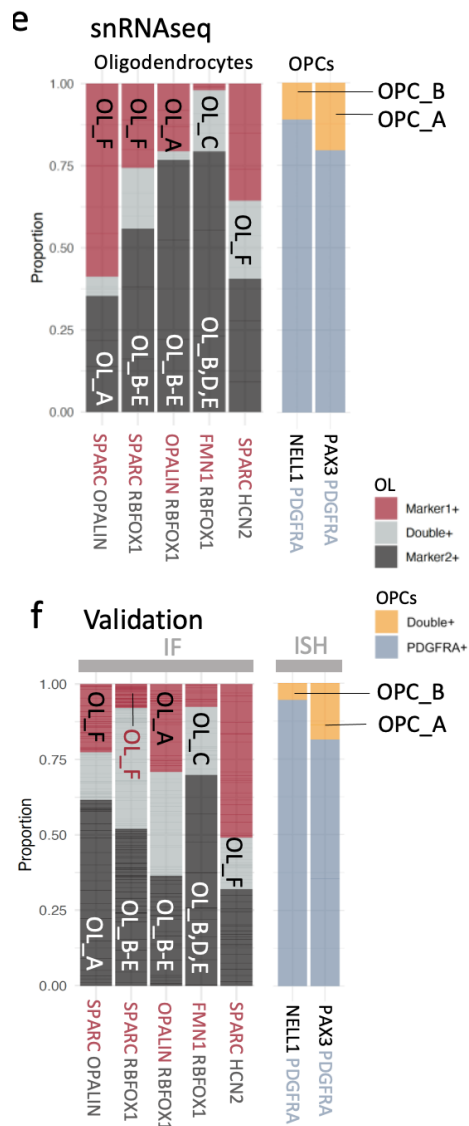


Fig 3 I am puzzled by the text here - if I look at fig 3 a-c my eye is drawn to a big increase in OPC-A and Oligo A,B,C in cervical spinal cord compared to motor cortex and to some extent cerebellum. However, the text wants to draw my attention to Oligo F where I see a few dots of increased expression in CSC compared to BA4 and CB - why is this? Is Oligo F particularly interesting? Fig 3d and e appears to be focusing again on this apparently minor subpopulation using IF markers, but it is very difficult to tell this from the labels or the figure legend

We indeed do think that Oligo_F is particularly interesting, based not only on the Milo results (noting that each dot in this plot does not represent a single cell but a neighbourhood) but also as the transcriptomic signature of this spinal cord selective Oligo_F cluster is very different from the other oligodendrocytes. Oligo_F expresses SPARC, usually associated with the astrocyte lineage, while being negative for astrocyte lineage markers such as SOX9, ALDH1L1 and GFAP. At the same time, Oligo_F also most highly expresses MPZ, a myelin gene associated with Schwann cells. However, Oligo_F is not a Schwann cell as it is negative for all other Schwann cell markers tested (Fig. S11). Del Rio Hortega originally described a 'schwannoid type IV oligodendrocyte', sparking our interest in validating this oligodendrocyte type in the human spinal cord.

We have added more information to the figure legend to better explain this interest and have added labels to the plot panels d-g to show clearly which oligodendroglia clusters we validated across the regions.

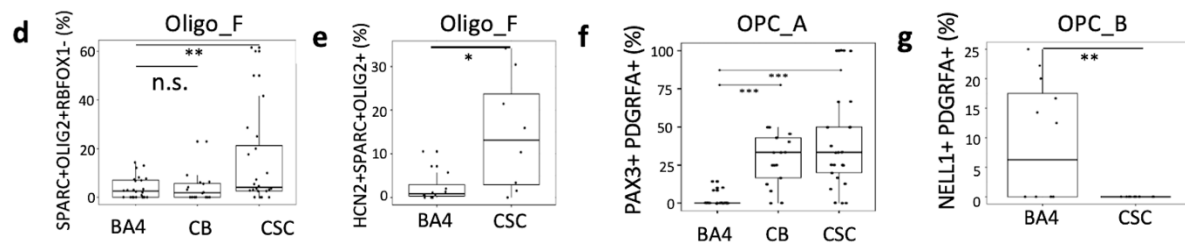


Fig 3h-m attempts to show differences in OPCs between different regions, but I wasn't sure if these belonged to group A or group B or both. I am also not sure why certain genes were picked on and others were ignored (as indicated by the arrows in h, j, k and l) The plots in i and m: I think 3i is showing me information about spinal cord OPCs and fig 3m is showing me information about spinal cord oligodendrocytes, but this is just not at all clear from looking at the figure - basic labeling and use of keys would greatly aid the reader in determining this

We have now written the comparisons on panels and expanded the legends to ensure no confusion. The many differentially expressed genes show that oligodendroglia vary significantly with anatomical region, and we provide the full results as supplementary files for the interested reader, as well as considering their combined influence via gene ontology analyses. However, we use red arrows to highlight genes to the reader that we found particularly interesting and have discussed further in the main text. We indicate this in the figure caption.

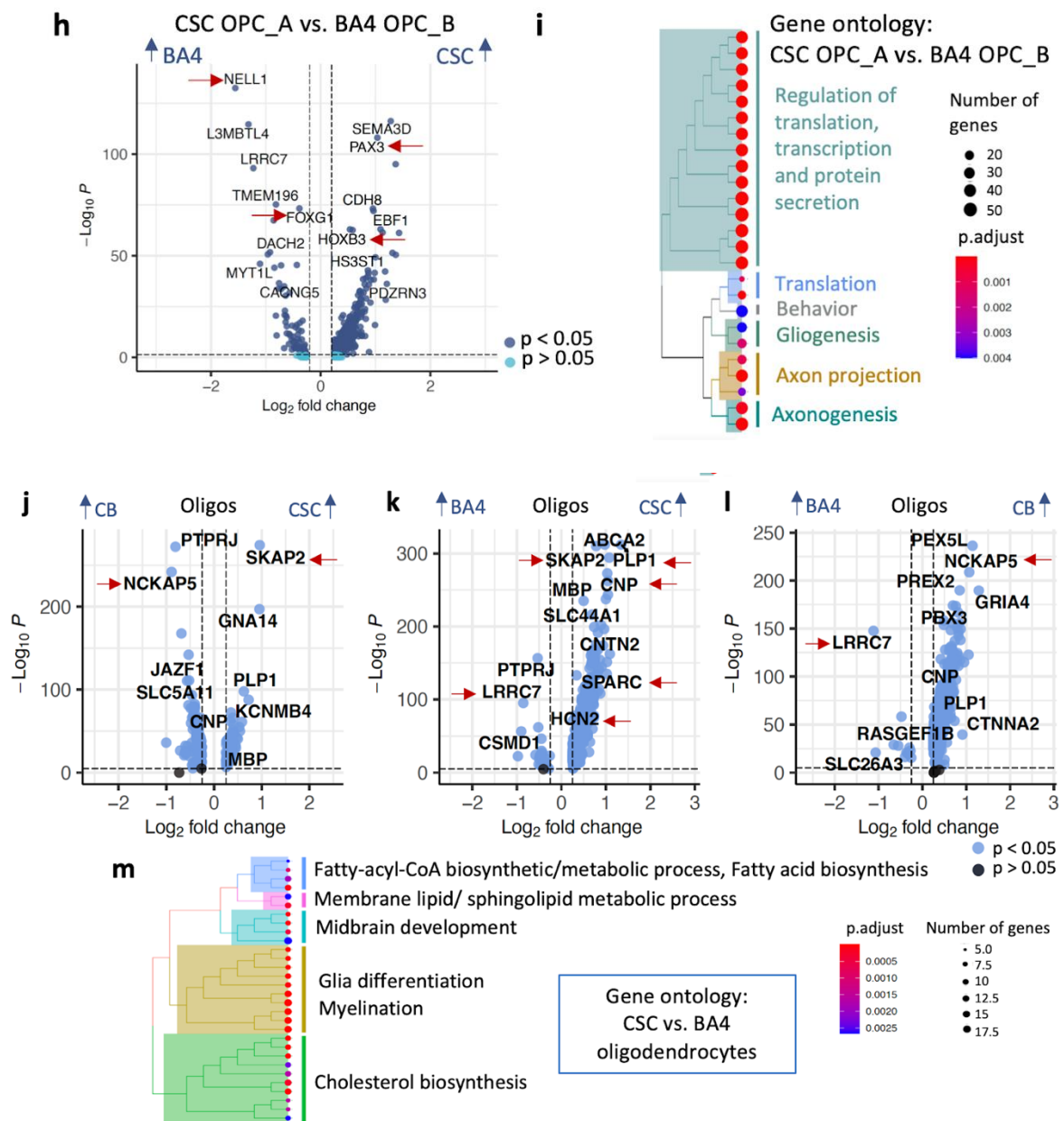


Fig 4

The age and sex differences seem fairly minimal, though a few genes are affected - however, linking all of this to multiple sclerosis (MS) is a mute point, since these are normal subjects and not subjects with the additional genetic risk factors seen in MS

We agree that sex differences are not big across all glia lineages in our dataset, which is interesting as sex differences have been described in rodents and there are sex differences in the risk of diagnosis of demyelinating and neurodegenerative diseases.

Fig 5

I guess the authors realize that they don't actually have data from MS brains, so they are correlating their findings with other databases - not quite good enough I think!

I wasn't entirely clear as to the point being made in regard to previous data with MS

brains - are the authors saying this has all been done before (in which case why do this study on normal brains) or are they saying that combining their data with other datasets adds something, and if so what?

We reiterate that our aim was to study glial transcriptomic signatures in health, and it is important to understand glial diversity in the normal condition so we can subsequently better understand disease.

Our lab (and others) have indeed conducted similar studies in MS, PD, AD, HD etc (many cited in our article) but without comparing regions (or indeed sex or age).

Comparing our dataset to previous datasets is obviously good practice and we found it useful. By comparing our data to our previous MS brain dataset, we provide further evidence that Oligo_F is spinal cord selective (not present in the brain dataset) and that oligodendrocyte clusters enriched in MS are not present in normal CNS. By comparison to mouse data, we found that transitional oligodendroglia states (COPs and newly formed oligodendrocytes) are more abundant in the mouse than human indicating the relative lack of OPC differentiation in the healthy human CNS.

Fig 6

More of the same, but this time in astrocytes...

Fig 7

More of the same, but this time in microglia...

We were also interested in astrocyte and microglia changes, which are equally interesting with marked regional differences. Our scientific colleagues in these fields are already finding these data (from our preprint) very useful.

Discussion

There is a lot of speculation going on in the discussion, perhaps a side effect of data overload! I think speculations about multiple sclerosis simply cannot be made from this dataset, since it involves putatively normal brains (whatever that means)

In the discussion, we speculate on what we think the most interesting aspects of these differences mean for humans in health and in their propensity to diseases. This includes multiple sclerosis but also other diseases. We feel this is justified in the discussion section, have made it clear that these are hypotheses and hope this will inspire others to think more about regional differences in glial biology in their research to understand and treat neurodegenerative diseases with regional susceptibility.

Reviewer #2: In this manuscript Seeker et al. attempt to address the heterogeneity of glia in human CNS white matter. The authors hypothesize that glial diversity is an important mediator of region, age and sex differences in the normal human CNS. They used single nucleus RNA sequencing (snRNA-seq) of young and aged males and females from Primary motor cortex (Brodmann area 4; BA4), cerebellum (CB) and cervical spinal cord (CSC)

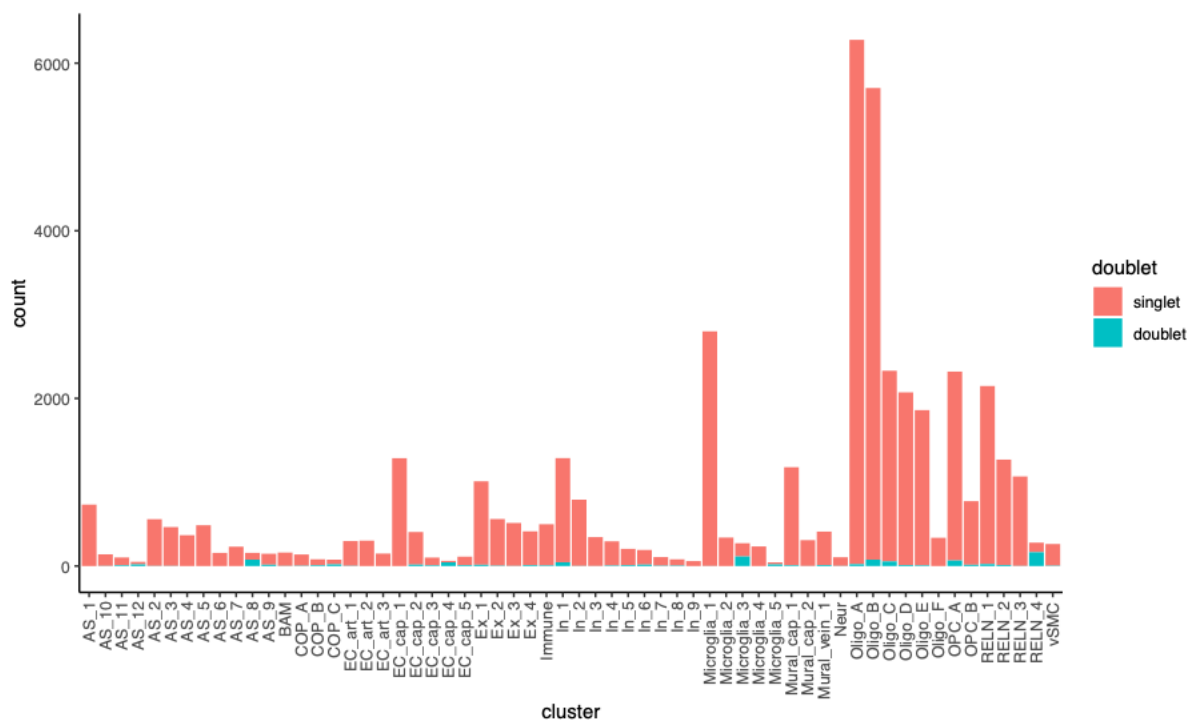
Going through the figures and data it was evident that there could be potential issues with analysis strategy and data validation which could have led to grave misinterpretation of data.

Overall, this manuscript of low standard and should not be considered before major changes in data analysis, interpretation and validation.

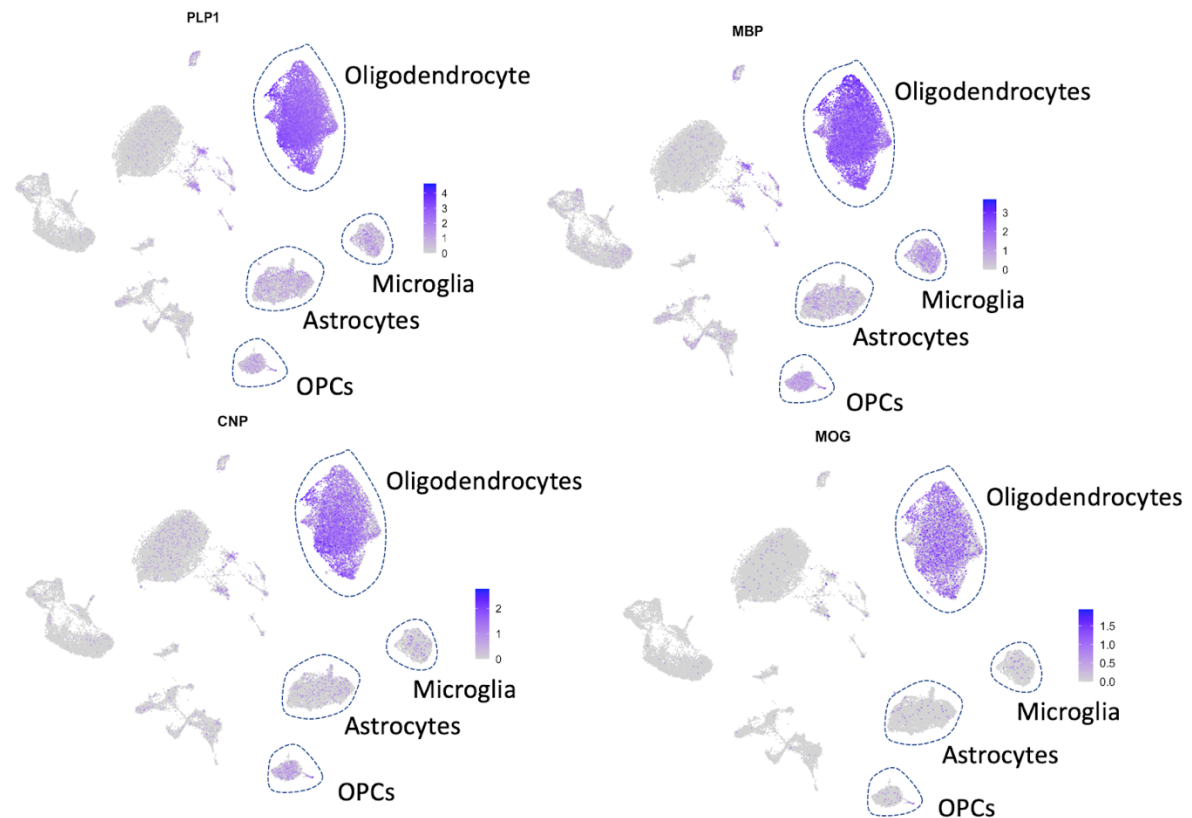
With respect, we disagree that this is low standard work with misinterpretation of data. We were very careful with our planning, analysis and validation of the results, as we are well aware of potential pitfalls in snRNAseq data. We opted for strict quality control but then inclusion of data that passed this, in the spirit of openness and allowing others to use our full data. We appreciate the opportunity to defend our strategy.

One major concern of this reviewer is whether we have sufficiently addressed the question of doublets/nuclei containing transcripts classically assigned to different broad cell types, and so will deal with this first.

We indeed ran a doublet detection algorithm (scDblFinder v 1.6.0) at the appropriate stage of our analysis (after empty droplets were removed but only minimal QC was performed,) on each sample separately as recommended, and detected a very low percentage of potential doublets (2.2% in the retained data). We have added detailed information on the doublet analysis approach and results in the metadata and shiny apps which we will make publicly available (L197-201, 629, 674-675). We have also created a new supplementary figure (**Error! Reference source not found.**) that shows the location of detected 'doublets' in clusters. As we only detected very few potential doublets, our strategy was to flag but not remove them. In particular, this reviewer was concerned about doublets in the large oligodendrocyte clusters Oligo_B and D, but these are clearly not affected.



Our clusters Microglia_3 and astrocyte AS_8 had a higher proportion of potential doublets but nuclei that express transcripts classically associated with two different broad cell types may also represent transitional stages/dedifferentiated cells or true cells with overlap transcriptomes. These latter cells are not well understood, but widely reported in other single cell/nuclei RNAseq studies. For example, our cluster Microglia_3 contains nuclei with transcripts associated with myelin normally associated with oligodendrocytes, as well as classic microglial gene transcripts. This is also seen in other published datasets, and we show below the example from the dataset



Astrocytes and oligodendrocytes develop from a common precursor, and so perhaps it is not surprising that these cells exist and these remain of interest. Therefore, we chose to retain these in case other researchers wished to study them further.

To be as clear as possible, we provide doublet analysis results in the metadata and in the shiny app. We also added new supplementary files that show UMAP plots coloured for doublet score for each glia type. We described our doublet detection method in the methods section (L197-201) and discussed the possibility of a few specific clusters being affected by doublets in the results (L 628-630, 674-675). We have removed one feature plot from Fig. 6b to avoid distractions, though left the markers in Fig. 6a.

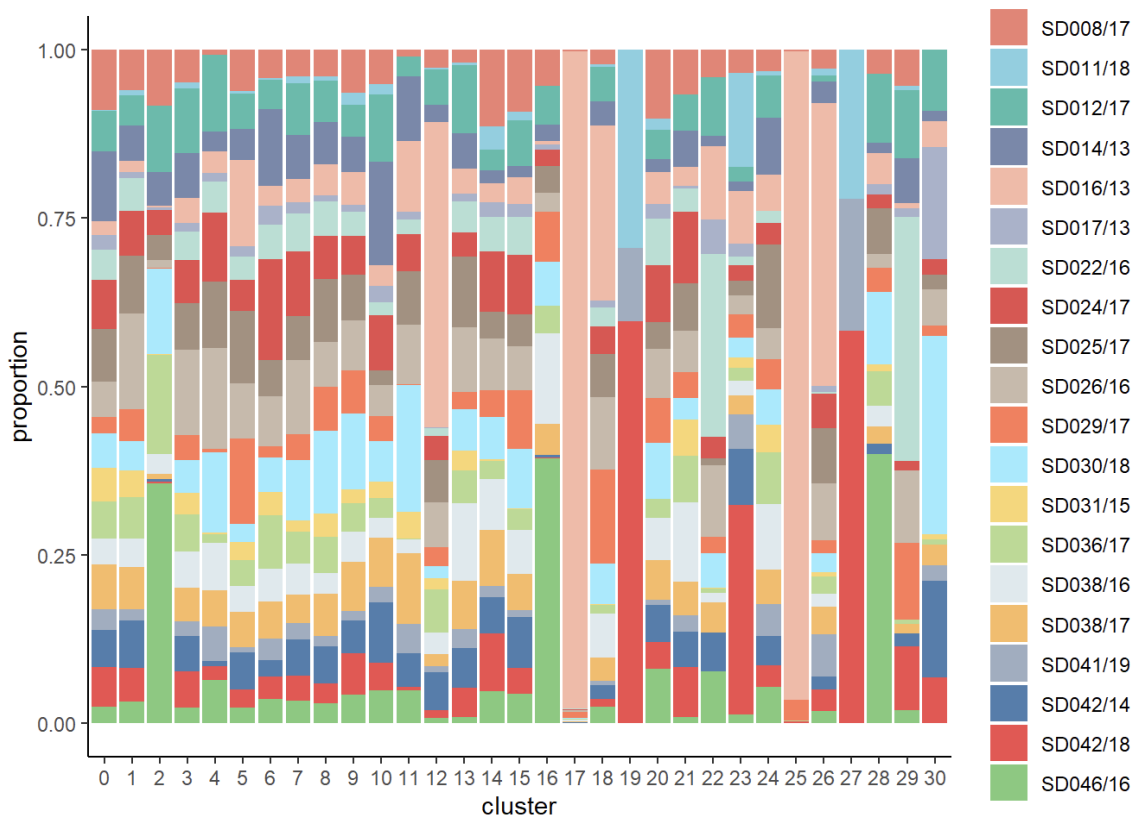
However, it is important to reiterate that these few and small clusters are not the focus of our paper, and we do not wish these to distract from the main messages of our paper, which do not involve these clusters.

Main points:

"Clusters had to contain nuclei of at least 8 donors, while donors were only considered if they contributed at least 2% to the total cluster size." How was this criteria to manually curate clusters decided?

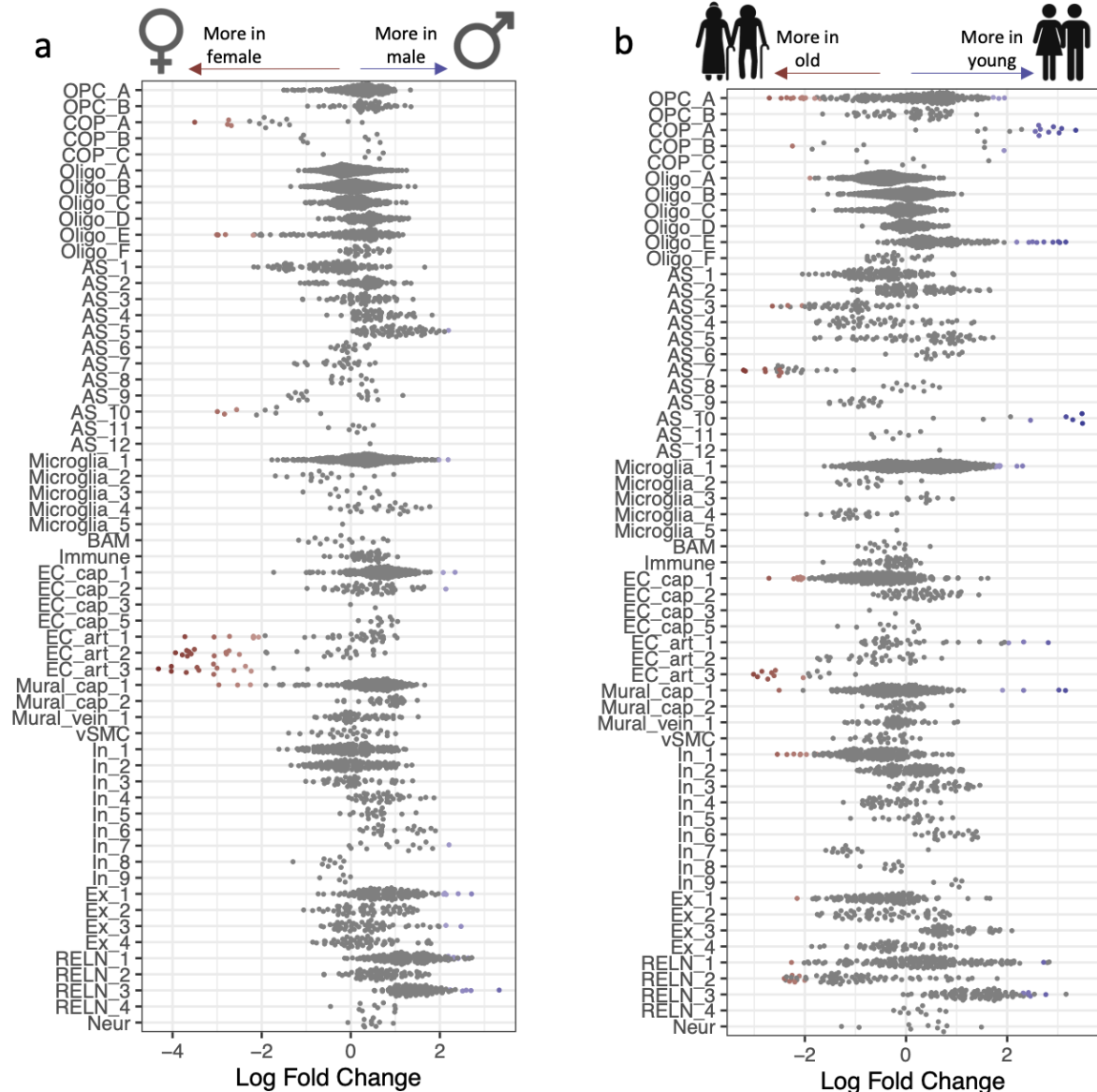
We tested different approaches to filter out clusters that were mainly composed of nuclei from specific/few donors, to avoid individual donor effects skewing the analysis. Either by removing clusters where one donor contributed > 40% nuclei or removing clusters that were made up of less than 8 donors contributing at least 2% nuclei flagged the same clusters as dubiously generalisable. These thresholds filtered out clusters 17, 19, 25 and 27 with disproportionate contributions from donors SD016/13 and SD042/18.

The QC was performed iteratively, starting with lax QC thresholds, and increasing these so not to lose clusters specific to a certain tissue, age and sex combination (>5 as this is group size) but ensuring that the remaining clusters are not due to variation within a few donors and in the end ensuring good quality data. The proportion plot below illustrates our strategy.



Human data consists of gender specific/enriched clusters some which do not represent biologically meaningful differences. Was the gender proportionality quantified to check male/female sex of ratio of each cluster? Was any data integration performed?

There were no sex-specific clusters in our glia datasets (before or after above quality control). We used Milo to statistically test whether our glial clusters (oligodendroglia, microglia and astrocytes) depend on sex differences after controlling for tissue region and age (e.g. in Fig 4g), but they did not. We did the same for age (controlling for region and sex), as shown below and as supplementary figures (Figure SX 2).



We carefully planned our experiment, processing all samples over 2 weeks, under the same conditions (same lab, same people conducting the experiment). We randomised samples balanced by group onto the 10X chips and to sequencing pools and each pool was sequenced on two different lanes to avoid batch effects. cDNA was generated on several days, but the cDNA libraries were processed in parallel on only 2 days further reducing batch effects. We were successful in this, as shown in Fig. S1 h-i) negating the need for data integration.

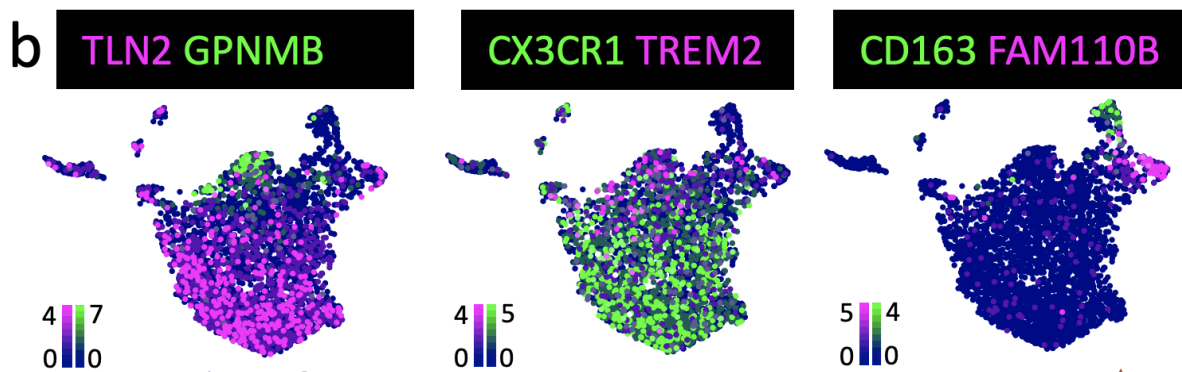
Sup fig. 1 j-m: which statistical test was used to calculate significance? What does *** mean? Since the sample size is very large for single cell dataset (which is also the case here), are the p values scaled accordingly? Considering the sample size, *** might not be significant. (Lindley's Paradox).

We used linear models on the response variables that all followed a normal distribution with subsequent ANOVA. We have added this information and the significance levels used to the figure caption. The *** was less than 2×10^{-16} so unlikely to become non-

significant even after strict adjustments. The analysis script is provided within the github repository.

Is Fig. 2a Feature plot? The scale for expression is missing. Similar issues for Fig. 6b and 7b.

We have added scale bars as shown below for Fig. 7b. All genes shown in Feature plots are also represented in dot plots with scales.



Presence of the Oligo-B, and D populations can be explained by generation of homotypic doublets from Oligo-F and C. Since the gene counts are high in QC analysis, which could be potential doublets, was any computational doublet detection and elimination performed? If not why?

We performed a doublet detection analysis as described above and there is no evidence that Oligos_B and D are doublets.

Fig. 2: How do authors explain the high variability in proportionality for each combination of genes in oligodendrocytes between snRNA-seq (e) and IF validation (f)? Also, a label to indicate the expected Oligo-cluster which is detected for each bar would be helpful. Additionally, A Marimekko plot for distribution of different Oligo-clusters in each brain region will be very informative and help better interpretation of data.

We were agreeably surprised to see how well the RNA and protein measures aligned, as RNA and protein expression are well-described to not correlate perfectly. The plots show that even at the protein level cluster markers for oligodendrocytes are distinct, and as our validations are all performed on different donor samples, generalisable. We have added more labels to this plot to make it easier to understand and also provide more explanation in the figure caption.

We show a stacked bar graph as an alternative to a Marimekko plot below, which we will include as a supplementary figure (Figure SX 3).

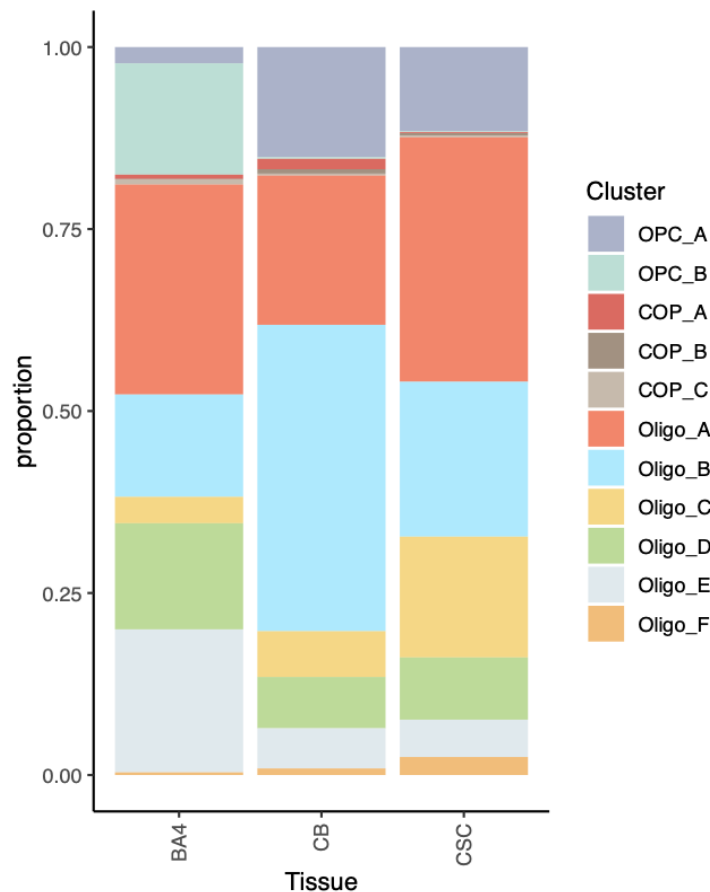


Figure 3 volcano plots:

Human protein atlas database and Brain RNA-Seq database search for expression of HOXB3 does not show its expression in OPCs or in fact in any CNS cells. Although there is no solid guidelines for setting FC cut-off values, the DE testing is known to enhance the small differences and cut-off values of 0.25 with Log2 scale need to be validated via independent methods.

The problem here is that the Human Protein Atlas has captured very few OPCs (286) at the single cell level (see picture below) and therefore is underpowered to detect HOXB3 expression (we captured >10x more OPCs). In the same human protein atlas, but examining CNS expression, HOXB3 is detectable in the human pons, medulla oblongata, spinal cord and overall white matter consistent with our results. PAX3 is another marker for OPC_A, which is more highly expressed, and we focussed on PAX_3 for validation of this cluster.

c-42 Oligodendrocyte precursor cells

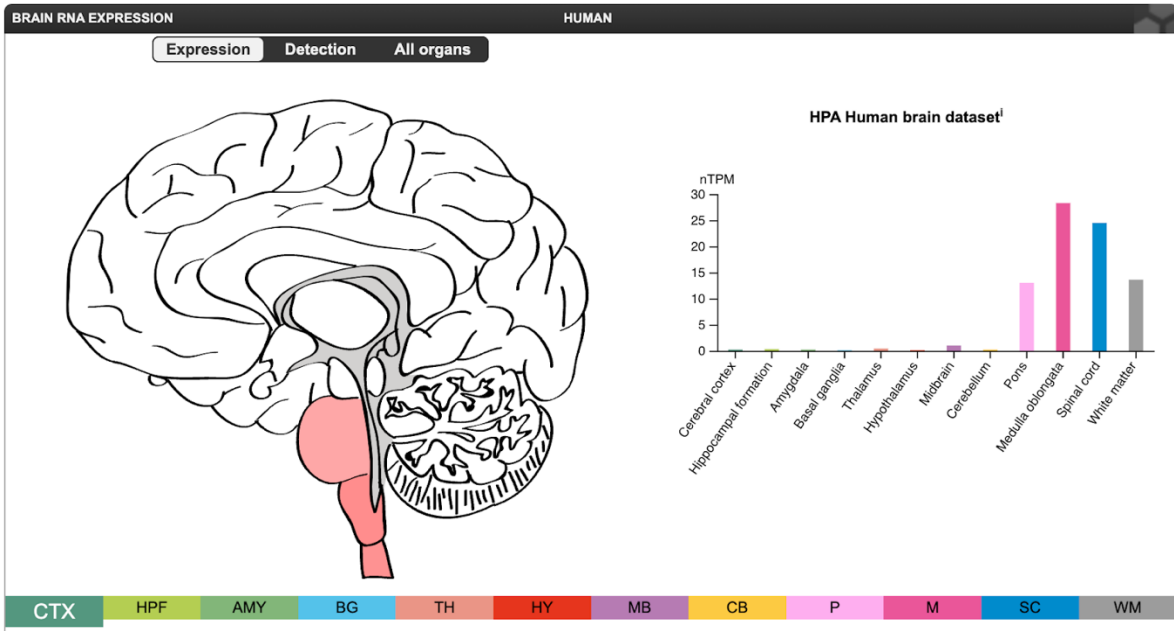
c-43 Microglial cells

c-44 Excitatory neuron

c-42
Oligodendrocyte precursor cells
Glial cells
Cell count: 286
Read count: 0
Expression: 0.0 nTPM

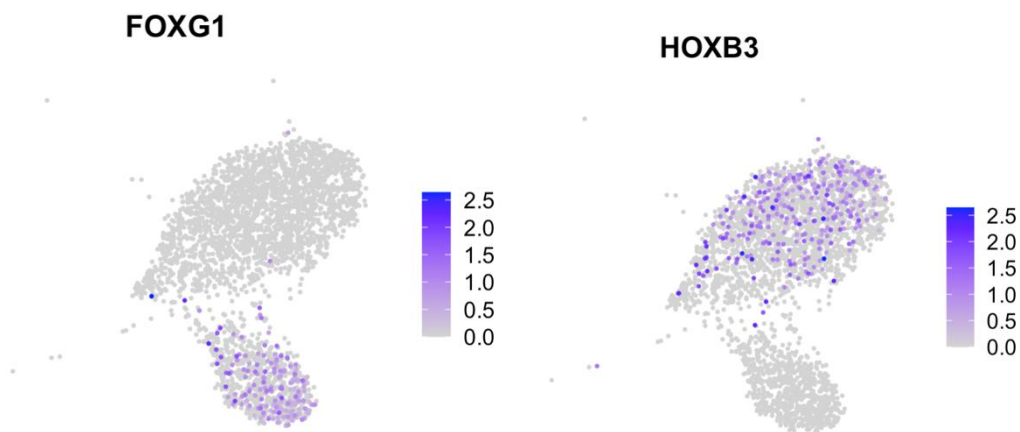
GENERAL INFORMATION ¹	
Human gene name ¹	HOXB3
Mouse gene name	Hoxb3
Human gene description ¹	Homeobox B3
Predicted location ¹	Intracellular
Mouse gene	ENSMUSG00000048763 (version 103)
Pig gene	ENSSSCG00000017534 (version 103)
Antibodies in assay ¹	No antibodies in assay

HUMAN PROTEIN ATLAS INFORMATION			
Tissue specificity ¹	Tissue enhanced (epididymis)		
	Human brain	Pig brain	Mouse brain
Regional specificity ¹	Group enriched (medulla oblongata, pons, spinal cord, white matter)	Group enriched (medulla oblongata, pons, spinal cord)	Region enriched (pons and medulla)
	Tau specificity score ¹	0.72	0.88
Regional distribution ¹	Detected in many	Detected in some	Detected in single



Since it is a pseudo-bulk analysis, it is also important to display the proportions of OPCs that could express these genes as high expression in very few cells could also give these results.

We agree and provide additional feature plots to show that these genes are expressed widely in OPCs. We also provide a shiny app where users can create a variety of plots that may address their own biological questions more specifically (https://seeker-science.shinyapps.io/shiny_app_multi/).



In addition to this, why do the authors focus their attention on only one gene for each CNS regions? There are other genes which show much more differential expression between the groups. Overall, using only a couple of genes to interpret a possible biological function of a cell without any experimental and independent validation cannot be trustworthy. Additionally, to solidify the transcriptomics based findings authors should validate the expression of FOXG1, HOXB3, and SKAP2 in situ via immunolabelling or RNAscope.

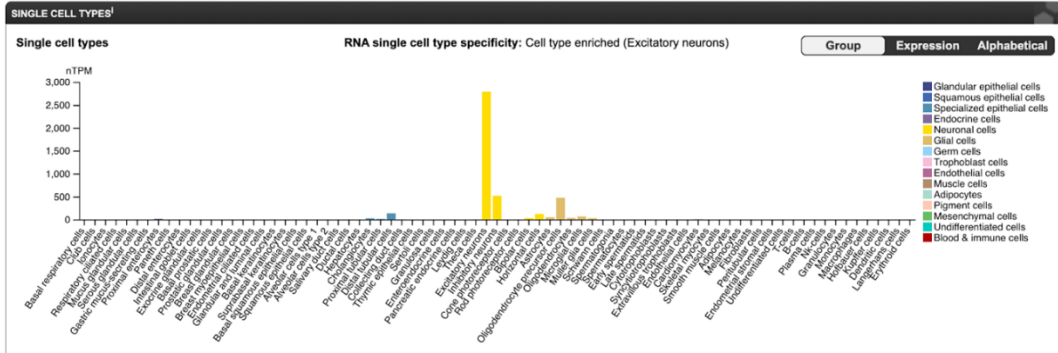
Indeed, we found many interesting genes differentially expressed in our analysis. The validation of OPC_A and OPC_B using PAX3 and NELL1 (that also express HOXB3 and FOXG1 respectively) was so clear that we decided not to add further validation here in a paper already data-heavy. SKAP2 is interesting as it has also recently been reported to show increased expression in mouse spinal cord OPCs compared to brain [5], leading to increased myelination. However, it has not been described in human. Furthermore, we wanted to validate the novel finding of increased SPARC expression in CSC oligodendrocytes.

Figure 4:

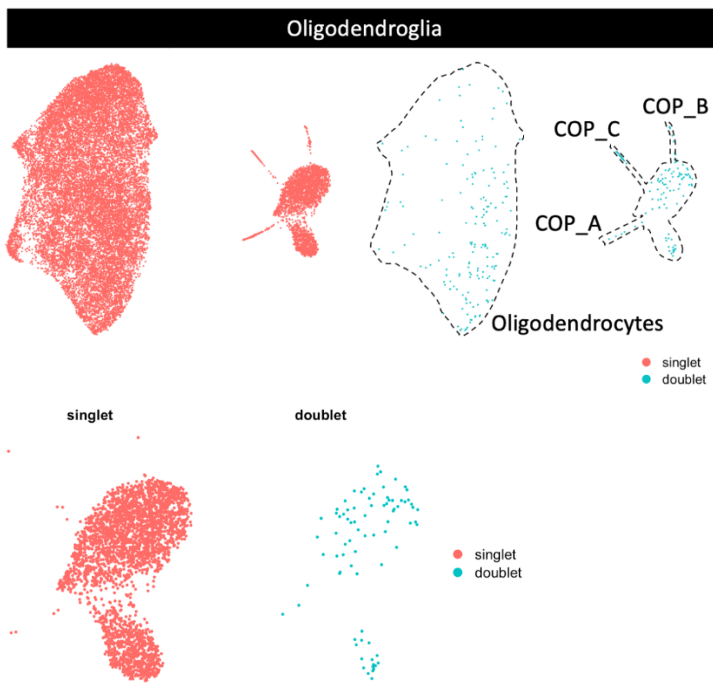
Based on the transcriptional data authors aim to address the question whether changes in oligodendroglia transcriptional signatures also differ with age which could be a plausible reason for myelin quality deterioration during aging. DE analysis shows that it's the OPCs which are altered but not the Oligodendrocytes. Here the aged OPC have expression of RALYL which is a neuronal gene and thus again the issue of presence of doublets comes.

OPCs are known to express multiple genes that are traditionally thought of as neuronal. These include neurotransmitter receptors [1, 4], and other neuronal genes including RALYL, and reflect their more recently described roles over and above simply differentiating into oligodendrocytes. RALYL is expressed in OPCs even at the protein level as shown in the above-mentioned human protein atlas:

GENERAL INFORMATION ¹		HUMAN PROTEIN ATLAS INFORMATION ¹	
Gene name ¹	RALYL	Single cell type expression cluster ¹	Neurons - Neuronal signaling (mainly)
Gene description ¹	RALYL RNA binding protein like	Single cell type specificity ¹	Cell type enriched (Excitatory neurons)
Predicted location ¹	Intracellular	Tau specificity score ¹	0.89
Number of transcripts ¹	10	Immune cell specificity ¹	Not detected in immune cells
		Immune cell distribution ¹	Not detected
		Protein evidence ¹	Evidence at protein level

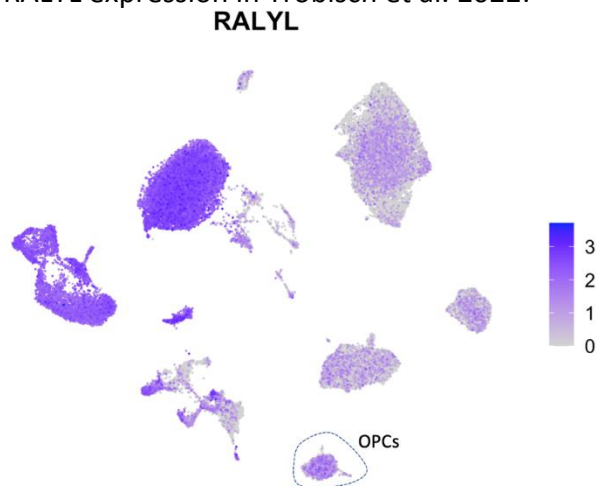


We are certain that our results are not driven by doublets as only a very small proportion of nuclei in our dataset (2.2%) are detected as potential doublets (now in Figure SX 1). Even after removing the few potential doublets within our OPCs, RALYL is still widely expressed as in other datasets including Trobisch et al. 2022 [7].



RALYL expression after removal of doublets in our dataset:

RALYL expression in Trobisch et al. 2022:



Finally, based on the DE analysis shown in figure 4 authors conclude that "age-related oligodendrocyte and myelin changes may be influenced by transcriptional changes in the OPC". However, what is puzzling is that the oligodendrocytes do not show changes in gene expression and so even if OPCs were altered it's difficult to believe authors proposal that changes in OPCs lead to deteriorating myelination upon ageing. And again, experimental evidence for any of the author's explanations is missing. This issue of over interpretation of data continues with regards to expression of gonosomal genes in the analysis of gender enriched/specific gene expression also.

Our reasoning was that OPCs are needed to replace oligodendrocytes over ageing, which is less efficient with age, and hence aged OPC changes may contribute to this. Functional studies in rodents show declining OPC function with age (Neumann et al. 2019), and we were seeking a human OPC ageing signature equivalent. Unfortunately, we cannot yet functionally validate this in human cells, as ES/iPS-derived human oligodendrocytes are not sufficiently mature in vitro.

We have reduced our speculation about the gonosomal genes.

Figure 5: Possible issues with the evidence for Oligo-F being human specific
Authors use Seurat's CCA and integrate their data with various mouse and human datasets. In order to integrate the data authors convert the human gene symbols to mouse genes. Upon integrating the data authors observe presence of SPARC+ Oligos (Oligo-F) in the human data but not in the mouse data. It's worth noting that in human SPARC is expressed in Oligodendrocytes and microglia at a similar level but in mice SPARC is expressed by microglia at much higher levels compared to oligodendrocytes. These differences in the expression could possibly affect data integration. Perhaps, authors could simply verify presence/absence of SPARC+ Oligos (Oligo-F) via immunolabelling or RNAscope.

This is not an issue with this comparison as we only integrated the subsetted oligodendrocytes. We agree that validation of SPARC+ Oligo_F Oligos would be interesting.

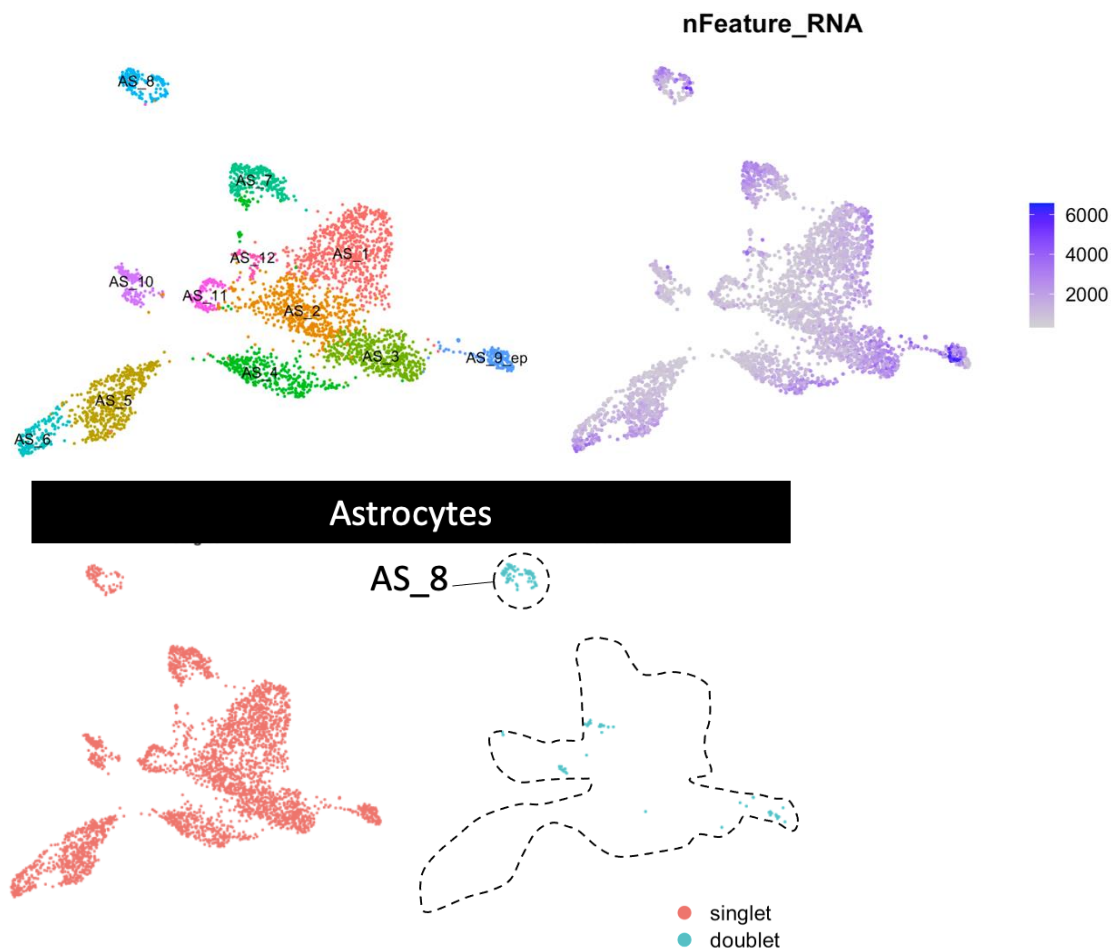
Figure 6: Astrocyte heterogeneity

Along with Oligodendroglia authors also address the astrocyte heterogeneity in WM. IN

Figure 6 authors show several distinct transcriptional states. However, already based on the Dotplot shown and the genes represented this proposed heterogeneity could be due to contamination of other cell types generating heterotypic doublets in the data. Several genes which are well known and have specific expression non-astrocytic cells are shown as the genes enriched in astrocyte clusters e.g. ELMO1, NKAIN2, PLP1 and others.

While it could be a novel discovery, the major issue here is that possible contamination of other cell types in astrocytes is not addressed and it is not shown that there are no doublets also. In order to deal with this discrepancy authors cite a bio-archive manuscript which in this reviewer's opinion is not a solid evidence to support their claims as those data might not be peer reviewed. There is no IF or RNAscope verification also. Thus overall due to severe issues with data analysis strategy, it is very difficult to grasp the proposed astrocyte heterogeneity.

As above, only astrocyte cluster AS_8 may contain some doublets (figure below), and does express myelin genes.



We agree that this possibility should be stated in the manuscript and we have therefore changed the results section at line 629 to reflect this, and added the doublet detection strategy to our methods section (L 197- 201) and in Figure SX 1. As overlap nuclei/cells, which do not fulfil criteria for doublets, but express markers traditionally assigned to different broad cell types are increasingly described in (published and preprint) literature,

we prefer to leave these cells in our dataset. Other resources have set a precedent for this e.g. the human protein atlas and Trobisch et al. 2022 [7], where, for example, ELMO1, NKAIN2 and PLP1 are shown as expressed at low levels in astrocytes.

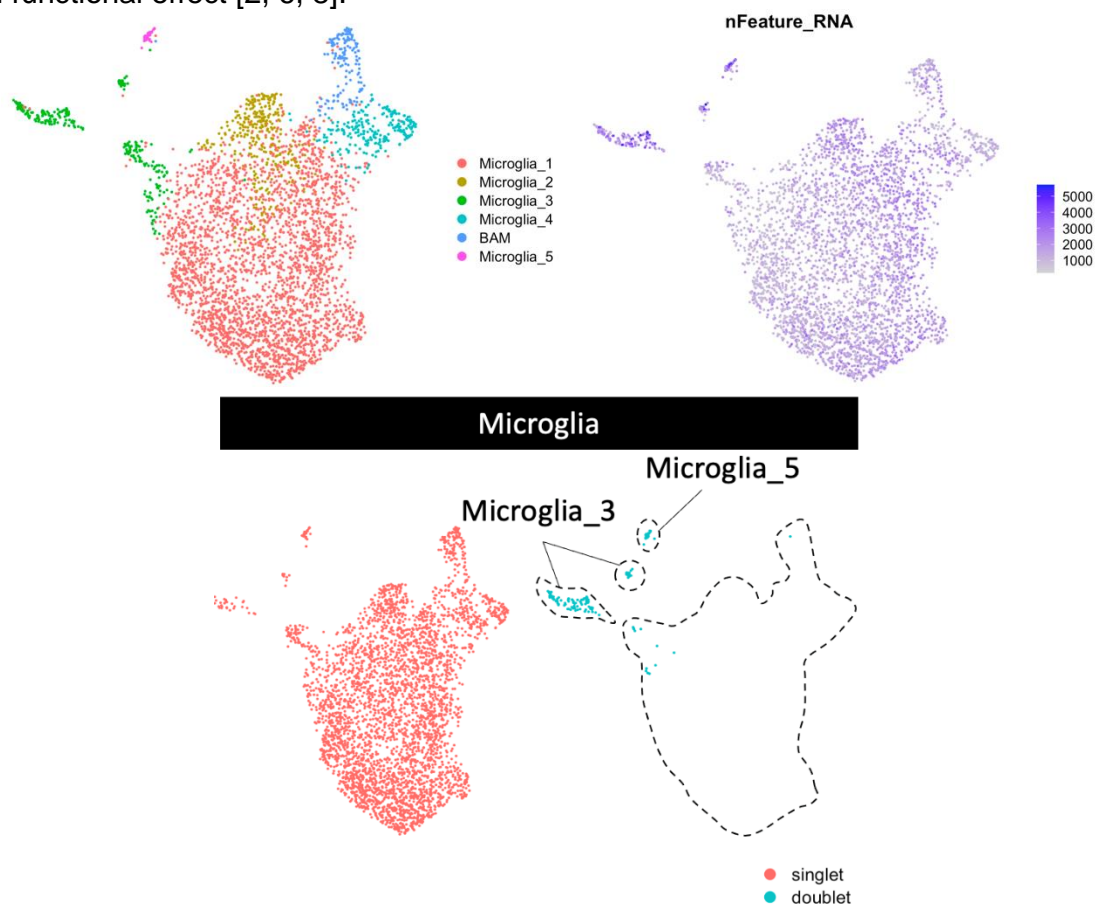
However, the astrocyte diversity that we observed across tissues is not explained by this.

Figure 7: microglia heterogeneity

The issues with astrocyte analysis are also present in the microglia analysis with expression of non-microglial genes contributing to the heterogeneity. E.g. PLP1, EDIL3, (Oligodendrocyte lineage) and CXCR4 (hematopoietic cell origin) which is due to presence of doublets.

As we explain above, Microglia_3 cluster may contain some doublets, and we clarify this in lines 674-675 and in Figure SX 1. However, microglia expressing markers classically found in other broad cell types e.g. myelin gene transcripts such as PLP1 and EDIL3 are also described in other datasets, perhaps secondary to phagocytosis. However, again, our marked regional microglia heterogeneity does not depend on this.

The CXCR4-expressing Microglia_4 cluster shows no evidence of doublets, and the published literature shows that microglia express CXCR4 at the mRNA and protein level, with functional effect [2, 6, 8].



References

1. Akay LA, Effenberger AH, Tsai LH (2021) Cell of all trades: Oligodendrocyte precursor cells in synaptic, vascular, and immune function. *Genes Dev* 35:180–198. doi: 10.1101/GAD.344218.120
2. Asensio VC, Campbell IL (1999) Chemokines in the CNS: Plurifunctional mediators in diverse states. *Trends Neurosci* 22:504–512. doi: 10.1016/S0166-2236(99)01453-8
3. Bakken TE, Jorstad NL, Hu Q, Lake BB, Tian W, Kalmbach BE, Crow M, Hodge RD, Krienen FM, Sorensen SA, Eggermont J, Yao Z, Aevermann BD, Aldridge AI, Bartlett A, Bertagnolli D, Casper T, Castanon RG, Crichton K, Daigle TL, Dalley R, Dee N, Dembrow N, Diep D, Ding SL, Dong W, Fang R, Fischer S, Goldman M, Goldy J, Graybuck LT, Herb BR, Hou X, Kancherla J, Kroll M, Lathia K, van Lew B, Li YE, Liu CS, Liu H, Lucero JD, Mahurkar A, McMillen D, Miller JA, Moussa M, Nery JR, Nicovich PR, Niu SY, Orvis J, Osteen JK, Owen S, Palmer CR, Pham T, Plongthongkum N, Poirion O, Reed NM, Rimorin C, Rivkin A, Romanow WJ, Sedeño-Cortés AE, Siletti K, Somasundaram S, Sulc J, Tieu M, Torkelson A, Tung H, Wang X, Xie F, Yanny AM, Zhang R, Ament SA, Behrens MM, Bravo HC, Chun J, Dobin A, Gillis J, Hertzano R, Hof PR, Höllt T, Horwitz GD, Keene CD, Kharchenko P V., Ko AL, Lelieveldt BP, Luo C, Mukamel EA, Pinto-Duarte A, Preissl S, Regev A, Ren B, Scheuermann RH, Smith K, Spain WJ, White OR, Koch C, Hawrylycz M, Tasic B, Macosko EZ, McCarroll SA, Ting JT, Zeng H, Zhang K, Feng G, Ecker JR, Linnarsson S, Lein ES (2021) Comparative cellular analysis of motor cortex in human, marmoset and mouse. *Nature* 598:111–119. doi: 10.1038/s41586-021-03465-8
4. Fernandez-Castaneda A, Gaultier A (2016) Adult oligodendrocyte progenitor cells – Multifaceted regulators of the CNS in health and disease. *Brain Behav Immun* 57:1–7. doi: 10.1016/j.bbi.2016.01.005
5. Ghelman J, Grewing L, Windener F, Albrecht S, Zarbock A, Kuhlmann T (2021) SKAP2 as a new regulator of oligodendroglial migration and myelin sheath formation. *Glia* 69:2699–2716. doi: 10.1002/glia.24066
6. Hattori Y, Miyata T (2018) Microglia extensively survey the developing cortex via the CXCL12/CXCR4 system to help neural progenitors to acquire differentiated properties. *Genes to Cells* 23:915–922. doi: 10.1111/gtc.12632
7. Trobisch T, Zulji A, Stevens NA, Schwarz S, Wischnewski S, Öztürk M, Perales-Patón J, Haeussler M, Saez-Rodriguez J, Velmeshev D, Schirmer L (2022) Cross-regional homeostatic and reactive glial signatures in multiple sclerosis. *Acta Neuropathol* 144:987–1003. doi: 10.1007/s00401-022-02497-2
8. Wang X, Li C, Chen Y, Hao Y, Zhou W, Chen C, Yu Z (2008) Hypoxia enhances CXCR4 expression favoring microglia migration via HIF-1 α activation. *Biochem Biophys Res Commun* 371:283–288. doi: 10.1016/j.bbrc.2008.04.055